

## REPORT DOCUMENTATION PAGE

1a. REPORT SECURITY CLASSIFICATION Unclassified		1b. RESTRICTIVE MARKINGS None	
2a. SECURITY CLASSIFICATION AUTHORITY		3. DISTRIBUTION/AVAILABILITY OF REPORT Approved for Public Release Distribution Unlimited	
2b. DECLASSIFICATION/DOWNGRADING SCHEDULE			
4. PERFORMING ORGANIZATION REPORT NUMBER(S) AFWAL-TR-84-3084		5. MONITORING ORGANIZATION REPORT NUMBER(S)	
6a. NAME OF PERFORMING ORGANIZATION AFWAL/FIGC	6b. OFFICE SYMBOL (If applicable) AFWAL/FIGC	7a. NAME OF MONITORING ORGANIZATION	
6c. ADDRESS (City, State and ZIP Code) Wright-Patterson AFB, OH 45433		7b. ADDRESS (City, State and ZIP Code) Wright-Patterson AFB, OH 45433	
8a. NAME OF FUNDING/SPONSORING ORGANIZATION	8b. OFFICE SYMBOL (If applicable) AFWAL/FIGC	9. PROCUREMENT INSTRUMENT IDENTIFICATION NUMBER	
8c. ADDRESS (City, State and ZIP Code) Wright-Patterson AFB, OH 45433		10. SOURCE OF FUNDING NOS.	
		PROGRAM ELEMENT NO. 62201F	PROJECT NO. 2403
		TASK NO. 05	WORK UNIT NO. 52
11. TITLE (Include Security Classification) Validation of USAF Stability and Control DATCOM (over)			
12. PERSONAL AUTHOR(S) Sharpes, Daniel Gregory			
13a. TYPE OF REPORT Final	13b. TIME COVERED FROM 1 Nov 80 to 30 Apr 84	14. DATE OF REPORT (Yr., Mo., Day) July 1985	15. PAGE COUNT 213
16. SUPPLEMENTARY NOTATION			
17. COSATI CODES		18. SUBJECT TERMS (Continue on reverse if necessary and identify by block number)	
FIELD	GROUP	Datcom, Stability and Control, Aerodynamics, Stability Derivative Estimation, Design Methodologies, Sweptforward (over)	
19. ABSTRACT (Continue on reverse if necessary and identify by block number)			
A detailed review of USAF Stability and Control Datcom methodologies was conducted to determine their validity for application to straight tapered, sweptforward wing configurations. To the extent possible the format found in the Datcom is repeated in this report.			
Several methods were modified to enable more accurate coefficient prediction (e.g., Wing Zero-Lift Angle of Attack, Downwash and Yawing Moment due to Yaw Rate) irrespective of sweep sign. At supersonic speeds, the reversibility theorem enabled most methodologies to be used without any modifications to account for sweptforward leading-edge designs. For the methodologies validated, sweptforward-wing estimation results were generally as accurate as the sweptback-wing results presented in the Datcom. Unfortunately, lack of test data prevented validation of several empirical methodologies (e.g., Subsonic High Angle-of-Attack Pitching Moment and Transonic Pitching Moment). No estimation (over)			
20. DISTRIBUTION/AVAILABILITY OF ABSTRACT UNCLASSIFIED/UNLIMITED <input type="checkbox"/> SAME AS RPT. <input checked="" type="checkbox"/> DTIC USERS <input type="checkbox"/>		21. ABSTRACT SECURITY CLASSIFICATION Unclassified	
22a. NAME OF RESPONSIBLE INDIVIDUAL Daniel G. Sharpes		22b. TELEPHONE NUMBER (Include Area Code) (513) 476-2087	22c. OFFICE SYMBOL AFWAL/FIGC

- 11. Methodologies for Straight-Tapered Sweptforward Wings
- 18. Wings, Forward Swept Wings
- 19. methodologies are proposed in these cases.

## FOREWORD

This report describes an in-house effort of the Control Dynamics Branch, Flight Control Division, Flight Dynamics Laboratory, Air Force Wright Aeronautical Laboratories, Wright-Patterson Air Force Base, Ohio under Work Unit 24030552, "Stability and Control Design Methods".

The work reported herein was performed during the period 1 November 1980 to 30 April 1984 by the author Lt Daniel Sharpes (AFWAL/FIGC), Project Engineer. The report was released by the author in August 1984.

This report is a complement to the USAF Stability and Control Datcom (AFWAL-TR-83-3048) and was written to expedite use of the Datcom in estimating straight-tapered sweptforward wing stability and control characteristics.

Special thanks are in order for Dana Bauer for her patient endurance at the word processor.

# *Contrails*

TABLE OF CONTENTS

<u>Section</u>	<u>Page</u>
INTRODUCTION	1
VALIDATION OF DATCOM METHODOLOGIES	
4.1 Wings at Angle of Attack	2
4.3 Wing-Body, Tail-Body Combinations at Angle of Attack	40
4.4 Wing-Wing Combinations at Angle of Attack	53
4.5 Wing-Body-Tail Combinations at Angle of Attack	57
4.6 Power Effects at Angle of Attack	61
4.7 Ground Effects at Angle of Attack	61
4.8 Low-Aspect-Ratio Wings and Wing-Body Combinations at Angle of Attack	61
5.1 Wings in Sideslip	62
5.2 Wing-Body Combinations in Sideslip	70
5.3 Tail-Body Combinations in Sideslip	73
5.4 Flow Fields in Sideslip	78
5.5 Low-Aspect-Ratio Wings and Wing-Body Combinations at Angle of Attack	78
5.6 Wing-Body-Tail Combinations in Sideslip	79
6.1 Symmetrically Deflected Flaps and Control Devices on Wing-Body and Tail-Body Combinations	84
6.2 Asymmetrically Deflected Controls on on Wing-Body and Tail-Body Combinations	98
6.3 Special Control Methods	101

TABLE OF CONTENTS (concl'd)

<u>Section</u>	<u>Page</u>
7.1 Wing Dynamic Derivatives	108
7.3 Wing-Body Dynamic Derivatives	126
7.4 Wing-Body-Tail Dynamic Derivatives	134
APPENDIX - Summary of Datcom Modifications Necessary to Estimate Forward Swept Wing Stability and Control Characteristics	145
REFERENCES	160

LIST OF ILLUSTRATIONS

<u>FIGURE</u>		<u>PAGE</u>
1	Zero-Lift Angle of Attack Correlation	
	a) Current Datcom Method	2
	b) Using Equation 2	3
2	Effect of Linear Twist on Wing Zero-Lift Angle of Attack	
	a) Taper Ratio = 0.0	4
	b) Taper Ratio = 0.5	5
	c) Taper Ratio = 1.0	6
3	Transonic Wing-Body Lift-Curve Slope Correlation	
	a) $\Lambda c/4 = -28^\circ$ , $A = 4.0$	8
	b) $\Lambda c/4 = -48^\circ$ , $A = 2.8$	8
4	Effect of Reynolds Number on Maximum Lift Method Accuracy	
	a) $C_{L_{max}}$	13
	b) $\alpha_{C_{L_{max}}}$	14
5	Effect of Linear Twist on Wing Zero-Lift Pitching Moment	
	a) Taper Ratio = 0.0	16
	b) Taper Ratio = 0.5	17
	c) Taper Ratio = 1.0	18
6	Wing Aerodynamic-Center Position	
	a) Taper Ratio = 0.0	21
	b) Taper Ratio = 0.2	21
	c) Taper Ratio = 0.25	22
	d) Taper Ratio = 0.33	22
	e) Taper Ratio = 0.5	23
	f) Taper Ratio = 1.0	24
7	Datcom Figure 4.1.4.3-25, "Empirical Pitch-Up Boundary"	26
8	Lift-Dependent Drag Factor Due to Linear Twist	
	a) Taper Ratio = 0.1	30
	b) Taper Ratio = 0.2	31
	c) Taper Ratio = 0.25	32
	d) Taper Ratio = 0.3	33
	e) Taper Ratio = 0.4	34
	f) Taper Ratio = 0.5	35
	g) Taper Ratio = 0.6	36
	h) Taper Ratio = 0.75	37
	i) Taper Ratio = 1.0	38

LIST OF ILLUSTRATIONS (Cont'd)

·0

<u>FIGURE</u>		<u>PAGE</u>
9	Forward Swept Wing Wing-Body Maximum Lift Correction Factor a) $C_{L_{max}}$ b) $\alpha_{C_{L_{max}}}$	43 44
10	Effective Wing Aspect Ratio and Span For Sweptforward Planforms	52
11	Wing-Vortex Lateral Positions at Subsonic Speeds	54
12	Wing-Vortex Lateral Positions at Supersonic Speeds	56
13	Comparison of Calculated and Experimental Values of $C_{Y_B}$	62
14	Datcom Figure 5.1.2.1-27, "Wing Sweep Contribution to $C_{\ell_B}$ "; (b) $\lambda = .5$	64
15	Comparison of Calculated and Experimental Values of $C_{\ell_B}$	65
16	Comparison of Calculated and Experimental Values of $C_{n_B}$	68
17	Planform Correction Factor - Trailing-Edge Flaps (Replaces Datcom Figure 6.1.4.3-10)	86
18	Spanwise Load Distribution Due to Symmetric Flap Deflection a) $\frac{BA}{\kappa_{av}} = 2$ b) $\frac{BA}{\kappa_{av}} = 6$ c) $\frac{BA}{\kappa_{av}} = 10$	89 89 89
19	Pitching-Moment Derivative for <u>Untapered</u> Trailing-Edge Control Surfaces <u>Located at the Wing Tip</u>	90



<u>FIGURE</u>		<u>PAGE</u>
20	Pitching-Moment Derivative for <u>Tapered Trailing-Edge Control Surfaces Having Outboard Edge Coincident with Wing Tip</u>	
	a) $\frac{\text{TAN } \Lambda_{\text{HL}}}{\beta} = -.20$	91
	b) $\frac{\text{TAN } \Lambda_{\text{HL}}}{\beta} = -.40$	91
	c) $\frac{\text{TAN } \Lambda_{\text{HL}}}{\beta} = -.60$	91
	d) $\frac{\text{TAN } \Lambda_{\text{HL}}}{\beta} = -.80$	91
21	Supersonic Theoretical Hinge-Moment Derivative $C_{h\delta}$	
	a) $\frac{\text{TAN } \Lambda_{\text{HL}}}{\beta} = -.20$	96
	b) $\frac{\text{TAN } \Lambda_{\text{HL}}}{\beta} = -.40$	96
	c) $\frac{\text{TAN } \Lambda_{\text{HL}}}{\beta} = -.60$	96
	d) $\frac{\text{TAN } \Lambda_{\text{HL}}}{\beta} = -.80$	96
22	Rolling-Moment Derivative for <u>Tapered Control Surfaces Having Outboard Edge Coincident with Wing Tip</u>	
	a) $\frac{\text{TAN } \Lambda_{\text{HL}}}{\beta} = -.20$	99
	b) $\frac{\text{TAN } \Lambda_{\text{HL}}}{\beta} = -.40$	99
	c) $\frac{\text{TAN } \Lambda_{\text{HL}}}{\beta} = -.60$	100
	d) $\frac{\text{TAN } \Lambda_{\text{HL}}}{\beta} = -.80$	100

## LIST OF ILLUSTRATIONS (Concluded)

<u>FIGURE</u>		<u>PAGE</u>
23	<u>Rolling-Moment Derivative for Tapered Control Surfaces Having Outboard Edge Not Coincident with Wing-Tip</u>	
	a) $\frac{\text{TAN } \Lambda}{\beta} \text{HL} = -.20$	101
	b) $\frac{\text{TAN } \Lambda}{\beta} \text{HL} = -.40$	101
	c) $\frac{\text{TAN } \Lambda}{\beta} \text{HL} = -.60$	102
	d) $\frac{\text{TAN } \Lambda}{\beta} \text{HL} = -.80$	102
24	<u>Rolling-Moment Derivative for Untapered Control Surfaces Having Outboard Edge Coincident with Wing Tip</u>	103
25	<u>Rolling Moment Derivative for Untapered Control Surfaces Having Outboard Edge Not Coincident with Wing Tip</u>	103
26	<u>Roll-Damping Parameter at Zero Lift</u>	
	a) Taper Ratio = 0.0)	113
	b) Taper Ratio = 0.25	114
	c) Taper Ratio = 0.5	115
	d) Taper Ratio = 1.0	116
27	<u>Low-Speed Drag-Due-To-Lift Yaw-Damping Parameter</u>	121
28	<u>Low-Speed Profile-Drag Yaw-Damping Parameter</u>	122

## LIST OF TABLES

<u>TABLE</u>		<u>PAGE</u>
1	Subsonic Wing-Alone Lift-Curve Slope Data Summary and Substantiation	161
2	Supersonic Wing-Body Normal-Force-Curve Slope Data Summary and Substantiation	161
3	Subsonic Wing-Alone Lift Variation with Angle of Attack Data Summary and Substantiation	162
4	Maximum Lift and Angle of Attack for Maximum Lift for Wing-Alone Configurations at Subsonic Speeds	165
5	Wing-Alone Zero-Lift Pitching Moment Data Summary and Substantiation	165
6	Subsonic Wing-Alone Aerodynamics-Center Location Data Summary and Substantiation	166
7	Supersonic Wing-Body Aerodynamic Center Location Data Summary and Substantiation	167
8	Zero-Lift Drag Data Summary and Substantiation	168
9	Subsonic Wing-Alone Drag Due to Lift Data Summary and Substantiation	169
10	Transonic Wing-Body Drag Due to Lift and Data Summary and Substantiation	171
11	Supersonic Wing-Body Drag Due to Lift Data Summary and Substantiation	173
12	Subsonic Wing-Body Lift-Curve Slope Data Summary and Substantiation	174
13	Subsonic Wing-Body Lift Variation with Angle of Attack Data Summary and Substantiation	175
14	Subsonic Wing-Body Maximum Lift Data Summary and Substantiation	176
15	Subsonic Wing-Body Aerodynamic-Center Location	176
16	Subsonic Wing-Body Zero-Lift Drag Data Summary and Substantiation	176

<u>TABLE</u>		<u>PAGE</u>
17	Supersonic Wing-Body Zero-Lift Drag Data Summary and Substantiation	177
18	Subsonic Wing-Body Drag Due to Lift Data Summary and Substantiation	177
19	Subsonic Downwash - Method 1 Data Summary and Substantiation	178
20	Subsonic Downwash Gradient - Method 2 Data Summary and Substantiation	179
21	Downwash Due to Flap Deflection Data Summary and Substantiation	179
22	Subsonic Dynamic Pressure Ratio Data Summary and Substantiation	179
23	Transonic Wing-Body Rolling Moment Due to Sideslip Data Summary and Substantiation	180
24	Supersonic Wing-Body Rolling Moment Due to Sideslip Data Summary and Substantiation	181
25	Subsonic Wing-Body Rolling Moment Due to Sideslip Data Summary and Substantiation	181
26	Subsonic Wing-Body-Tail Rolling Moment Due to Sideslip Data Summary and Substantiation	182
27	Effect of Control Surface Deflection on Lift Data Summary and Substantiation	183
28	Effect of Control Surface Deflection on Lift-Curve Slope Data Summary and Substantiation	184
29	Effect of Control Surface Deflection on Maximum Lift Coefficient Data Summary and Substantiation	185
30	Effect of Control Surface Deflection on Pitching Moment Data Summary and Substantiation	186
31	Effect of Angle of Attack on Control Surface Hinge Moment Data Summary and Substantiation	187
32	Effect of Control Surface Deflection on Rolling Moment Data Summary and Substantiation	187

# Contrails

AFWAL-TR-84-3084

<u>TABLE</u>		<u>PAGE</u>
33	Effect of Control Surface Deflection on Yawing Moment Data Summary and Substantiation	188
34	Subsonic Wing-Alone $C_{Lq}$ Data Summary and Substantiation	188
35	Subsonic Wing-Alone $C_{mq}$ Data Summary and Substantiation	189
36	Subsonic Wing-Alone $C_{Yp}$ Data Summary and Substantiation	190
37	Subsonic Wing-Alone $C_{\ell p}$ Data Summary and Substantiation	190

LIST OF SYMBOLS

## ENGLISH SYMBOLS

$A, AR$	Wing aspect ratio
$A_{eff}$	Effective wing aspect ratio
$b$	Wing span
$b_{eff}$	Effective wing span
$b_f$	Total span of flaps, measured normal to the plane of symmetry
$C_2$	Empirical taper ratio constant
$c_{f_r}$	Root chord of flap measured parallel to the plane of symmetry
$c_{f_t}$	Tip chord of flap measured parallel to the plane of symmetry
$c_r$	Root chord
$c_t$	Tip chord
$\bar{c}$	Wing mean aerodynamic chord
$d$	Maximum fuselage diameter
$e$	Oswald efficiency factor for induced drag
$\frac{G}{\delta}$	Subsonic spanwise loading coefficient
$h_H$	Height of aft-surface MAC quarter-chord point above or below the forward surface root chord, measured in plane of symmetry normal to forward surface root chord, positive for aft-surface MAC above root chord plane
$K_{B(W)}$	Ratio of the lift of the body in the presence of the wing to that of the wing alone
$K_N$	Ratio of the body-nose lift to that of wing alone
$K_{W(B)}$	Ratio of the lift of the wing in the presence of the body to that of the wing alone
$K_\Lambda$	Flap span factor

$K_{B(W)}$	Ratio of lift-curve slope of body in presence of wing to that of wing alone
$K_{W(B)}$	Ratio of lift-curve slope of wing in presence of body to that of wing alone
M	Mach number
NDM	No Datcom method
n	Chordwise distance from wing apex to the pitching-moment reference center measured in root chords, positive for reference center aft of apex
$\frac{q}{q_\infty}$	Average dynamic pressure ratio
Re	Reynolds number
$S_e$	Exposed wing area
$S_w$	Wing area
v	induced-drag factor
w	induced-drag factor
$X_{a.c.}$	Distance between aerodynamic center and wing apex, parallel to the MAC, positive for a.c. aft of wing apex
$\bar{X}$	Distance between a.c. and c.g., positive when c.g. is ahead of a.c.
y	Lateral coordinate measured positive to right of plane of symmetry

## GREEK SYMBOLS

$\alpha$	Angle of attack, degrees
$\alpha_{C_L \max}$	Wing angle of attack at maximum lift coefficient
$\alpha_0$	Angle of attack at zero lift
$\Delta\alpha_0$	Change in wing zero-lift angle of attack due to linear wing twist
$\beta$	Mach number parameter, $\sqrt{M^2-1}$ or $\sqrt{1-M^2}$
$\Gamma$	Dihedral angle, positive wing tips up
$\Delta$	Increment, difference between test and calculated values
$\epsilon$	Downwash angle in plane of symmetry
$\Delta\epsilon$	Downwash increment due to flaps
$\frac{\partial\epsilon}{\partial\alpha}$	Downwash gradient acting on the aft surface
$\eta$	Dimensionless span station, $\frac{y}{b/2}$
$\eta_f$	Dimensionless distance from plane of symmetry to edge of flap or control surface
$\eta_{\text{stall}}$	Spanwise location where stall will first occur on an untwisted, tapered wing
$\theta$	Linear angle of twist of wing tip with respect to root, negative for washout
$\kappa, \kappa_{av}$	Ratio of two-dimensional lift-curve slope at appropriate Mach number to $2\pi$
$\Lambda$	Surface sweep angle (positive for sweepback)
$\Lambda_\beta$	Compressible sweep parameter, $\tan^{-1} \left( \frac{\tan \Lambda_{C/4}}{\beta} \right)$
$\lambda$	Taper ratio, $\frac{C_t}{C_r}$



## COEFFICIENTS AND DERIVATIVES

$C_D$	Drag coefficient
$C_{D_L}$	Drag coefficient due to lift
$C_{D_q}$	Drag pitching derivative
$C_{D_0}$	Zero-lift drag coefficient
$C_{D_\alpha}$	Change in drag coefficient with variation in rate of change of angle of attack
$C_{h_\alpha}$	Rate of change of hinge moment with angle of attack at constant flap or control deflection
$C_{h_\delta}$	Rate of change of hinge moment with control surface deflection at constant angle of attack
$C_{h_\delta}'$	Value of derivative for zero-thickness control surface
$\Delta C_{h_\alpha}$	Increment in derivative accounting for induced-camber effects
$C_L$	Lift coefficient
$C_{L_i}$	Rate of change of lift coefficient with wing incidence
$C_{L_{max}}$	Maximum lift coefficient
$C_{L_q}$	Lift pitching derivative
$C_{L_\alpha}$	Lift-curve slope
$(C_{L_\alpha})_\delta$	Lift-curve slope of the flap-deflected wing
$C_{L_\alpha}$	Change in lift coefficient with variation in rate of change of angle of attack

# Contrails

AFWAL-TR-84-3084

$C_{L\delta}$	Rate of change of lift coefficient with wing flap deflection at constant angle of attack
$\Delta C_L$	Increment of wing lift coefficient due to flap or control surface deflection
$\Delta C_{L_{max}}$	Increment in wing maximum lift coefficient due to flap deflection
$C_\ell$	Rolling moment coefficient
$C_{\ell'_p}$	Rotary derivative
$C_{\ell'_r}$	Rotary derivative
$C_{\ell_\beta}$	Rate of change of rolling moment with sideslip angle
$C_{\ell'_\beta}$	Change in rolling moment coefficient with variation in the rate of change of sideslip angle
$C_{\ell_\delta}$	Rate of change of rolling moment with control deflection
$C_m$	Pitching moment coefficient
$C_{m_q}$	Pitching moment pitching derivative
$C_{m_0}$	Pitching moment coefficient at zero lift
$C_{m_\alpha}$	Rate of change of pitching moment coefficient with angle of attack
$C_{m'_\alpha}$	Rate of change of pitching moment coefficient with rate of change of angle of attack
$C_{m_\delta}$	Rate of change of pitching moment coefficient with rate of change of angle of attack

# Contrails

AFWAL-TR-84-3084

$\Delta C_{m_0}$	Increment in pitching moment coefficient at zero lift due to linear twist
$\frac{dC_m}{dC_L}$	Wing pitching-moment-curve slope
$C_N$	Normal force coefficient
$C_{N_\alpha}$	Rate of change of normal-force coefficient with angle of attack
$C_n$	Yawing-moment coefficient
$C_{n_p}$	Rotary derivative
$C_{n_r}$	Rotary derivative
$C_{n_\beta}$	Rate of change of yawing moment with sideslip
$C_{n_{\dot{\beta}}}$	Change in yawing moment coefficient with variation in the rate of change of sideslip angle
$\Delta C_n$	Yawing moment due to aileron deflection
$C_Y$	Side-force coefficient
$C_{Y_p}$	Rotary derivative
$C_{Y_r}$	Rotary derivative
$C_{Y_\beta}$	Rate of change of side force with sideslip angle
$C_{Y_{\dot{\beta}}}$	Change in side-force coefficient with variation in the rate of change of sideslip angle

## ABBREVIATIONS

ASW	Aft swept wing
CALC	Calculated value
c/2	Mid-chord
c/4	Quarter-chord
e	exposed
FSW	Forward swept wing
HL	Hinge line
i	Inboard
LE	Leading edge
o	outboard
TEST	Tested value
TE	Trailing edge
W	Wing
WB	Wing-body

## INTRODUCTION

When the USAF Stability and Control Datcom (Reference 1) was first being written, forward swept wing designs were not seriously considered and so were generally ignored in that text's prediction methodologies. Since then, advances in material technology has made sweptforward wings a viable design option, thus mandating the validation of Datcom relations and charts for sweptforward wing configurations.

A broad data search was begun in August of 1980 which eventually netted numerous configurations tested at speeds from low subsonic to supersonic. Interestingly, the majority of the data came from NACA in the 1946-49 time period. Pre-World War II drag data were also located for several German planforms.

The method of validation was performed in the following manner. The foundation of each of the Datcom methods was reviewed to determine its applicability to negative sweep angles. If the methodology appeared to be applicable, comparisons were made between calculated and wind tunnel tested values for those coefficients where data existed. Good agreement indicated that no major modifications were necessary. Poor agreement dictated a review of the methodology and its source, continuing for as many iterations as necessary to improve method accuracy. The situations where no tunnel data were located are so noted and the methodologies should be used with care. In some instances the methodology was not substantiated with test data. This was because those relations were strongly dependent on other methodologies whose results had already been correlated with test data (The wing-body-tail methods are an example, being made up of wing, wing-body and wing-wing relations).

The results of those validation efforts are contained herein and are presented in a format that the Datcom user will find most useful. The appendix lists the modifications necessary to enable the prediction of forward swept wing stability and control characteristics with the Datcom. The tables located in back of the report are similar to the Datcom tables and give the designer an idea of overall method accuracy.

4.1 WINGS AT ANGLE OF ATTACK

4.1.3.1 Wing Zero-Lift Angle of Attack

A. Subsonic

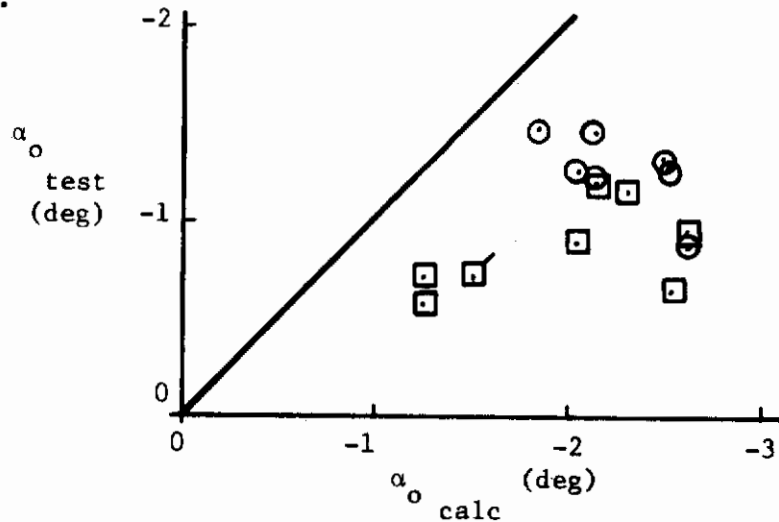
Datcom Equation 4.1.3.1-b,

$$(\alpha_0)_{\theta=0} = \tan^{-1} \left[ \tan (\alpha_0)_{\theta=0} \frac{1}{\cos \Lambda} \right] \quad (1)$$

which is used to correct the airfoil zero-lift angle of attack for sweep, was found to consistently overestimate the true angle for both aft- and forwardswept wings (Figure 1a). A new sweep correction equation,

$$(\alpha_0)_{\theta=0} = (\alpha_0)_{\theta=0, \Lambda=0} \cos^2 \Lambda \quad (2)$$

was developed and gave better agreement with test data than Equation 1 did (Figure 1b). It is recommended that Equation 2 be used in place of Datcom Equation 4.1.3.1-b, (Equation 1).



(a) Current Datcom Method

- Sweptback
- Sweptforward

Note: Flagged values denote wing twist

Figure 1. Zero-Lift Angle of Attack Correlation

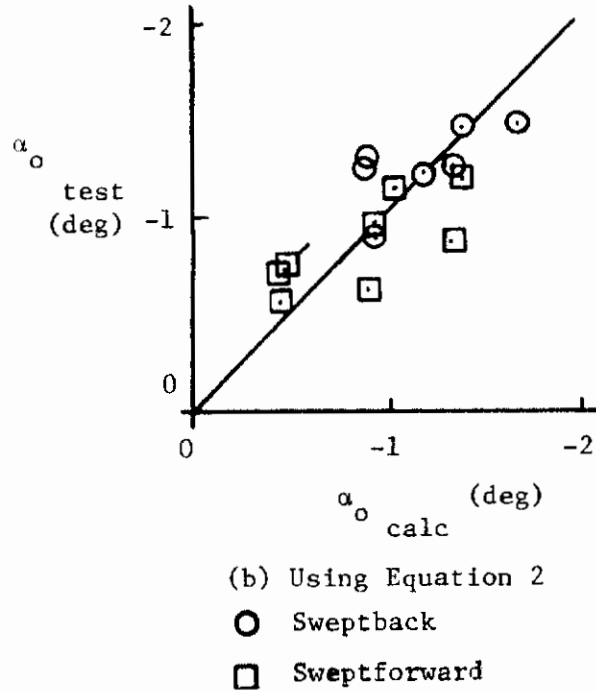


Figure 1. Zero-Lift Angle of Attack Correlation

The twist effect charts (Datcom Figure 4.1.3.1-4), developed by DeYoung and Harper (Reference 2), permitted estimation of twist effects for unswept and aft swept wings only. Following the procedure outlined in Reference 2, sweptforward wing twist effect factors were obtained. Expanded charts are presented in Figure 2 for taper ratios of 0.0 (Figure 2a), 0.5 (Figure 2b) and 1.0 (Figure 2c). As was the case for unswept and aft swept wings, insufficient data were found to substantiate the theoretical results.

#### B. Transonic

No Datcom method.

#### C. Supersonic

No Datcom method.

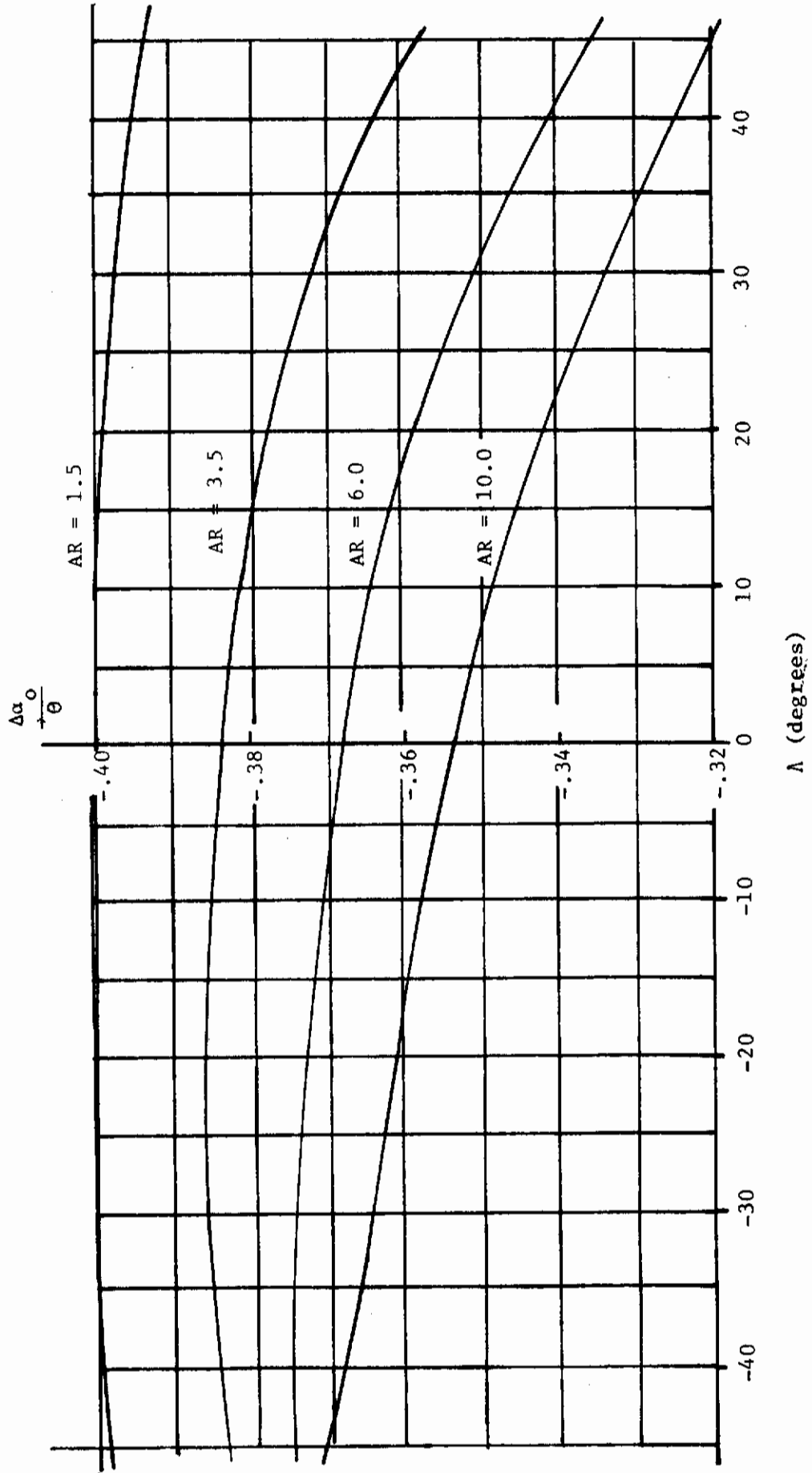
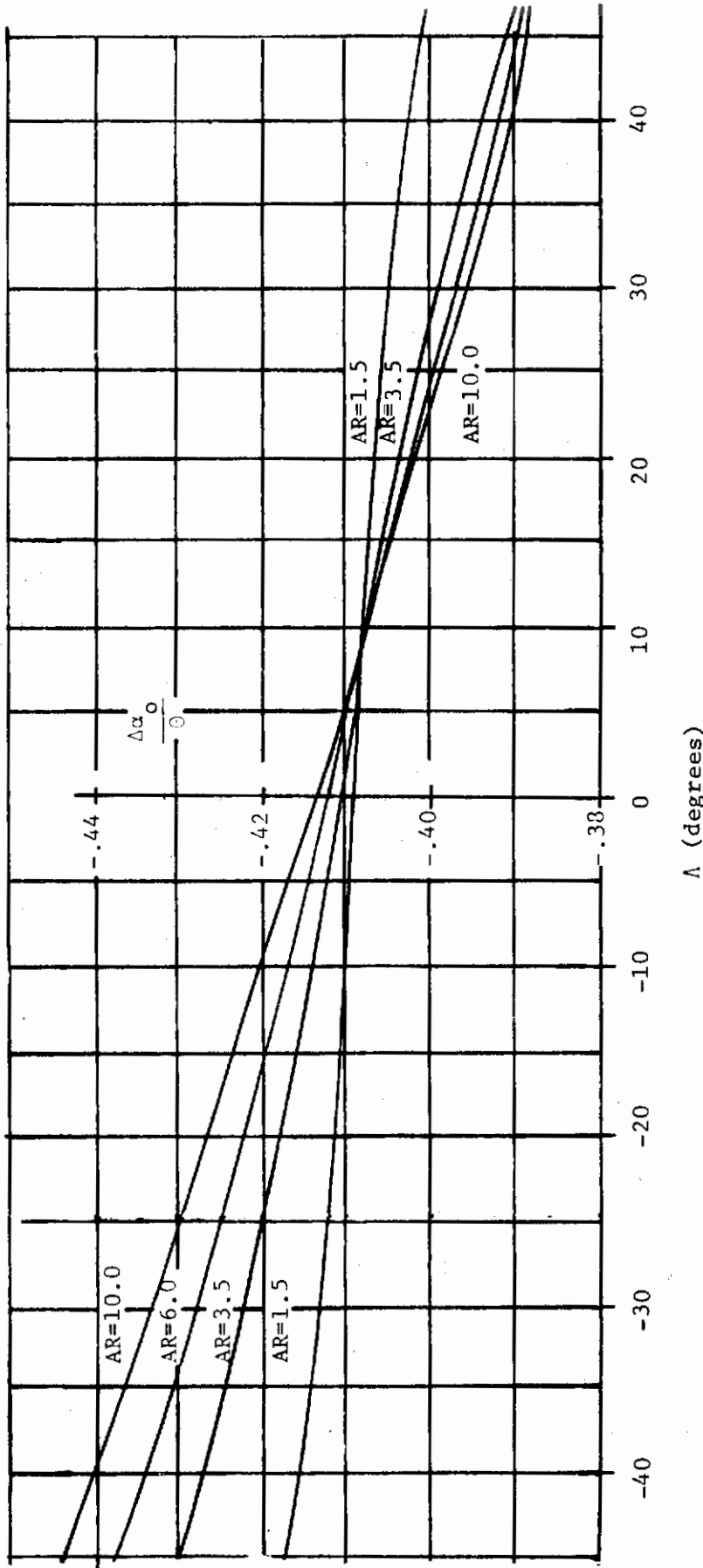


Figure 2. Effect of Linear Twist on Wing Zero-Lift Angle of Attack  
 a) Taper Ratio = 0.0





(b) Taper Ratio = 0.5

Figure 2. Effect of Linear Twist on Wing Zero-Lift Angle of Attack

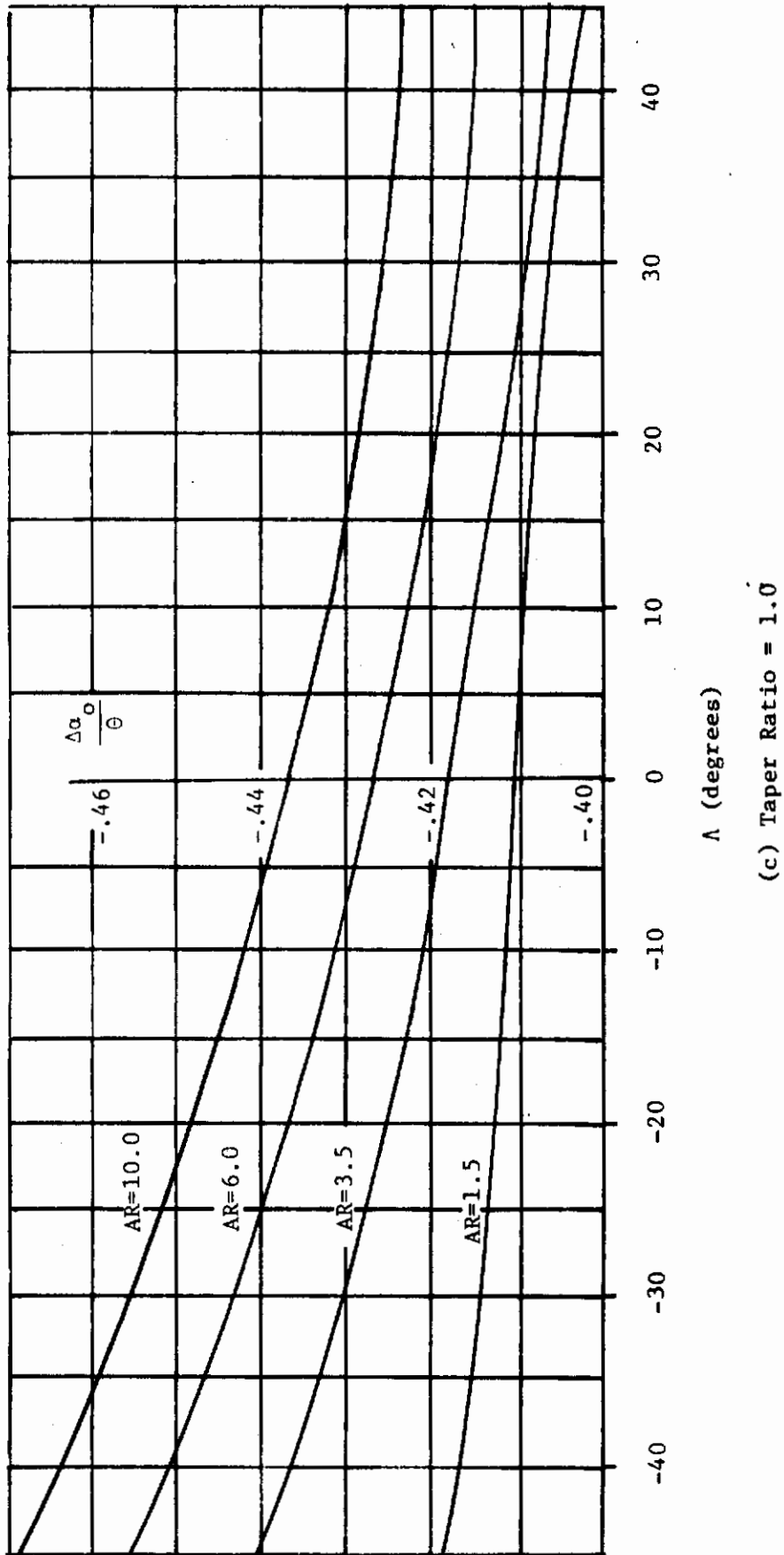


Figure 2. Effect of Linear Twist on Wing Zero-Lift Angle of Attack

## 4.1.3.2 WING LIFT-CURVE SLOPE

## A. Subsonic

Method 1 required no modifications to predict the sweptforward wing lift-curve slope. Good agreement (5.85% average error) was noted between predicted and test values. Table 1 contains a description of the planforms evaluated and the test and predicted lift curve slopes.

Method 2 is unsuitable for sweptforward planforms and should not be used.

## B. Transonic

No sweptforward-leading-edge wing-alone data were found but sufficient wing-body data were located to enable validation of the wing-alone prediction methodologies through wing-body analyses.

The absolute value of the mid-chord sweep angle should be used in Datcom Figure 4.1.3.2-53b, "Transonic Sweep Correction ...". No other modifications are necessary to predict transonic lift-curve slopes. Typical wing-body correlations between test and predicted lift-curve slopes are shown in Figure 3.

## C. Supersonic

Through the use of the reversibility theorem, the normal-force-curve slope of sweptforward planforms can be obtained from Datcom Figures 4.1.3.2-56a through -56f, "Wing Supersonic Normal-Force-Curve Slope", by inserting the absolute value of the trailing-edge sweep angle wherever the leading-edge sweep angle is called for. For

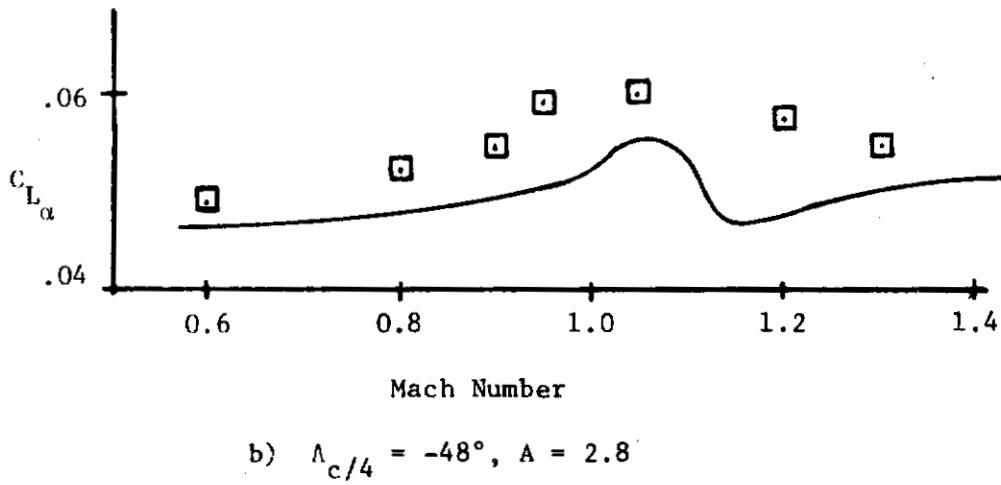
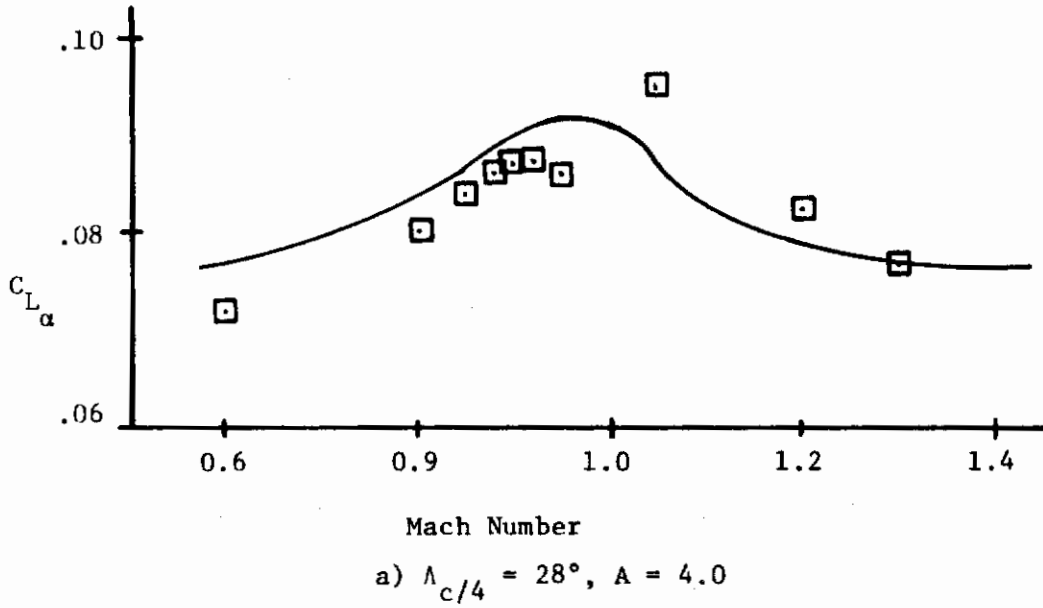


Figure 3. Transonic Wing-Body Lift-Curve Slope Correlation

AFWAL-TR-84-3084

sweptforward wings approaching the sonic-leading-edge condition, the absolute value of the leading-edge sweep angle should be used in Datcom Figure 4.1.3.2-60, "Supersonic Wing Lift-Curve-Slope Correction Factor..."

As was the case at transonic speeds, no wing-alone data were found, but wing-alone methods were validated through wing-body analysis. Wing-body results gave very good correlation (4.79% average error) with data. Table 2 contains a description of the planforms evaluated and their test and predicted normal-force-curve slopes.

#### D. Hypersonic

No data were found in this speed regime.

As the hypersonic methodology uses Datcom Figures 4.1.3.2-56a through -56f, the comments of Paragraph C are relevant here.

## 4.1.3.3 WING LIFT IN THE NONLINEAR ANGLE-OF-ATTACK RANGE

## A. Subsonic

The "General Method for Wings of Any Aspect Ratio" should be used to estimate forward swept wing lift in this angle of attack range. The absolute value of the leading-edge sweep angle should be used to obtain wing-shape parameter  $J$ . Table 3 shows good agreement (6.67% mean error) between estimated and test lift coefficients.

An occasional abnormality was noted for values of wing-shape parameter  $J$  greater than 1. This abnormality, the prediction of a false maximum lift peak, was explored by Williams and Vukelich (Reference 3). They suggest that when the false peak occurs, one replace the predicted lift values in the range between the angle of attack at which the lift curve slope ceases to be linear and the estimated angle of attack for maximum lift with a second-order polynomial such that the slope is zero at the maximum lift angle of attack. While this suggestion was not implemented, it would have reduced the 6.67% error noticeably. No other modifications are required other than those described in Paragraph A of Section 4.1.3.4, "Wing Maximum Lift".

No data were found for normal force at angles of attack beyond the stall. The modifications mentioned above should be sufficient to provide predictions of the normal force at post-stall angles of attack with accuracy comparable to aftswept wing results.

## B. Transonic

While no data were found for this speed range, the absolute value of the leading-edge sweep angle should be used in all equations as well as in Datcom Figures 4.1.3.3-59a, "Thickness Correction Factor ..." and 4.1.3.3-59b, "Supersonic Lift Variation ...". The modifications described in Paragraph C of Section 4.1.3.2, "Wing Lift-Curve Slope" should be utilized when estimating the wing normal-force-curve slope.

**C. Supersonic**

While no data were found for this speed range, the absolute value of the leading edge sweep angle should be used in all equations and in Datcom Figures 4.1.3.3-59a, "Thickness Correction Factor ..." and 4.1.3.3-59b, "Supersonic Lift Variation ...". The modifications described in Paragraph C of Section 4.1.3.2, "Wing Lift-Curve Slope" should be utilized when estimating the wing normal-force-curve slope.

**D. Hypersonic**

No modifications are required to predict the normal-force curve for this speed range other than those described in Paragraph C of this section and Paragraph D of Section 4.1.3.2, "Wing Lift-Curve Slope".

## 4.1.3.4 WING MAXIMUM LIFT

## A. Subsonic

Method 1 requires use of a wing spanwise-loading computer program. No modifications are required to the steps outlined in order to estimate maximum lift characteristics. However, the equation

$$\eta_{\text{stall}} = 1 - \lambda \quad (3)$$

(Datcom Equation 4.1.3.4-a), used to approximate the spanwise location where stall will first occur, should be applied cautiously, as stall tends to occur more inboard on forward swept wings than on aft swept wings.

Method 2 is an empirical relation for high-aspect-ratio wings. To estimate sweptforward maximum lift characteristics, the absolute value of the leading-edge sweep should be used in Datcom Figures 4.1.3.4-21a, "Subsonic Maximum Lift ..."; 4.1.3.4-21b, "Angle-of-Attack Increment ..."; and 4.1.3.4-22, Mach Number Correction ...". Modifications described in Section 4.1.3.1, "Wing Zero-Lift Angle of Attack", should be applied when estimating the zero-lift angle of attack.

Good agreement with test data was noted for the configurations analyzed. The average maximum lift coefficient error was 4.80% and the average error of the angle of attack for maximum lift coefficient was 2.45%. Table 4 contains a summary of the planform parameters with the test and estimated maximum lift characteristics.

Method 3, also empirical, is for low-aspect-ratio wings. Sweptforward wing maximum lift characteristics estimates can be obtained by using the absolute value of the leading-edge sweep angle in Datcom Figures 4.1.3.4-24a, "Maximum-Lift Increment..." and 4.1.3.4-25b, "Angle-of-Attack Increment...". Only one sweptforward planform was found for this class of aspect ratio. Estimation error was 15.70% for the maximum lift coefficient and 8.20% for the angle of attack for maximum lift coefficient.

The remaining planforms analyzed had borderline-aspect-ratio wings. Maximum lift characteristics were obtained by averaging results obtained from Methods 2 and 3. Average error was 5.55% in predicting the maximum lift coefficient and 5.55% in estimating the angle of attack for maximum lift coefficient.



Table 4 shows planform parameters along with test and predicted maximum lift values for the three aspect-ratio classifications.

The effect of Reynolds number was very noticeable in terms of method accuracy (Figure 4). Above a value of 2 million (based on mean aerodynamic chord length) good agreement was noted with Datcom estimates. Below that Reynolds number, however, the Datcom predictions correlated poorly with test results. Due to the many variables in wind tunnel testing (i.e., application and location of grit, inherent tunnel turbulence, etc), users of the Datcom maximum lift methodologies can only be alerted to discrepancies that may exist between test and predicted maximum lift values at lower Reynolds numbers.

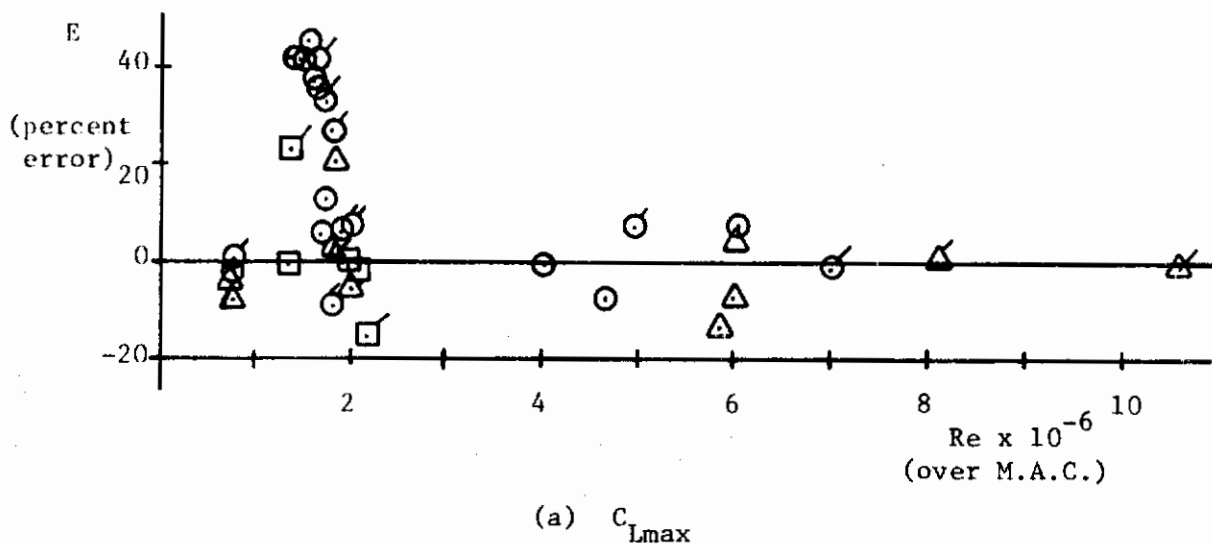


Figure 4. Effect of Reynolds Number on Maximum Lift Method

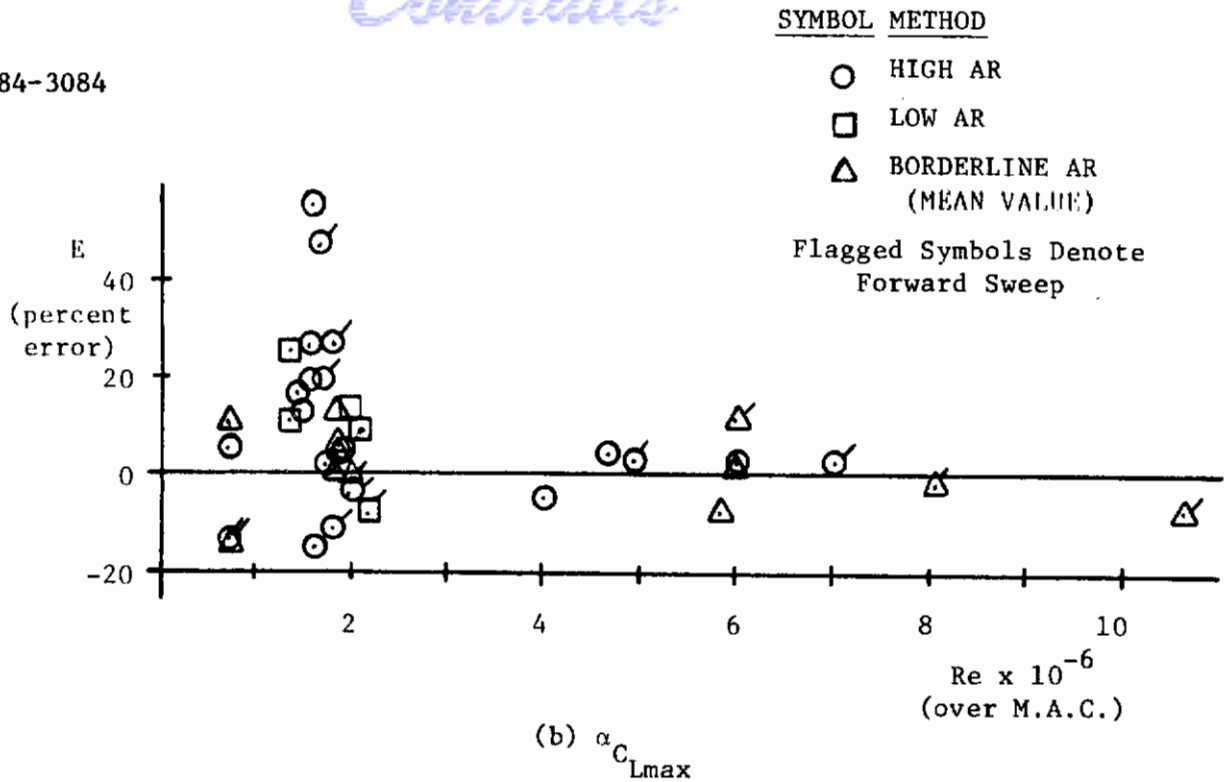


Figure 4. Effect of Reynolds Number on Maximum Lift Method

**B. Transonic**

The comments pertaining to Method 3 above are pertinent here. Also, the absolute value of the leading-edge sweep angle should be used in Datcom Figure 4.1.3.4-26b, "Maximum-Lift Correction Factor". No data were found in this speed range.

**C. Supersonic**

The comments in Paragraph C of Sections 4.1.3.2, "Wing Lift-Curve Slope" and 4.1.3.3, "Wing Lift in the Nonlinear Angle-of-Attack Range" are appropriate here. No other modifications are necessary.

No data were found in this speed range.

**D. Hypersonic**

The comments in Paragraph C of this section are appropriate here.

No data were found in this speed range.

## 4.1.4.1 WING ZERO-LIFT PITCHING MOMENT

## A. Subsonic

No modifications to the equations of Method 1 are required. The twist effect charts (Datcom Figure 4.1.4.1-5) were limited to unswept and aft swept wings. Charts based on DeYoung and Harper (Reference 2), expanded to include forward sweep, are presented in Figure 5 for taper ratios of 0.0 (Figure 5a), 0.5 (Figure 5b) and 1.0 (Figure 5c).

Insufficient data were found to substantiate the twist effect charts but eight planforms were available to validate the equations. The average difference between the test and predicted zero-lift pitching moment was 0.0030. Table 5 contains a summary of the planform parameters and the test and predicted pitching-moment values.

Method 2 is totally unsuited to forward-swept-wing planforms and should not be used.

*Contracts*

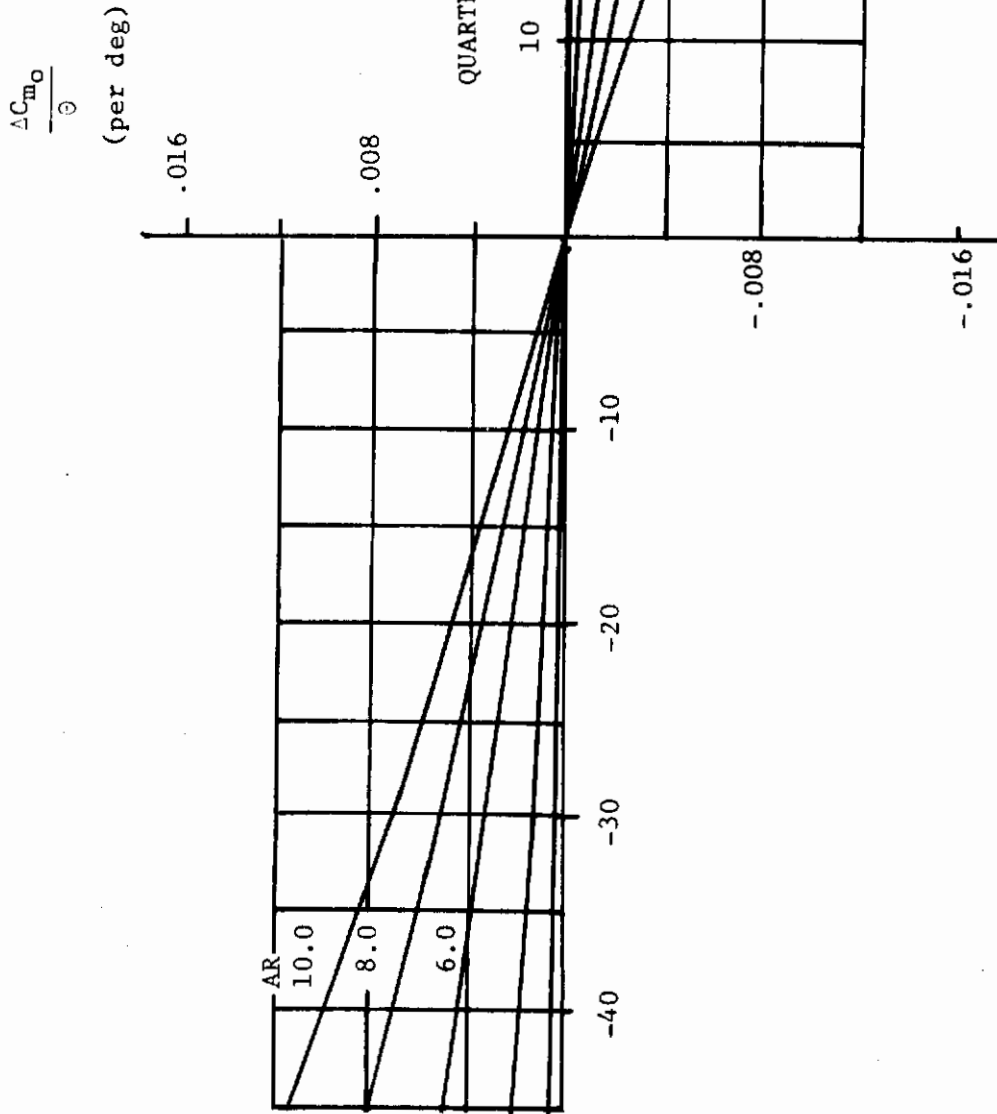
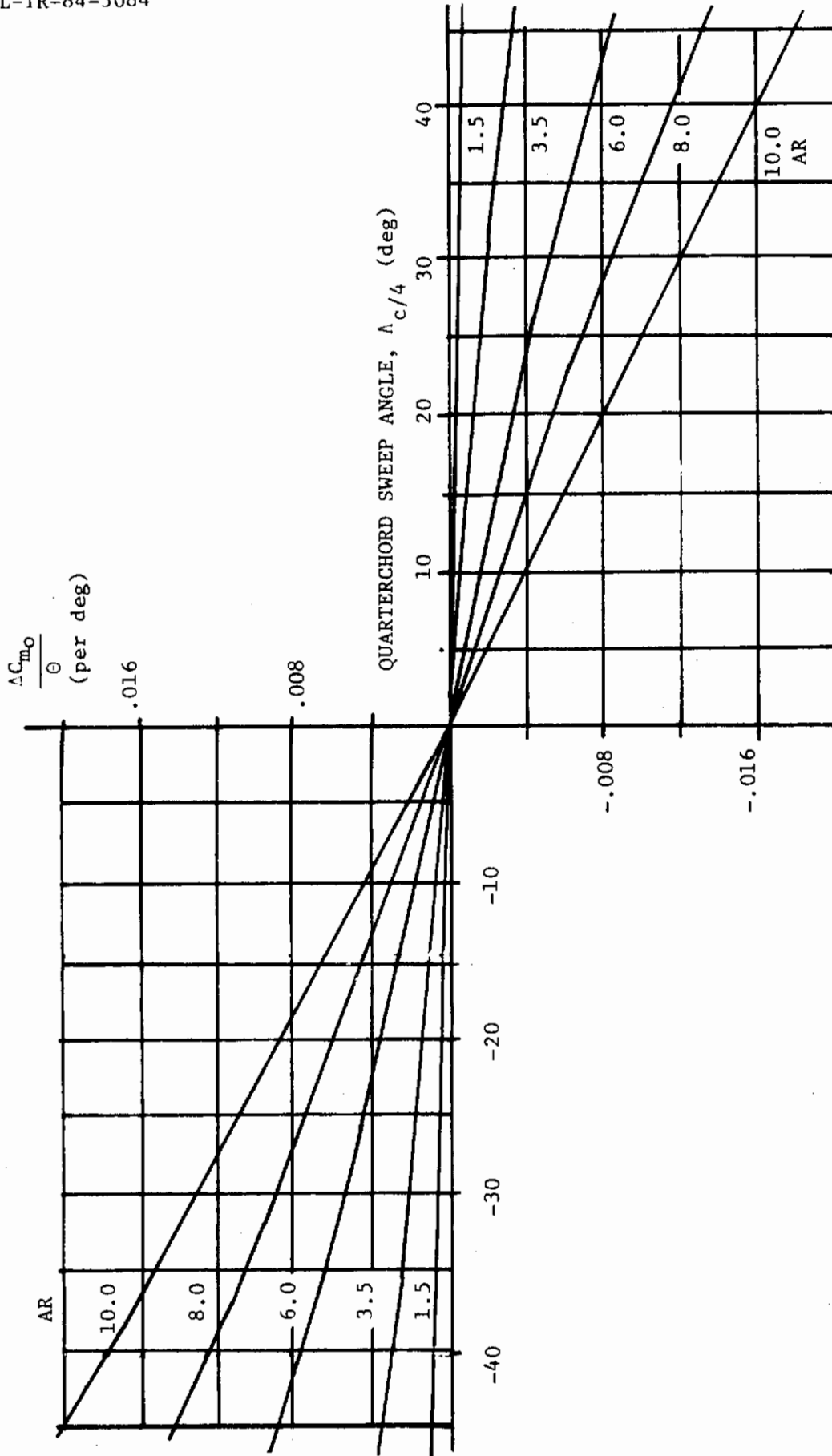


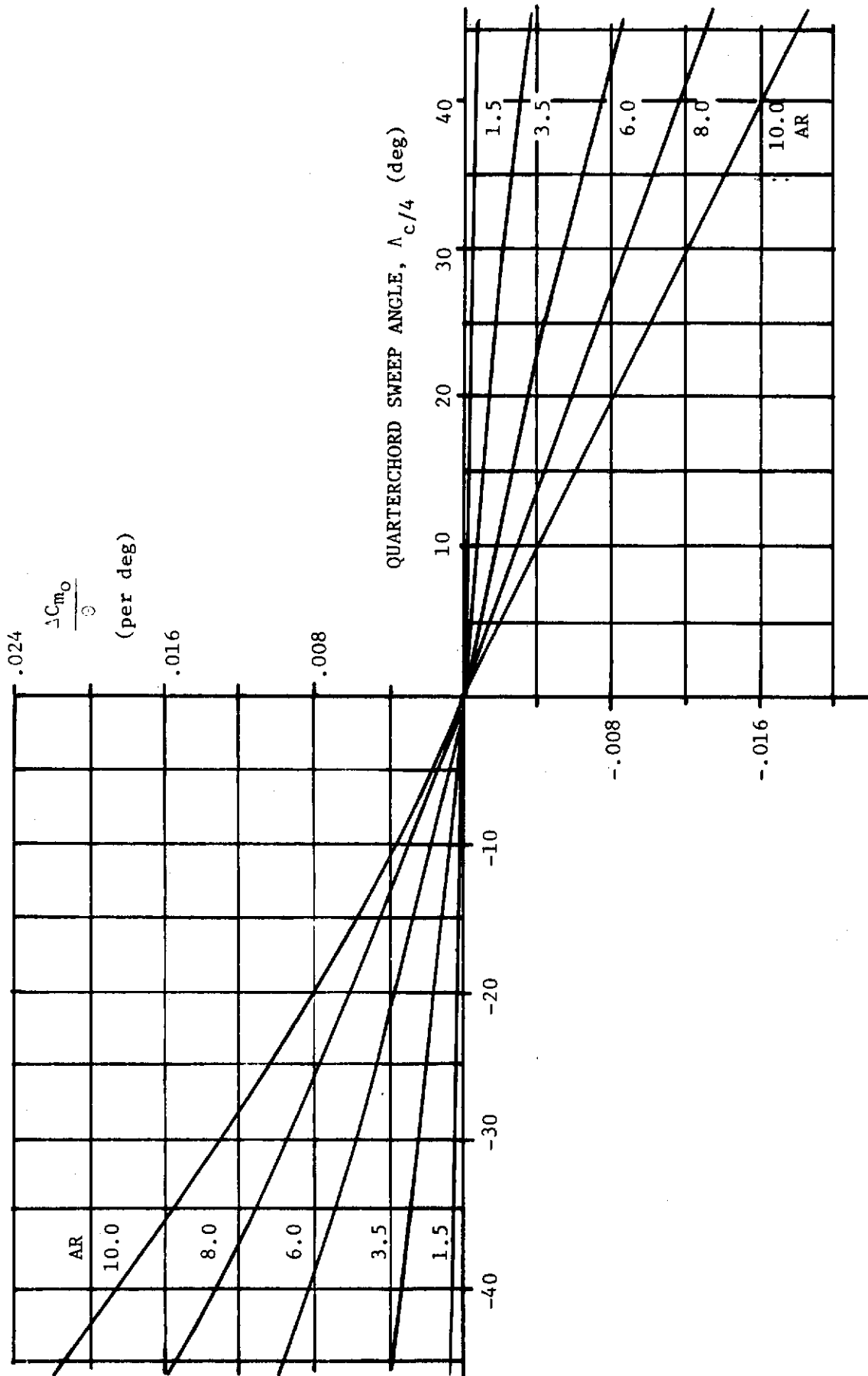
Figure 5. Effect of Linear Twist on Wing Zero-Lift Pitching Moment

a) Taper Ratio = 0.0



b) Taper Ratio = 0.5

Figure 5. Effect of Linear Twist on Wing Zero-Lift Pitching Moment



c) Taper Ratio = 1.0

Figure 5. Effect of Linear Twist on Wing Zero-Lift Pitching Moment

AFWAL-TR-84-3084

B. Transonic

No Datcom method.

C. Supersonic

No Datcom method.

## 4.1.4.2 WING PITCHING-MOMENT-CURVE SLOPE

## A. Subsonic

Estimation of the wing pitching-moment-curve slope is accomplished by using Datcom Equation 4.1.4.2-a

$$\frac{dC_m}{dC_L} = \left( n - \frac{x_{a.c.}}{c_r} \right) \frac{c_r}{\bar{c}} \quad (4)$$

While  $n$ ,  $c_r$ , and  $\bar{c}$  are planform dependent,  $\frac{x_{a.c.}}{c_r}$  is

obtained from Datcom Figures 4.1.4.2-26a through -26f, "Wing Aerodynamic-Center Position". The aerodynamic-center locations given by those charts are for aft swept wings only. Figure 6a through 6f should be used for sweptforward wing analysis. These charts were constructed by using a vortex-lattice computer code.

An average difference of 6.25% of the root chord was noted between test and predicted results using Method 1. Method 2 is totally unsuited for sweptforward wings and should not be used. Table 6 contains a summary of the planforms analyzed with their parameters, and predicted and test aerodynamic center locations.

## B. Transonic

The methods of this section are based entirely on aft swept wing data and should not be used to estimate sweptforward wing characteristics. No method is presented to estimate transonic forward sweptwing aerodynamic-center characteristics.



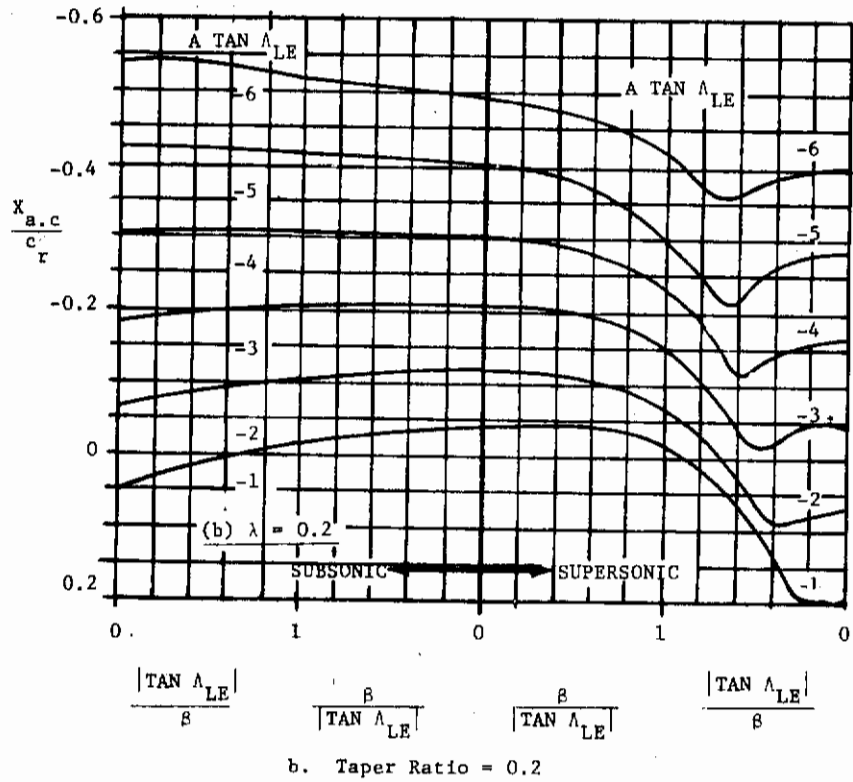
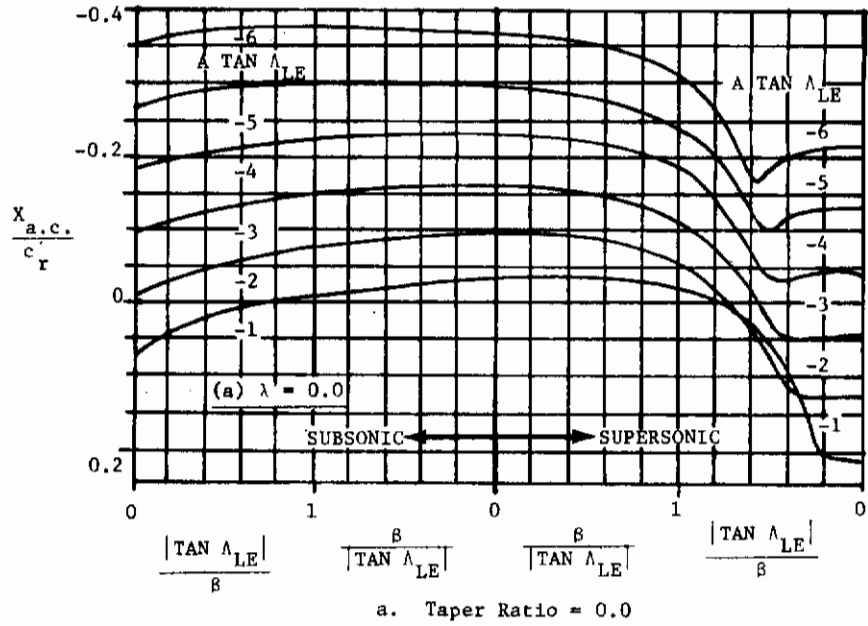


Figure 6. Wing Aerodynamic-Center Position

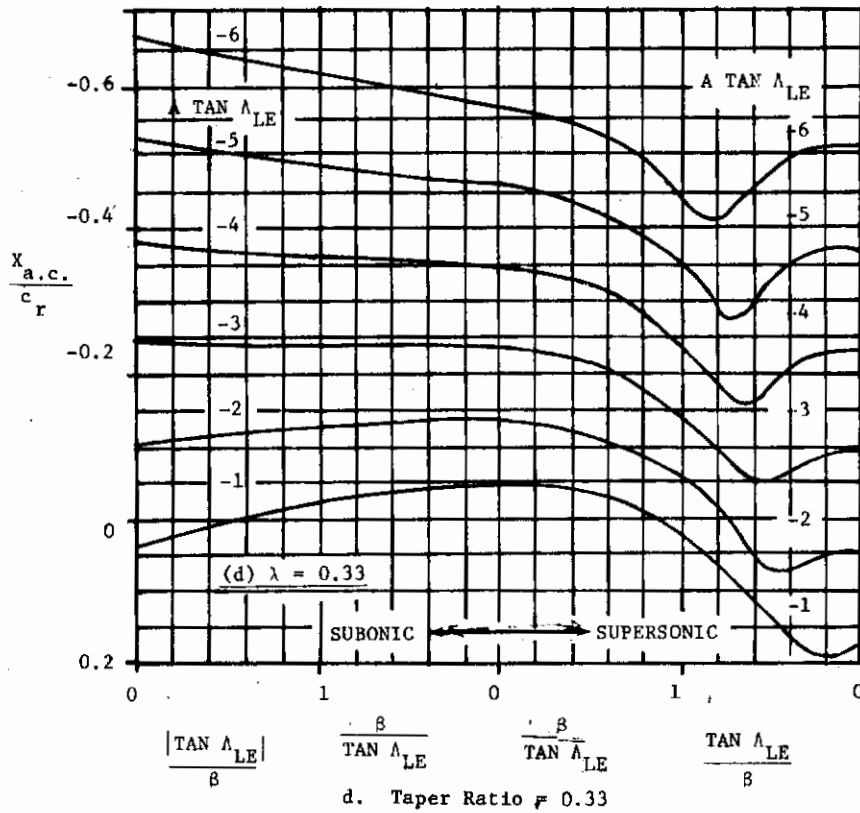
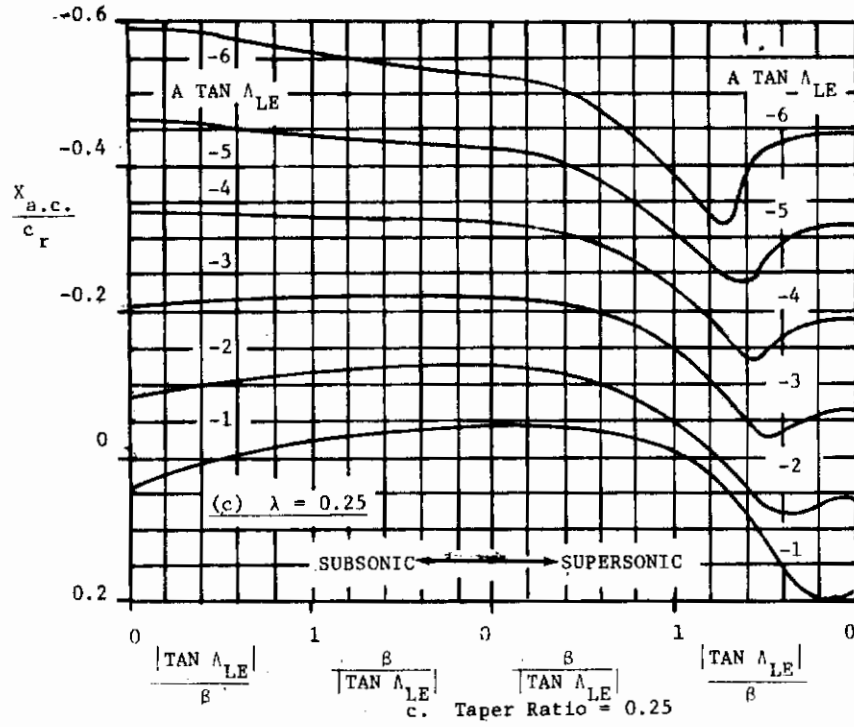
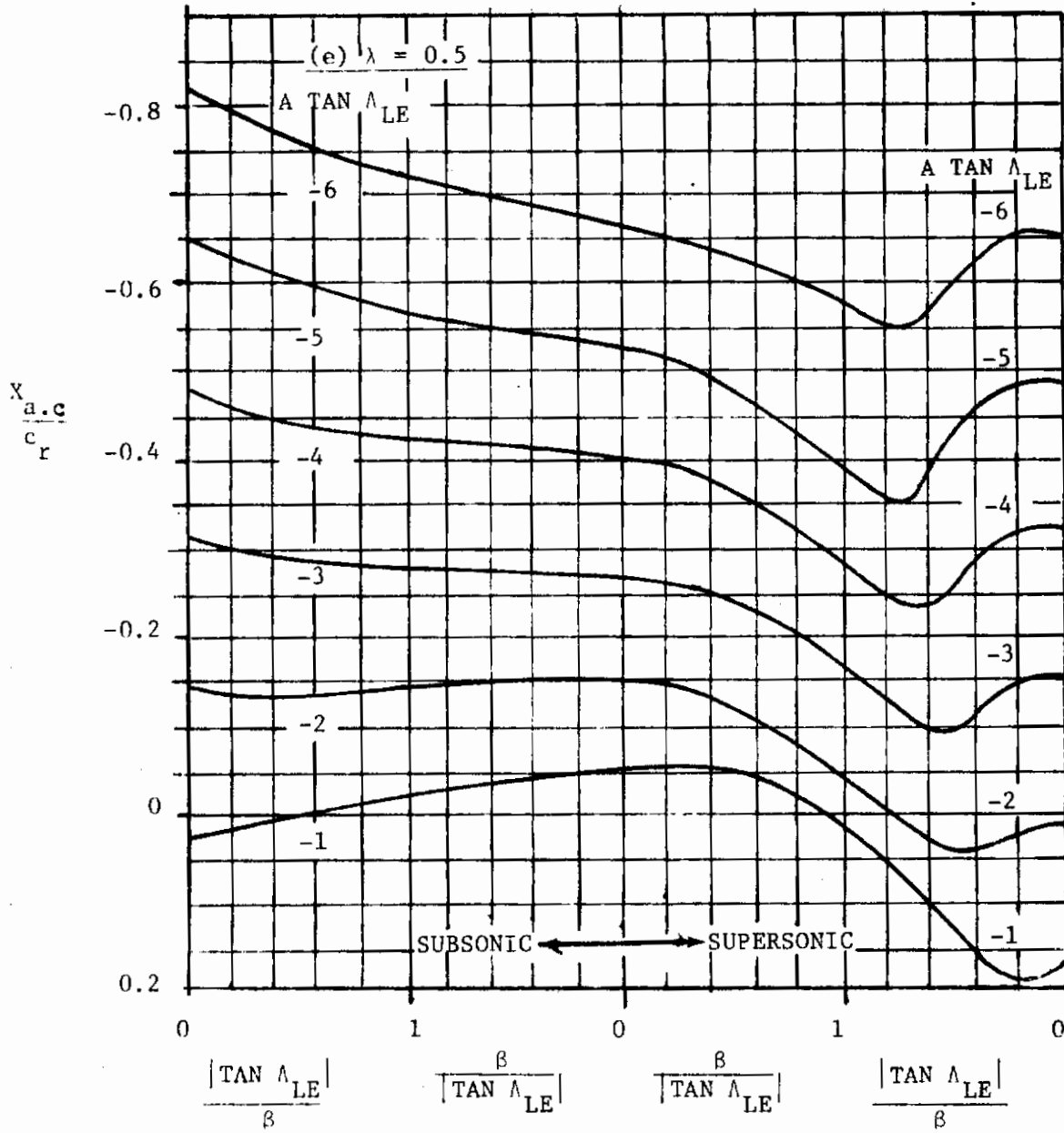
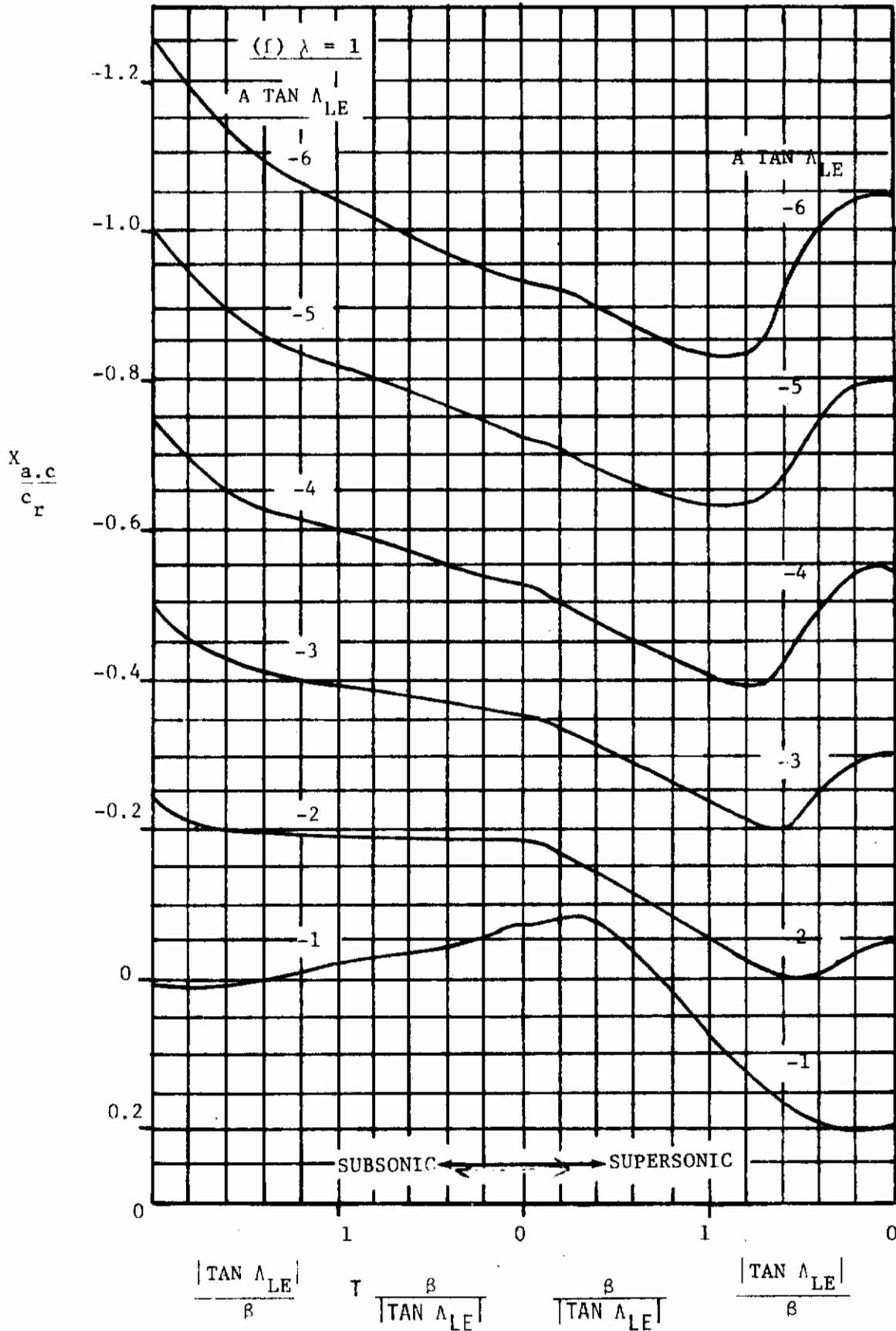


Figure 6. Wing Aerodynamic-Center Position



e. Taper Ratio = 0.5

Figure 6. Wing Aerodynamic-Center Position



f. Taper Ratio = 1.0

Figure 6. Wing Aerodynamic-Center Position

## C. Supersonic

The method discussed in Paragraph A of this section is also applicable to the supersonic speed range.

While no wing-alone data were found at this speed, wing-body prediction results showed fair agreement with test data, the average difference being 10.29% of the root chord. Table 7 contains a summary of the planforms analyzed, their parameters, and the test and predicted aerodynamic-center location.

## D. Hypersonic

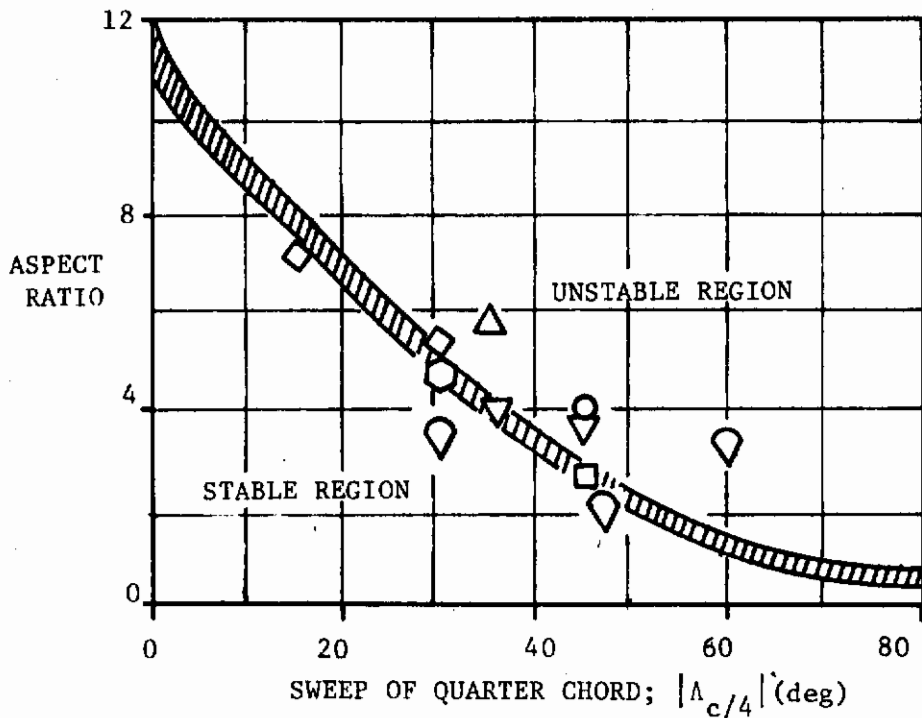
No data were found at this speed.

The method discussed in Paragraph A of this section is applicable in the hypersonic speed range. Values for  $\frac{x_{a.c.}}{c_r}$  would come from the extreme right-hand side of Figures 6a through 6f.

### 4.1.4.3 WING PITCHING MOMENT IN THE NONLINEAR ANGLE-OF-ATTACK RANGE

**A. Subsonic**

The methods presented in this section are empirical, based entirely on an aft swept wing data base. All attempts to predict sweptforward wing characteristics with any accuracy failed. However, as Figure 7 shows, overall trends can be obtained from Datcom Figure 4.1.4.3 -25, "Empirical Pitch-Up Boundary", by using the absolute value of the quarter-chord sweep angle.



Symbol	REF	$\Lambda_{c/4}$	ASPECT RATIO	$\lambda$	TESTED PITCH	CHART PITCH
⊙	RM L50F16	-45	4.00	.60	UP	UP
◻	RM L8G19	-45	2.61	1.00	DOWN	NEUTRAL
◊	RM L8H31	-30	5.36	.40	UP	UP
		-15	7.15	.45	DOWN	DOWN
◄	RM L9H18a	-32	5.79	.39	UP	UP
◄	RM L52D16	-45	3.55	.50	UP	UP
◊		-36	3.94	.63	DOWN	NEUTRAL
◊	RM A6K15	-30	4.69	.40	DOWN	NEUTRAL
◊	RM L7D23	-30	3.60	.35	DOWN	DOWN
		-47	2.10	.40	DOWN	DOWN
		-60	3.00	1.00	UP	UP

Figure 7. Datcom Figure 4.1.4.3-25, "Empirical Pitch-Up Boundary"

B. Transonic

No sweptforward wing method is presented. Do not use the existing Datcom method.

C. Supersonic

No sweptforward wing method is presented. Do not use the existing Datcom method.

## 4.1.5.1 WING ZERO-LIFT DRAG

## A. All Speeds

No modifications to the Datcom methods are required in any speed range. Table 8 contains a description of the planforms analyzed and their test and predicted values. As no transonic wing-along data were found, wing-body data and results are presented.

At subsonic speeds, the average difference between predicted and test drag values was .00855 (or 85.5 counts). At transonic speeds the difference was .02298 (229.8 counts) and at supersonic speeds the average difference was .03938 (393.8 counts). While these results are adequate for stability and control purposes, they should not be used for performance estimations.



## 4.1.5.2 WING DRAG AT ANGLE OF ATTACK

## A. Subsonic

Datcom Equation 4.1.5.2-h,

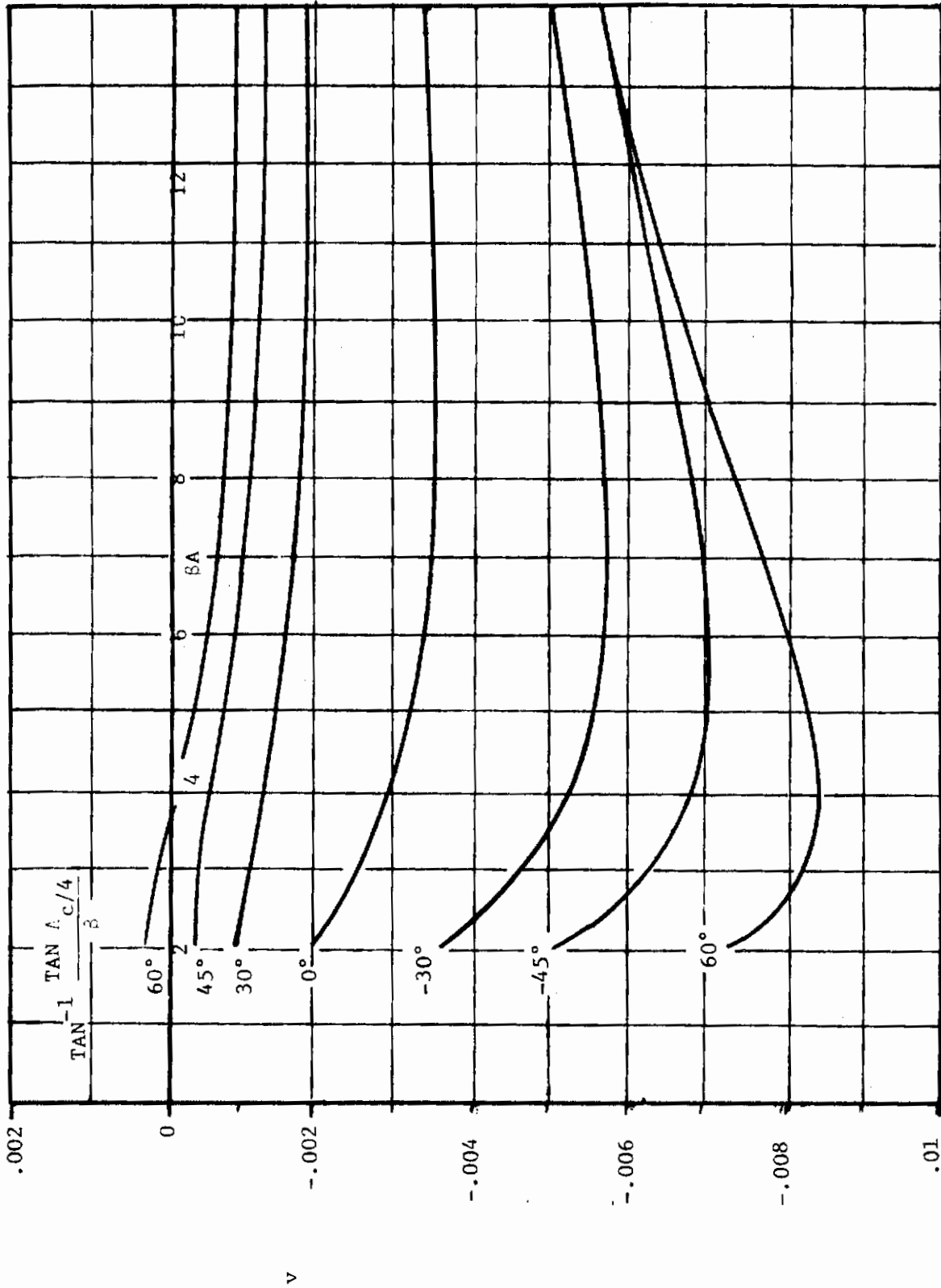
$$C_{D_L} = \frac{C_L^2}{\pi A e} + C_L \theta C_{l_{\alpha}} V + (\theta C_{l_{\alpha}})^2 w \quad (5)$$

is used to estimate wing drag at subsonic speeds. The absolute value of the designated sweep angle is used to obtain values of the span-efficiency factor  $e$  and zero-lift drag-due-to-twist factor,  $w$ . The induced-drag-due-to-twist factor  $v$ , should be obtained from Figure 8 for sweptforward wings. Figure 8 was developed from the methodologies outlined by Lundry in Reference 4. His work appears in the Datcom as Figures 4.1.5.2-42, "Lift-Dependent Drag Factor..." and 4.1.5.2-48, "Zero-Lift Drag Factor...".

An average difference between test and predicted values of 58.2 counts (.00582) was noted for the configurations studied. While this is adequate for stability and control purposes, performance estimates should not be based on Datcom predicted results. Table 9 contains a summary of the planforms examined, their parameters, and predicted and test drag values.

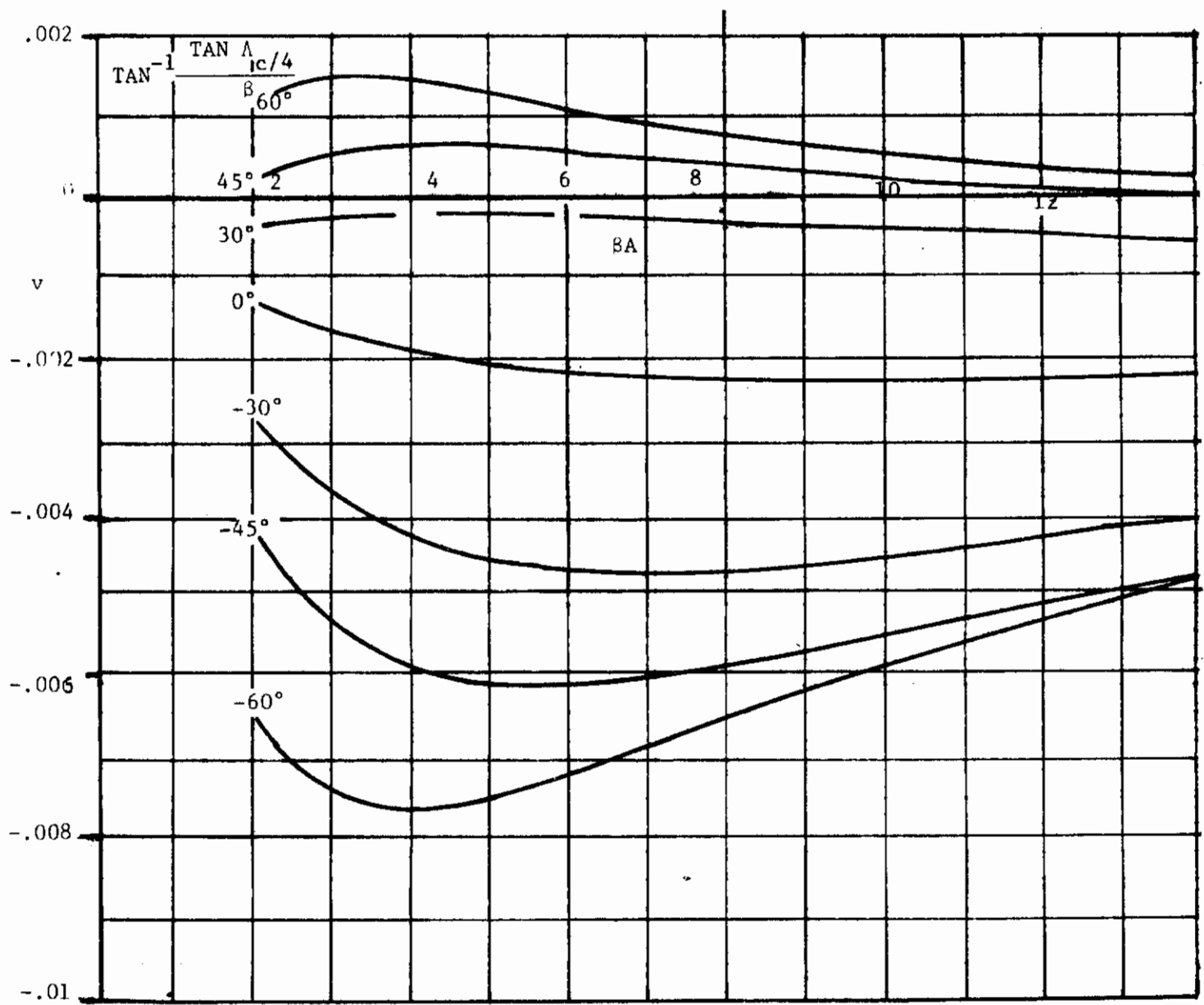
## B. Transonic

The methodology in this speed range is entirely empirical, based on aft swept wing data. Accuracy sufficient for stability and control analyses (average difference of 188.8 counts) was obtained for several sweptforward wing configurations by using the absolute value of the leading-edge sweep angle in Datcom Figure 4.1.5.2-55, "Transonic Drag Due to Lift".



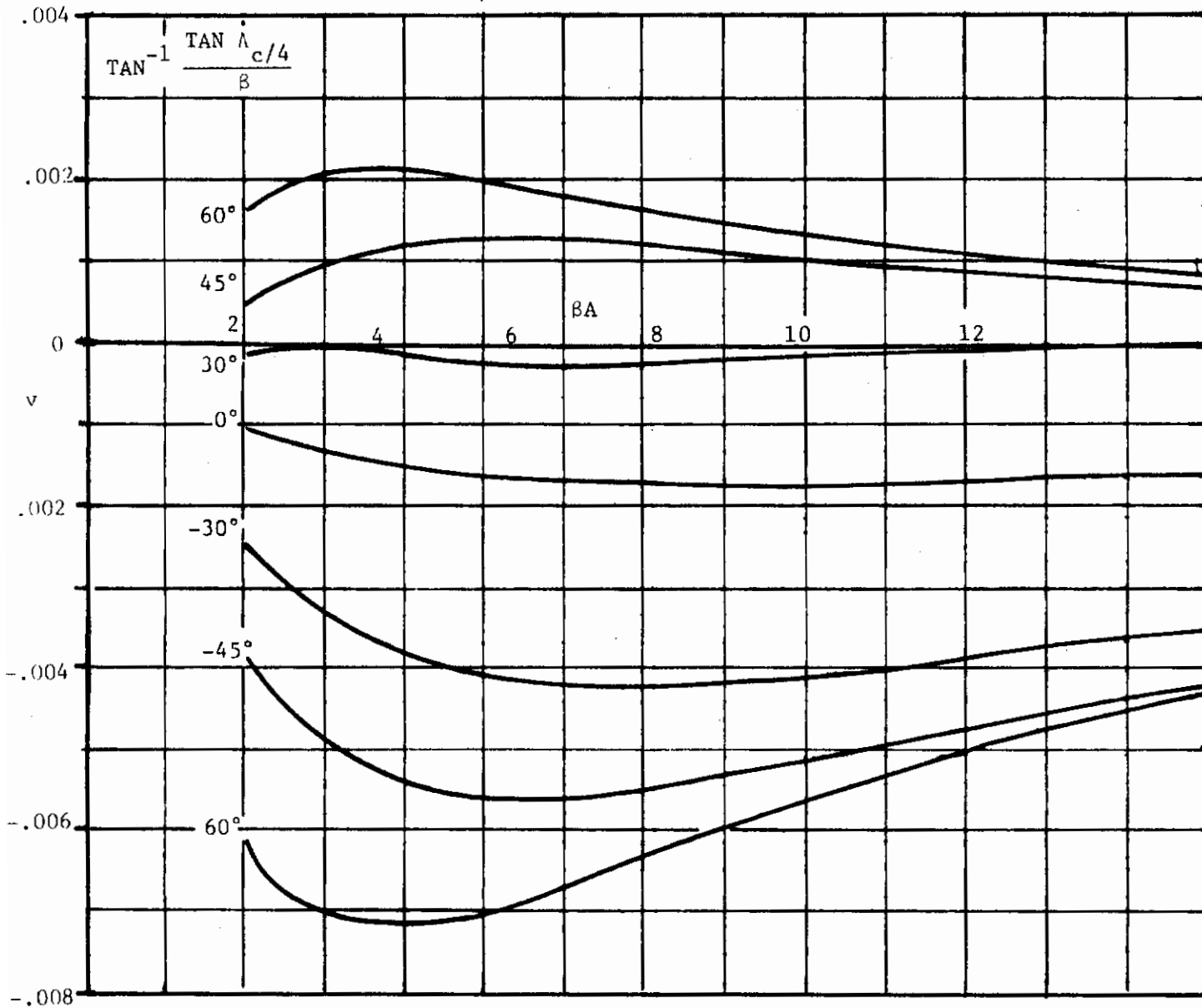
a. Taper Ratio = 0.1

Figure 8. Lift-Dependent Drag Factor Due to Linear Twist



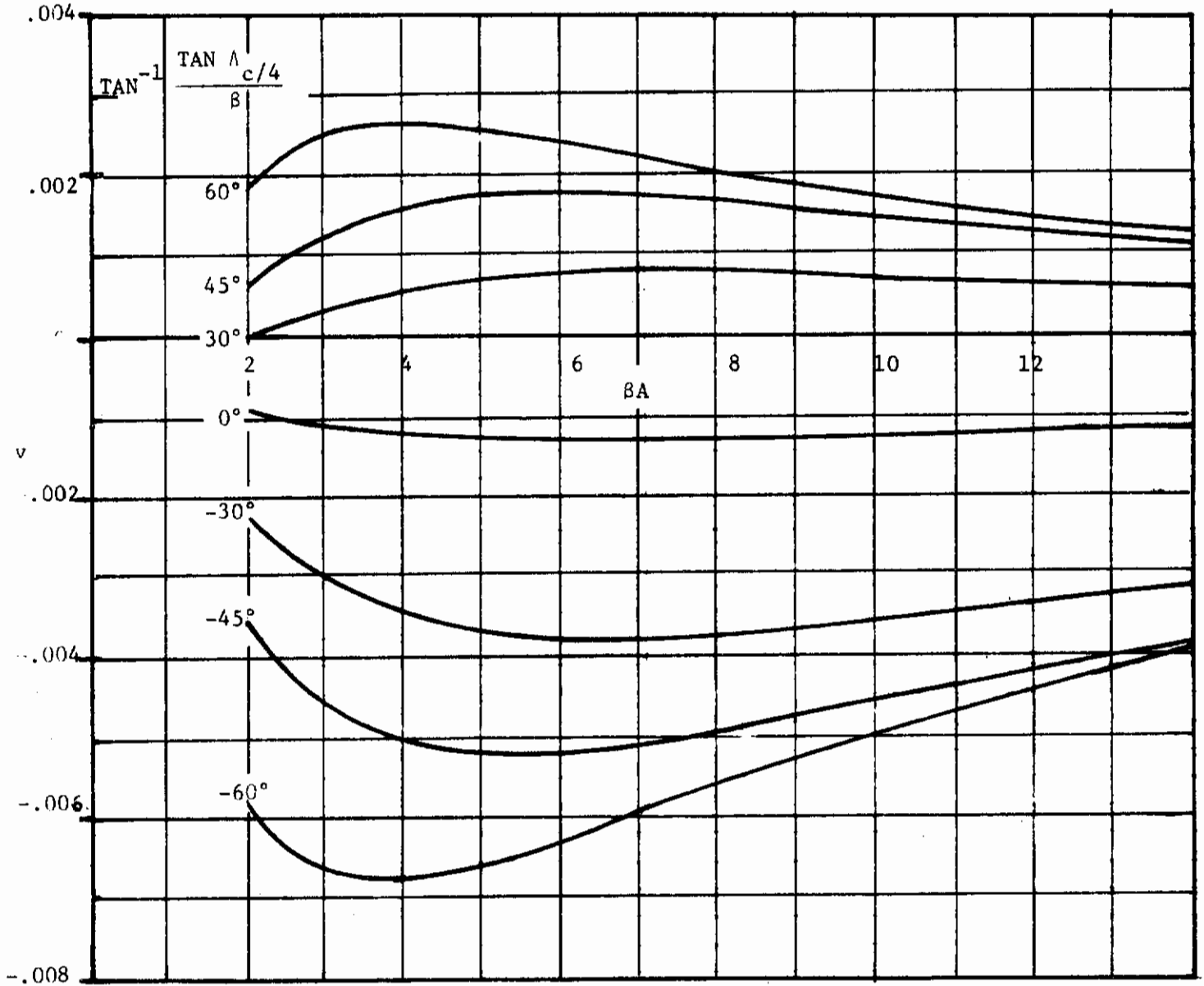
b. Taper Ratio = 0.2

Figure 8. Lift-Dependent Drag Factor Due to Linear Twist



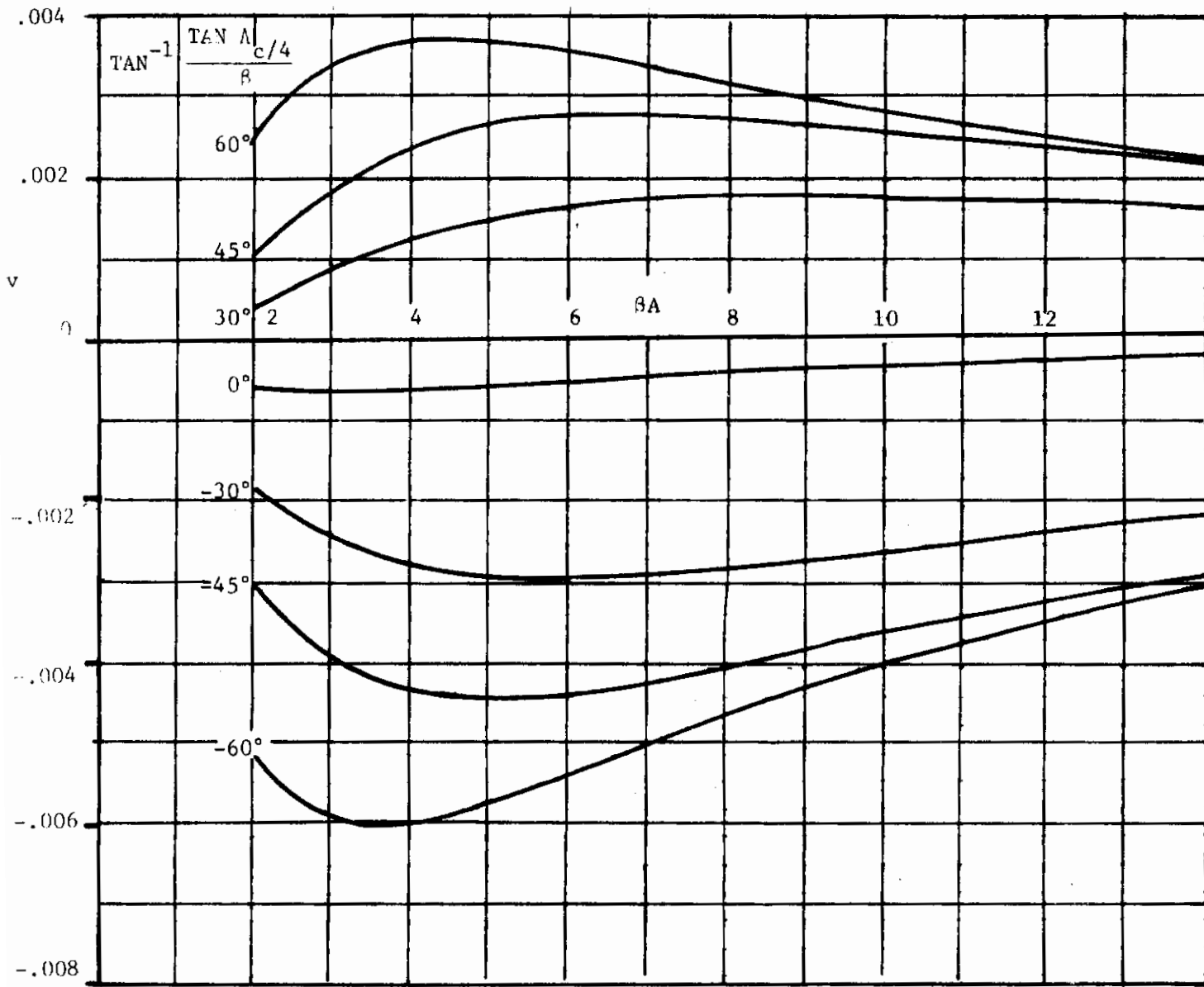
c. Taper Ratio = 0.25

Figure 8. Lift-Dependent Drag Factor Due to Linear Twist



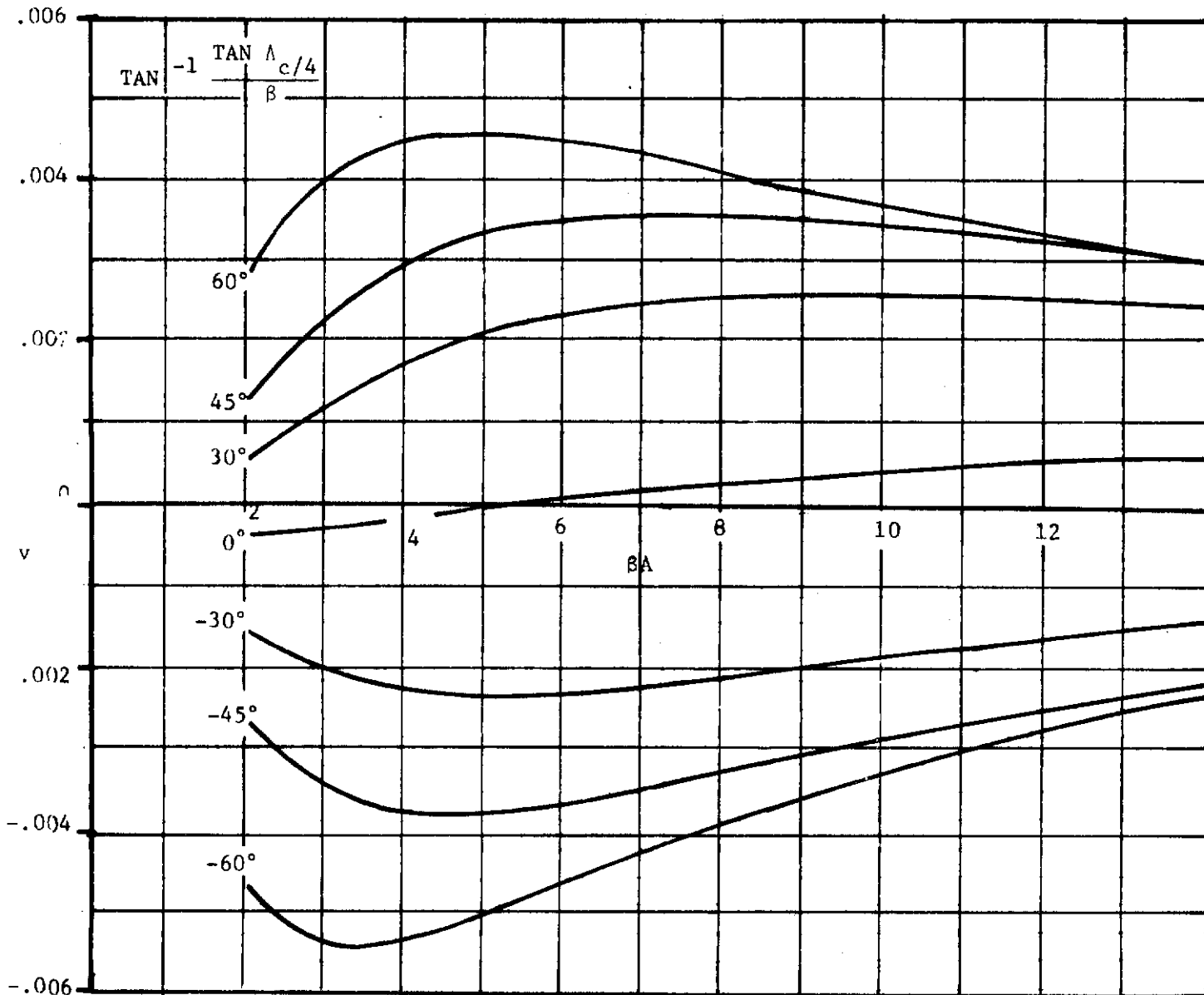
d. Taper Ratio = 0.3

Figure 8. Lift-Dependent Drag Factor Due to Linear Twist



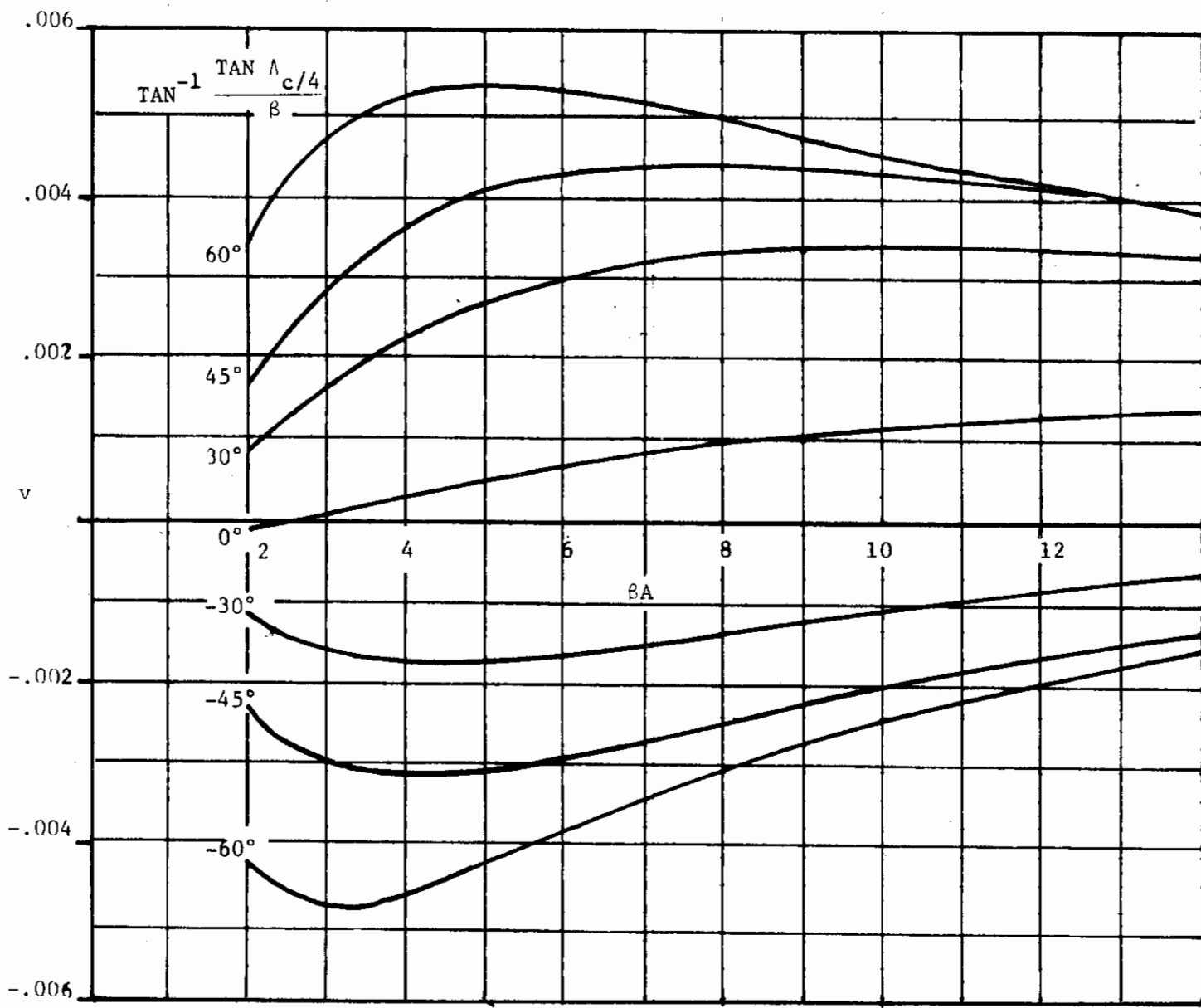
e. Taper Ratio = 0.4

Figure 8. Lift-Dependent Drag Factor Due to Linear Twist



f. Taper Ratio = 0.5

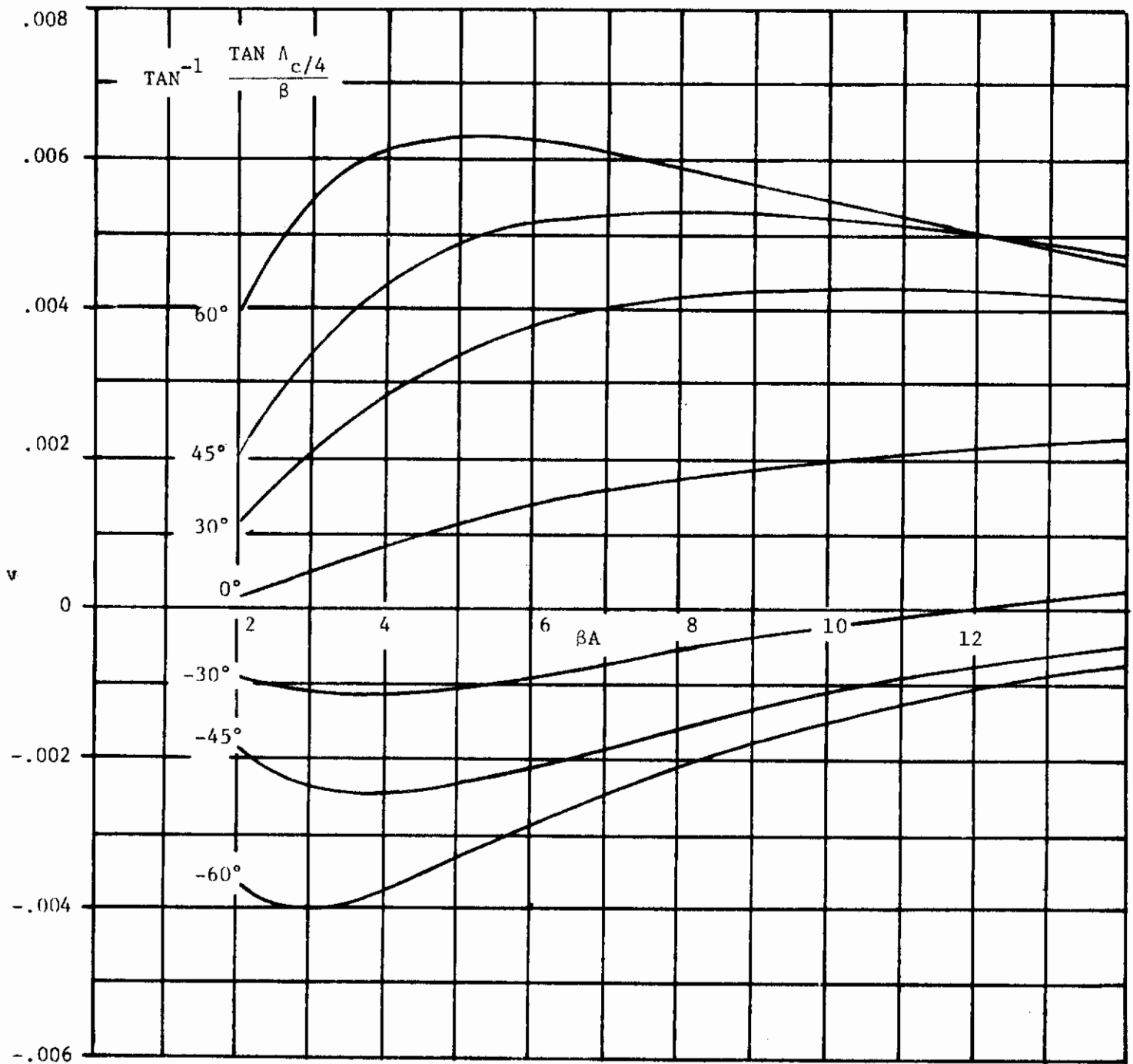
Figure 8. Lift-Dependent Drag Factor Due to Linear Twist



g. Taper Ratio = 0.6

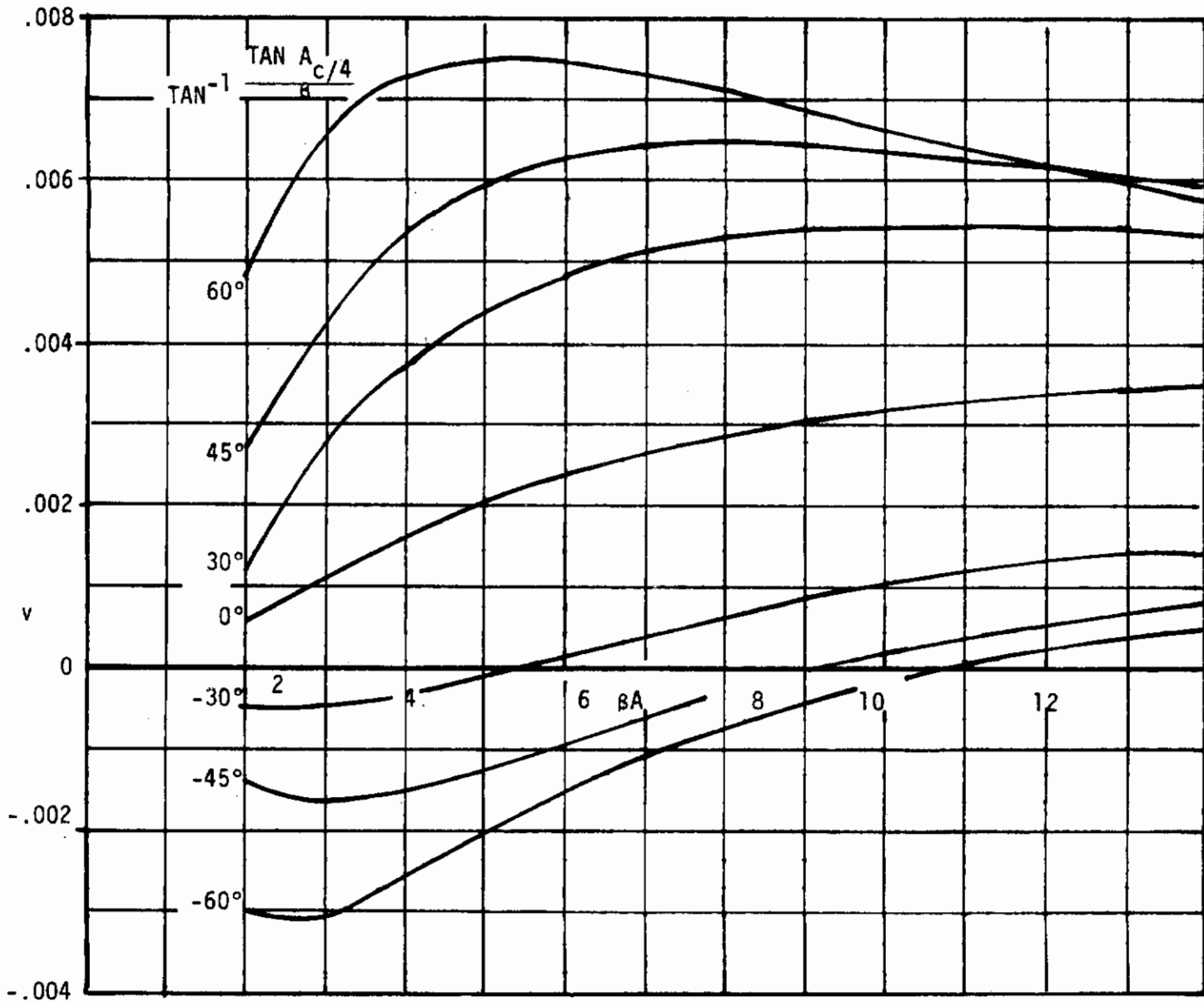
Figure 8. Lift-Dependent Drag Factor Due to Linear Twist





h. Taper Ratio = 0.75

Figure 8. Lift-Dependent Drag Factor Due to Linear Twist



1) Taper Ratio = 1.0

Figure 8. Lift-Dependent Drag Factor Due to Linear Twist

The wing-body planforms analyzed (no wing-alone data were found) are described in Table 10 along with predicted and test drag values. As has been mentioned, the Datcom predicted drag values should not be used for performance estimates.

### C. Supersonic

No modifications to the supersonic methodologies are required to estimate sweptforward-wing drag. Wing-body planforms were analyzed using wing-body relations, as no wing-alone data were available.

The difference between predicted and test drag values was an average of 215.6 counts. The individual predicted and test values, along with planform descriptions are listed in Table 11. As has been mentioned above, Datcom drag estimates should not be used for performance estimates.

4.3 WING-BODY, TAIL-BODY COMBINATIONS AT ANGLE OF ATTACK

4.3.1.2 WING-BODY LIFT-CURVE SLOPE

A. Subsonic

No modifications to either method are required. Good agreement between test and predicted lift-curve slopes (5.72% average error) was noted for the configurations analyzed. Table 12 contains a summary of the planforms, their parameters, and test and predicted lift-curve slopes.

B. Transonic

Two relations are used to predict transonic lift-curve slopes:

(C\_L\_alpha)\_WB = [K\_N + K\_w(B) + K\_B(w)] / (C\_L\_alpha)\_e \* (S\_e / S\_w) (6)

for panels fixed at zero incidence to the body and for panels capable of variable incidence relative to the body,

(C\_L\_i)\_WB = [k\_w(B) + k\_B(w)] (C\_L\_alpha)\_e \* (S\_e / S\_w) (7)

Modifications to the lift-curve slope of the exposed wing are discussed in Section 4.1.3.2 of this report. These modifications are also applicable when determining the factor K\_N. If the factor K\_B(w) is obtained from Datcom Figure 4.3.1.2-11, "Lift on Body in Presence of Wing...", the absolute value of the trailing-edge sweep angle should be inserted wherever the leading-edge sweep angle is called for.

Figure 3 shows typical wing-body lift-curve slope agreement.

C. Supersonic

The comments of Paragraph B above are applicable here.

# *Contrails*

AFWAL-TR-84-3084

Good agreement between test and predicted normal-force-curve slopes (4.80% error) was noted for the configurations analyzed. The data summary and substantiation for this speed range can be found in Table 2.

## 4.3.1.3 WING-BODY LIFT IN THE NONLINEAR ANGLE-OF-ATTACK RANGE

## A. Subsonic

No modifications to either method are required other than those described in Sections 4.1.3.3, "Wing Lift in the Nonlinear Angle-of-Attack Range" and 4.4.1, "Wing-Wing Combinations at Angle of Attack".

Table 13 contains a summary of the planforms, their parameters and test, and predicted lift coefficients in the nonlinear angle-of-attack range. An average error of 19.3% was noted from Method 1 and 14.5% from Method 2 for the planforms evaluated.

## B. Transonic

Although no data are available at this speed, no modifications to either method should be needed other than those discussed in Sections 4.1.3.2, "Wing Lift-Curve Slope"; 4.1.3.3, "Wing Lift in the Nonlinear Angle-of-Attack Range"; 4.3.1.2 "Wing-Body Lift-Curve Slope"; and 4.4.1, "Wing-Wing Combinations at Angle of Attack".

## C. Supersonic

The comments in Paragraph B of this section are appropriate here.

4.3.1.4 WING-BODY MAXIMUM LIFT

A. Subsonic

Method 1 requires use of a wing-body spanwise-loading computer program. The comments concerning Method 1 in Paragraph A of Section 4.1.3.4, "Wing Maximum Lift" are appropriate here.

Method 2 is based on empirical correlations and the wing-alone method of Datcom Section 4.1.3.4. To predict sweptforward wing maximum lift characteristics, Figure 9a should be used in place of Datcom Figure 4.3.1.4-12b, "Wing-Body Maximum Lift" and Figure 9b should be used in place of Datcom Figure 4.3.1.4-12c, "Angle of Attack for Maximum Lift". Figures 9a and 9b were developed from a vortex-lattice computer code.

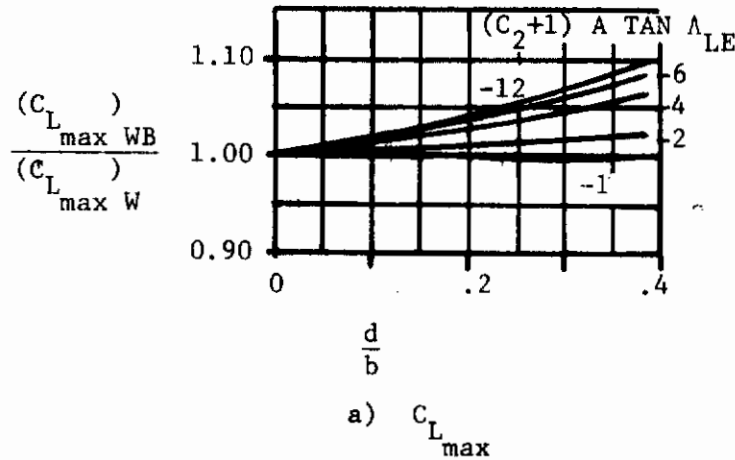


Figure 9. Forward Swept Wing Wing-Body Maximum Lift Correction Factor

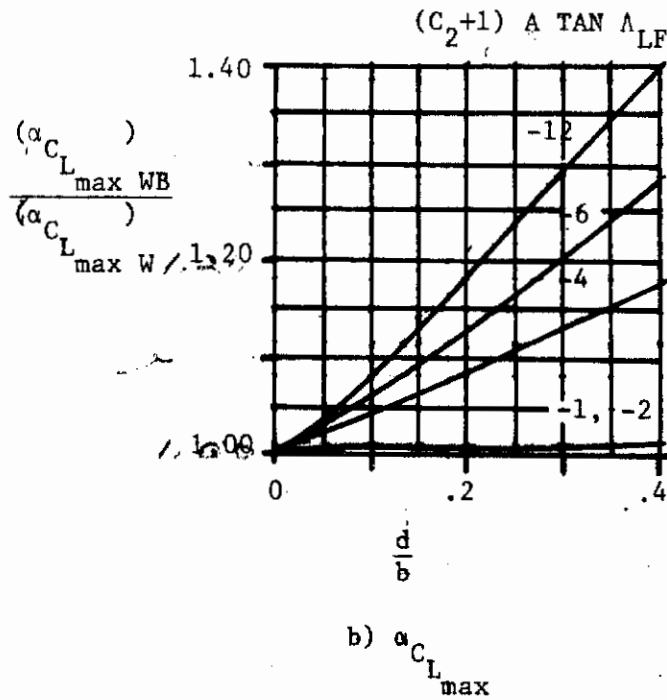


Figure 9. Forward Swept Wing Wing-Body Maximum Lift Correction Factor

Average errors of 12.4% and 17.0% were noted between test and predicted maximum lift coefficients and angles of attack for maximum lift, respectively. Table 14 presents a summary of the planforms, their parameters, and the test and predicted maximum lift values.

B. Transonic

No Datcom method is presented.



**C. Supersonic**

While no data were found in this speed range, no modifications should be necessary for either method other than those described in Paragraph C of Sections 4.1.3.4, "Wing Maximum Lift" and 4.3.1.2, "Wing-Body Lift-Curve Slope" for Method 1 and Section 4.3.1.3, "Wing-Body Lift in the Nonlinear Angle-of-Attack Range" for Method 2.

## 4.3.2.1 WING-BODY ZERO-LIFT PITCHING MOMENT

## A. Subsonic

No modifications to Method 1 are required other than those described in Paragraph A of Section 4.1.4.1, "Wing Zero-Lift Pitching Moment". Substantiation of this method was not performed. Several sweptforward configurations were analyzed using Method 2 with poor correlation noted between test and predicted values. Method 2, a linear regression method for fighter-type aircraft, should not be used to estimate forward-swept-wing characteristics.

## B. Transonic

The comments in Paragraph A of this section are appropriate here.

## C. Supersonic

There is no Datcom method appropriate for sweptforward configurations in this speed range.

## 4.3.2.2 WING-BODY PITCHING-MOMENT-CURVE SLOPE

## A. Subsonic

No modifications are necessary other than those described in Paragraph A of Section 4.1.4.2, "Wing Pitching-Moment-Curve Slope".

Good agreement was noted between test and predicted values (3.67% mean error). Table 15 contains a summary of the planforms studied, their parameters, and test and predicted values.

## B. Transonic

The methods in this speed range are based solely on empirical sweptback wing results and should not be used to predict sweptforward wing characteristics. No forward-swept-wing estimation method is presented.

## C. Supersonic

The absolute value of the leading-edge sweep angle should be used in Datcom Figures 4.3.2.2-36b, "Theoretical Aerodynamic-Center..." and 4.3.2.2-37, "Aerodynamic-Center Locations...". Also, the modifications described in Paragraph C of Sections 4.1.3.2, "Wing Lift-Curve Slope"; 4.1.4.2, "Wing Pitching-Moment-Curve Slope"; and 4.3.1.2, "Wing-Body Lift-Curve Slope" are appropriate here.

Fair agreement (10.29% mean error) was noted between test and predicted values. Table 7 contains a summary of the planforms, their parameters, and test and predicted values.

## 4.3.3.1 WING-BODY ZERO-LIFT DRAG

## A. Subsonic

No modifications to the Datcom methods are required at this speed. Agreement adequate for stability and control purposes (a mean difference of .00586, or 58.6 counts) was noted between test and predicted drag coefficients. Table 16 contains a summary of the wing-body planforms analyzed, their parameters, and predicted and test results. Datcom drag values should not be used for performance estimation.

## B. Transonic

No modifications to the Datcom methods are required at this speed.

Agreement adequate for stability and control purposes (a mean difference of 229.8 counts) was noted between test and predicted drag coefficients. Table 8 contains a summary of the wing-body planforms analyzed, their parameters, and predicted and test results.

Datcom drag values should not be used for performance estimation.

## C. Supersonic

The absolute value of the leading-edge sweep angle should be used in all the methodologies and figures at this speed. No other modifications are required.

Agreement adequate for stability and control purposes (a mean difference of 44.8 counts) was noted between test and predicted drag coefficients. Table 17 contains a summary of the wing-body planforms analyzed, their parameters, and predicted and test results.

Datcom drag values should not be used for performance estimation.

4.3.3.2 WING-BODY DRAG AT ANGLE OF ATTACK

A. Subsonic

Method 1 is a linear regression analysis for fighter-type aircraft. This method should not be used to estimate forward swept wing planform characteristics.

Method 2 can be used without any modifications other than those described in Paragraph A of Section 4.1.5.2, "Wing Drag at Angle of Attack". Agreement adequate for stability and control purposes (a mean difference of 169.0 counts) between test and predicted drag coefficients was noted. Table 18 contains a summary of the wing-body planforms analyzed, their parameters, and predicted and test results.

Datcom drag values should not be used for performance estimation.

B. Transonic

The comments concerning methodology use and modifications in Paragraph A of this section are applicable here.

Agreement adequate for stability and control purposes (an average difference of 188.8 counts) was noted between test and predicted drag coefficients. Table 10 contains a summary of the wing-body planforms analyzed, their parameters, and predicted and test results.

Datcom drag values should not be used for performance estimation.

C. Supersonic

The comments concerning methodology use and modification in Paragraph A of this section are applicable here.

Agreement adequate for stability and control purposes (an average difference of 215.6 counts) was noted between test and predicted drag coefficients. Table 11

AFWAL-TR-84-3084

contains a summary of the wing-body planforms analyzed, their parameters, and predicted and test results.

Datcom drag values should not be used for performance estimation.

## 4.4 WING-WING COMBINATIONS AT ANGLE OF ATTACK

## 4.4.1 WING-WING COMBINATIONS AT ANGLE OF ATTACK

## A. Subsonic

## DOWNWASH

For Method 1, Figure 10 (from Reference 3) should be used in place of Datcom Figure 4.4.1-66, "Effective Wing Aspect Ratio and Span..." when evaluating sweptforward wing planforms. (Increased accuracy can be obtained from Figure 10 and Datcom Figure 4.4.1-66 by multiplying the angle-of-attack parameter,  $\frac{\alpha - \alpha_o}{\alpha_{C_{L_{max}}} - \alpha_o}$ , by the Oswald efficiency factor,  $e$ , obtained from Datcom equation 4.1.5.2-i. The product of this operation,  $e \left( \frac{\alpha - \alpha_o}{\alpha_{C_{L_{max}}} - \alpha_o} \right)$ , should then be used in place of the angle-of-attack parameter called for in these figures.) The absolute value of the quarter-chord sweep angle should be used in Datcom Figure 4.4.1-67, "Downwash at the Plane of Symmetry...". There are no modifications to Method 1 other than those described in Paragraph A of Section 4.1.3.1, "Wing Zero-Lift Angle of Attack" and 4.1.3.4, "Wing Maximum Lift".

Very good agreement was noted between test and predicted downwash angles (average difference of  $1.37^\circ$ ). Table 19 contains a summary of the planforms analyzed, their parameters, and test and predicted results.

Method 2 is an empirical method for estimating the downwash gradient. No modifications are required.

Fair agreement was noted between test and predicted downwash gradients (average difference of = .0422). Table 20 contains a summary of the planforms analyzed, their parameters, and test and predicted results.

Method 3 estimates the effect of canards on aft lifting surfaces. Datcom Figure 4.4.1-71, "Wing-Vortex Lateral Position..." should be replaced with Figure 11 for both aft and forward swept wings. No other modifications are necessary other than

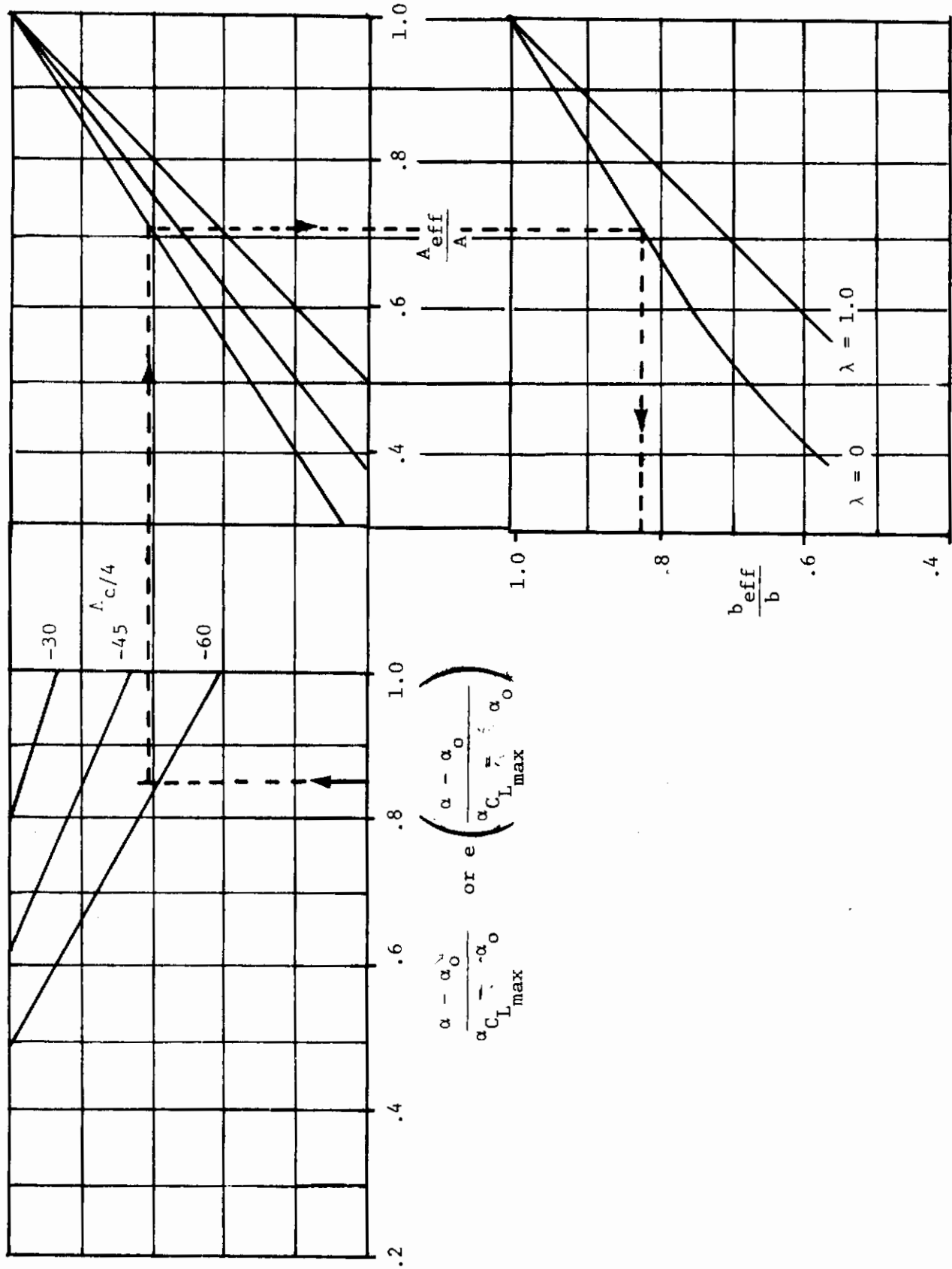


Figure 10. Effective Wing Aspect Ratio and Span for Sweptforward Planforms



AFWAL-TR-84-3084

those described in Paragraph A of Section 4.3.1.3, "Wing-Body Lift in the Nonlinear Angle-of-Attack Range."

No forward swept wing data were found. Correlation of Figure 11 (based on vortex-lattice code results) and Datcom Figure 4.4.1-71 with aft swept wing test data showed Figure 11 to be more accurate than Datcom Figure 4.4.1-71.

#### DOWNWASH DUE TO FLAP DEFLECTION

No modifications to this method are necessary. Good agreement was noted between test and predicted downwash angles (mean difference =  $1.9887^{\circ}$ ). Table 21 contains a summary of the planforms analyzed, their parameters, and test and predicted results.

#### UPWASH

The Datcom method applies to unswept wings only.

#### DYNAMIC PRESSURE RATIO

No modifications for this method are necessary.

Good agreement between test and predicted values was noted (average difference = .053). Table 22 contains a summary of the planforms analyzed, their parameters, and test and predicted ratios.

#### B. Transonic

##### DOWNWASH

No modifications seem required other than those discussed in Paragraph B of Sections 4.1.3.2, "Wing Lift-Curve Slope" and 4.1.3.3, "Wing Lift in the Nonlinear Angle-of-Attack Range."

No data were found to substantiate this section.

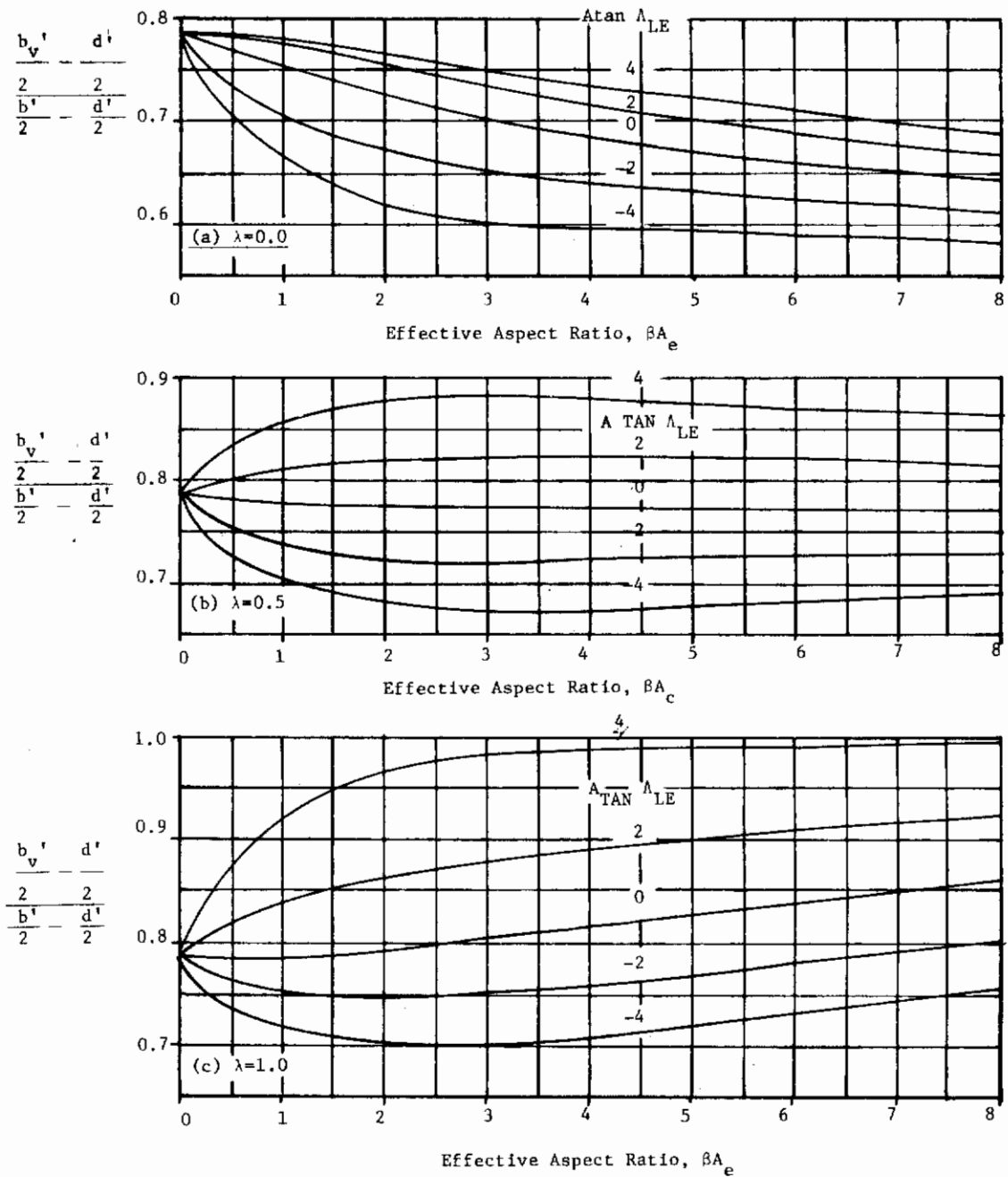


Figure 11. Wing-Vortex Lateral Positions at Subsonic Speeds

AFWAL-TR-84-3084

DYNAMIC PRESSURE RATIO

No modifications for this method are necessary.

C. Supersonic

DOWNWASH

No modifications to Method 1 are required. Method 2 is inapplicable to wings with sweptforward leading edges. However, rectangular wing results could be used as a rough approximation. For Method 3, Datcom Figure 4.4.1-80, "Wing Vortex Lateral Position..." should be replaced with Figure 12 for aft and forward swept wings. Figure 12 was obtained from a supersonic vortex-lattice code.

No data have been found to substantiate the previous modifications. Correlation of Figure 12 and Datcom Figure 4.4.1-80 with aft swept wing data indicates that better accuracy was obtained with values obtained from Figure 12.

DYNAMIC PRESSURE RATIO

No modifications appear to be required for this method.

No data have been found to substantiate this methodology.

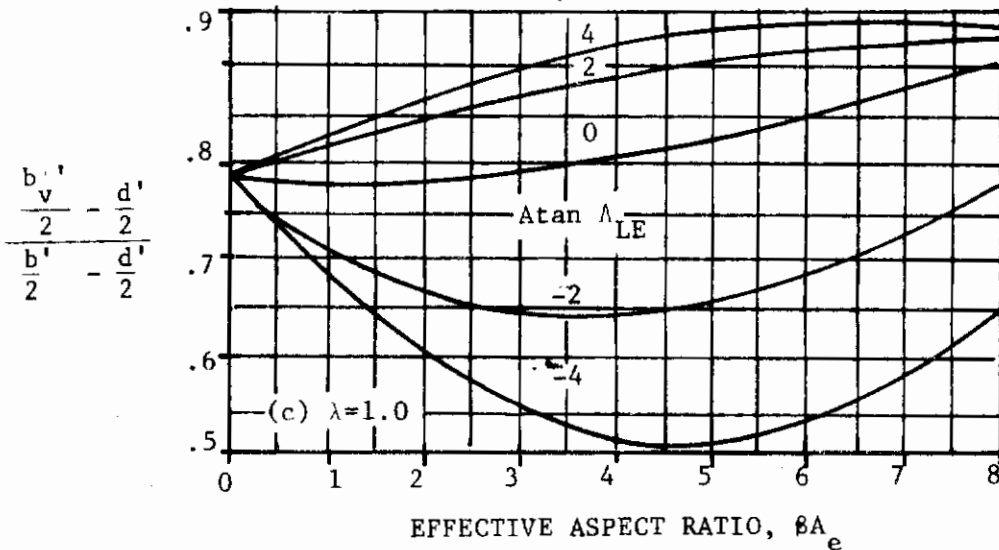
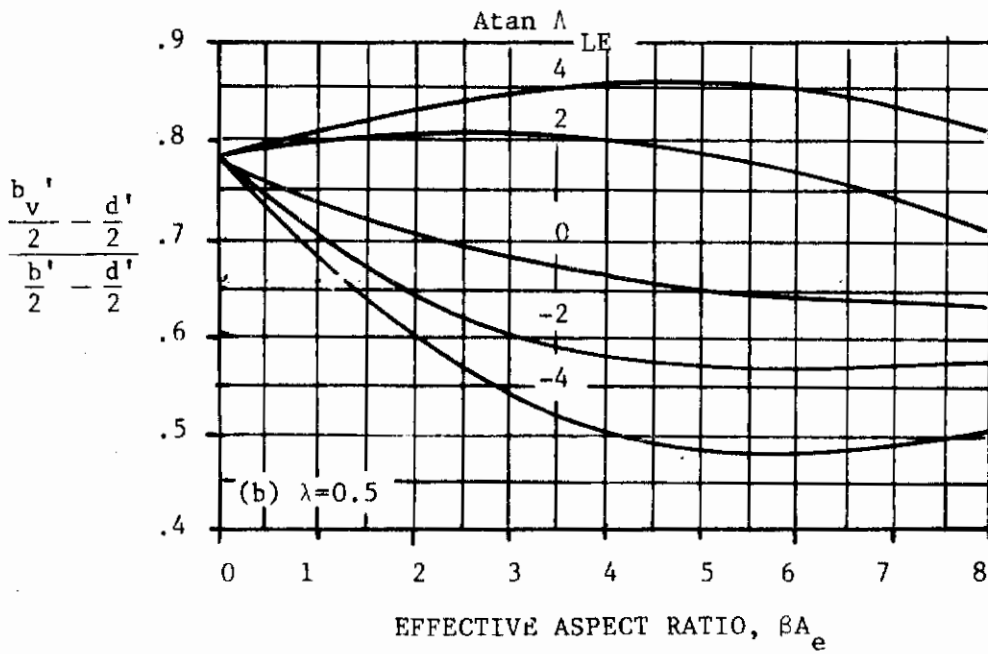
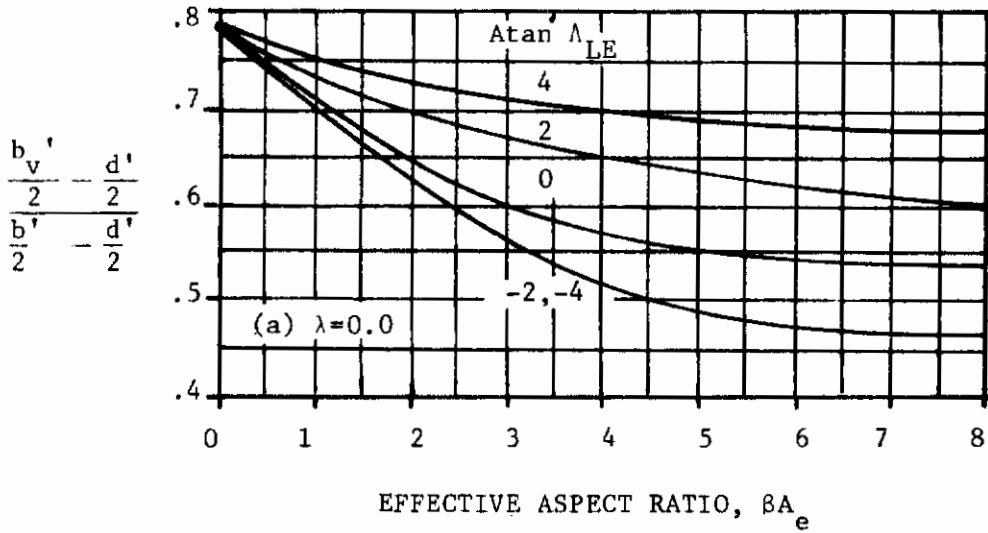


Figure 12. Wing-Vortex Lateral Positions at Supersonic Speeds

#### 4.5 WING-BODY-TAIL COMBINATIONS AT ANGLE OF ATTACK

No correlations between predicted results and test data were performed for wing-body-tail configurations. It was felt that validation of the wing-alone, wing-body, and wing-wing methodologies was sufficient.

##### 4.5.1.1 WING-BODY-TAIL LIFT-CURVE SLOPE

###### A. All Speeds

No modifications to either method are required other than those described in Sections 4.1.3.2, "Wing Lift-Cover Slope"; 4.3.1.2, "Wing-Body Lift-Curve Slope"; and 4.4.1, "Wing-Wing Combinations at Angle of Attack" in the appropriate speed range.

##### 4.5.1.2 WING-BODY-TAIL LIFT IN THE NONLINEAR ANGLE-OF-ATTACK RANGE

###### A. All Speeds

No modifications to either method are required other than those described in Sections 4.1.3.2, "Wing Lift-Curve Slope", 4.1.3.3, "Wing Lift in the Nonlinear Angle-of-Attack Range"; 4.1.3.4, "Wing Maximum Lift"; 4.3.1.2 "Wing-Body Lift-Curve Slope"; 4.3.1.3, "Wing-Body Lift in the Nonlinear Angle-of-Attack Range", and 4.4.1, "Wing-Wing Combinations at Angle of Attack" in the appropriate speed range.

4.5.1.3 WING-BODY-TAIL MAXIMUM LIFT

A. All Speeds

No modifications are necessary other than those described in Sections 4.1.4.1, "Wing Pitching-Moment-Curve Slope"; 4.1.4.3, "Wing Pitching Moment in the Nonlinear Angle-of-Attack Range"; 4.3.1.4, "Wing-Body Maximum Lift"; 4.3.2.2, "Wing-Body Pitching-Moment-Curve Slope"; 4.3.3.1, "Wing-Body Zero-Lift Drag"; 4.3.3.2, "Wing-Body Drag at Angle of Attack"; and 4.4.1, "Wing-Wing Combinations at Angle of Attack" in the appropriate speed range.

4.5.2.1 WING-BODY-TAIL PITCHING-MOMENT-CURVE SLOPE

A. All Speeds

No modifications to either method are required other than those described in Sections 4.3.1.2, "Wing-Body Lift-Curve Slope"; 4.3.2.2, "Wing-Body Pitching-Moment-Curve Slope"; 4.3.3.2, "Wing-Body Drag at Angle of Attack"; and 4.4.1, "Wing-Wing Combinations at Angle of Attack" in the appropriate speed range.

## 4.5.3.1 WING-BODY-TAIL ZERO-LIFT DRAG

## A. Subsonic

No modifications are necessary. Datcom drag values should not be used for performance estimation.

## B. Transonic

The absolute value of the quarter-chord sweep angle should be used in Datcom Figure 4.5.3.1-19, "Drag Divergence Mach Number Chart". No other modifications are necessary. Datcom drag values should not be used for performance estimation.

## C. Supersonic

No modifications are necessary other than those described in Paragraph C of Section 4.3.3.1, "Wing-Body Zero-Lift Drag". Datcom drag values should not be used for performance estimation.

## 4.5.3.2 WING-BODY-TAIL DRAG AT ANGLE OF ATTACK

## A. All Speeds

No modifications are necessary other than those described in Sections 4.1.3.1, "Wing Zero-Lift Angle of Attack"; 4.1.5.1, "Wing Zero-Lift Drag"; 4.3.1.2 "Wing-Body Lift-Curve Slope"; 4.3.2.1, "Wing-Body Zero-Lift Pitching Moment"; 4.3.2.2, "Wing-Body Pitching-Moment-Curve Slope"; 4.3.3.1, "Wing-Body Zero-Lift Drag"; 4.3.3.2, "Wing-Body Drag at Angle of Attack"; and 4.4.1, "Wing-Wing Combinations at Angle of Attack" in the appropriate speed range. Datcom drag values should not be used for performance estimation.



4.6 POWER EFFECTS AT ANGLE OF ATTACK

No modifications are expected other than those described for the power-off coefficients.

No data have been found to substantiate these methodologies.

4.7 GROUND EFFECTS AT ANGLE OF ATTACK

No modifications are expected other than those described for the out-of-ground-effect coefficients.

No data have been found to substantiate these methodologies.

4.8 LOW-ASPECT-RATIO WINGS AND WING-BODY COMBINATIONS AT ANGLE OF ATTACK

This section is based on delta wing shapes and should not be used for analysis of sweptforward planforms.

5.1 WINGS IN SIDESLIP

5.1.1.1 WING SIDESLIP DERIVATIVE  $C_{Y\beta}$  IN THE LINEAR ANGLE OF ATTACK RANGE<sup>B</sup>

A. Subsonic

No modifications for this method are required.

Fair accuracy was obtained, as shown in Figure 13, for the planforms analyzed.

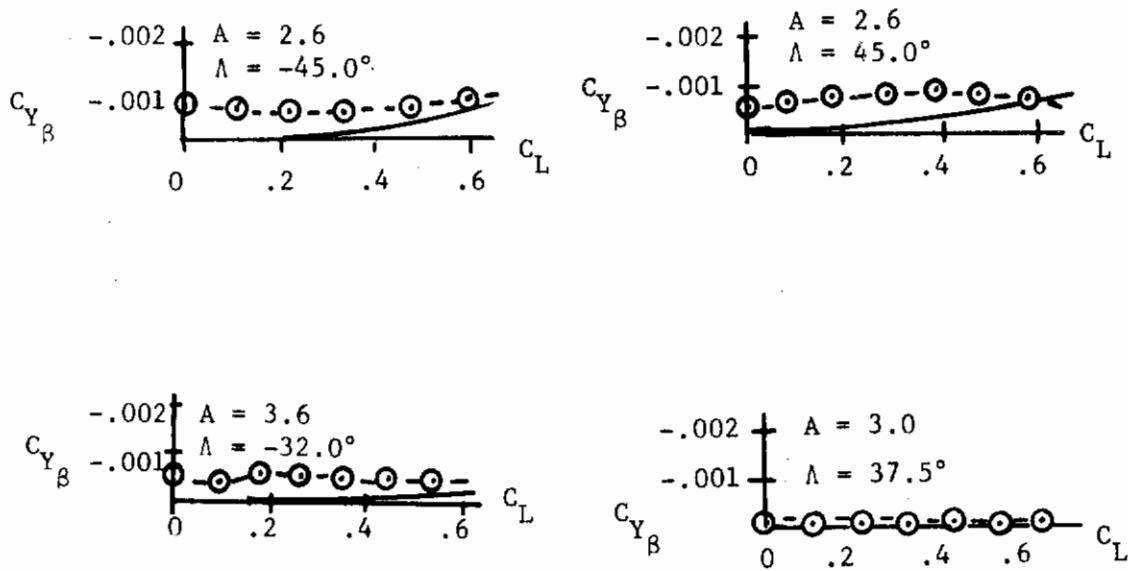


Figure 13. Comparison of Calculated and Experimental Values of  $C_{Y\beta}$

B. Transonic

No method is presented.

C. Supersonic

The existing relations do not account for wings with sweptforward leading edges. The rectangular planform methodology can be used for a first approximation.

5.1.2.1 WING SIDESLIP DERIVATIVE  $C_{l\beta}$  IN THE LINEAR ANGLE-OF-ATTACK

A. Subsonic

The only modification to this method is in adapting Datcom Figure 5.1.2.1-27, "Wing Sweep Contribution...". That figure, based on work done by Polhamus and Sleeman (Reference 5) was found to be oddly reflexive. Changing the sign of the midchord sweep angle (from positive to negative) results in a change of sign for the sweep contribution factor (from negative to positive) with the magnitude remaining unchanged. To illustrate, for a wing with an aspect ratio of 8.0, a taper ratio of 0.5 and a midchord sweep angle of 40 degrees, the sweep contribution factor is  $-.004$  (Figure 14). For the same wing sweptforward 40 degrees at the midchord point, its sweep contribution factor is  $.004$ . The sweep factor is then used in Datcom Equation 5.1.2.1-a just as the aft-swept sweep correction factor would be used.

Good agreement was noted between test and predicted rolling moments (Figure 15).

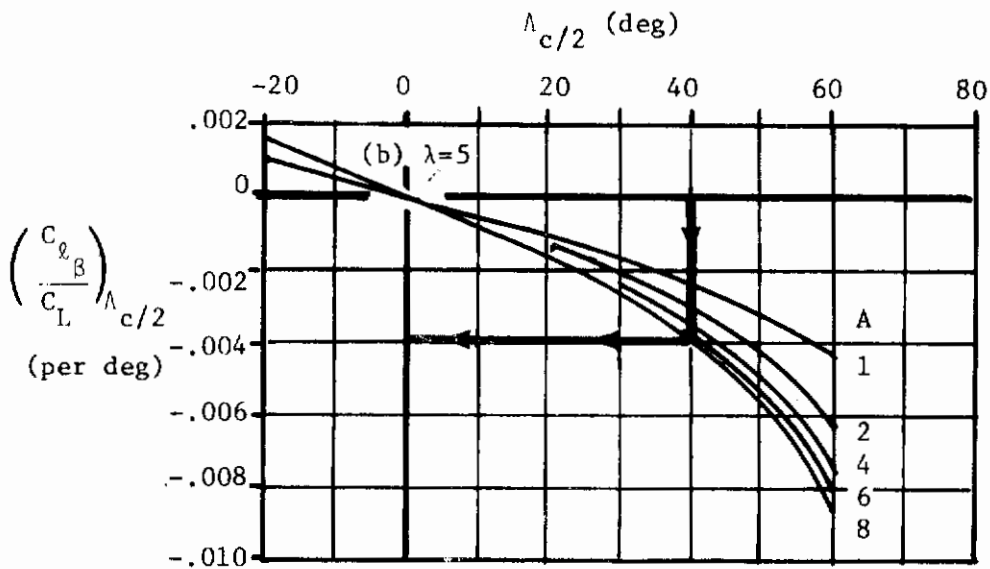


Figure 14. Datcom Figure 5.1.2.1-27, "Wing Sweep Contribution to  $C_{l\beta}$ "; (b)  $\lambda = .5$

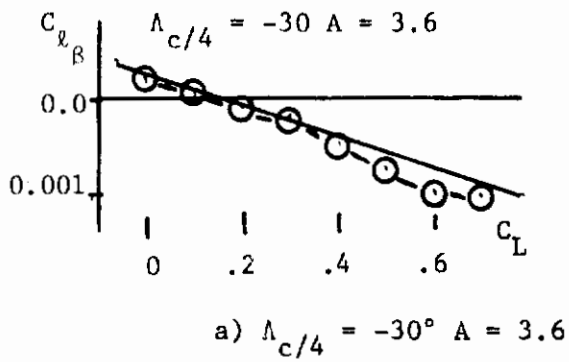
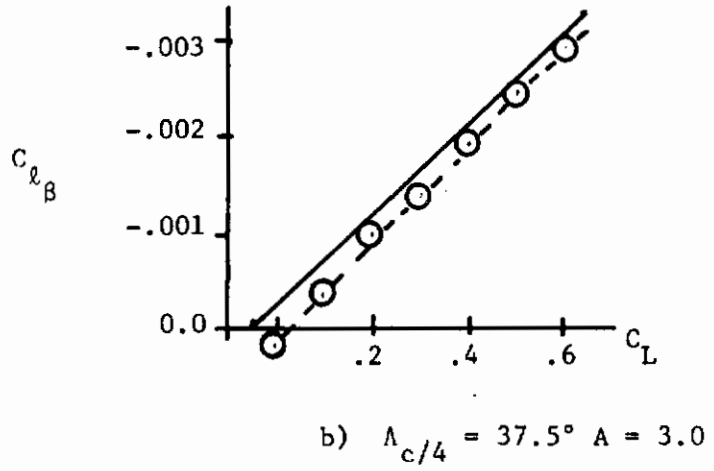


Figure 15. Comparison of Calculated and Experimental Values of  $C_{l_{\beta}}$

**B. Transonic**

No modifications to this method are required other than those described in Paragraphs A and C of this section and in Paragraph B of Section 4.1.3.2, "Wing Lift-Curve Slope".

While no wing-alone data were found at this speed, good agreement (average difference = .000879) was noted between test and predicted wing-body results. Table 23 contains a summary of the planforms analyzed, their parameters, and test and predicted results.

**C. Supersonic**

No modifications are necessary other than those described in Paragraph C of Sections 4.1.3.2, "Wing Lift-Cover Slope" and 7.1.2.2, "Wing Rolling Derivative  $C_{\ell p}$ ".

Good agreement (average difference = .000116) was noted between test and predicted wing-body values. No wing-alone data were found at this speed. Table 24 contains a summary of the planforms analyzed, their parameters, and test and predicted values.

5.1.2.2 WING ROLLING-MOMENT COEFFICIENT  $C_{l_2}$  AT ANGLE OF ATTACK

A. All Speeds

No modifications are necessary.

5.1.3.1 WING SIDESLIP DERIVATIVE  $C_{n\beta}$  IN THE LINEAR ANGLE-OF-ATTACK RANGE  $\beta$

A. Subsonic

No modifications to the methodologies are necessary. Good agreement (Figure 16) was noted between test and predicted results.

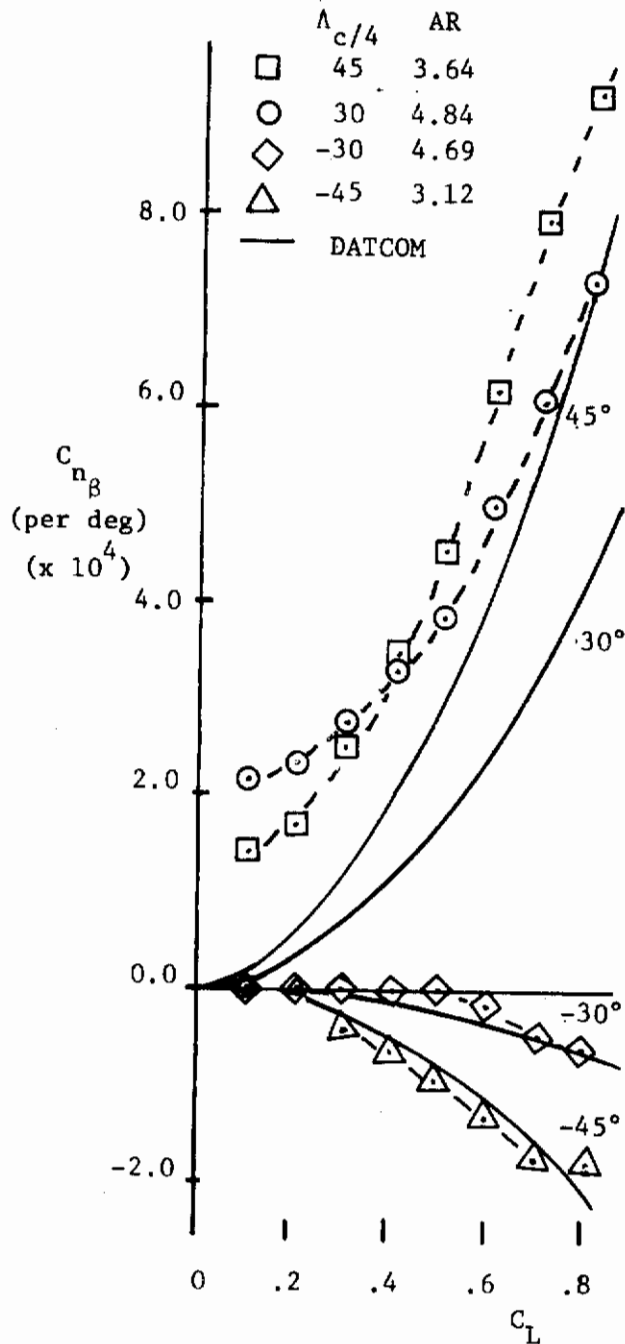


Figure 16. Comparison of Calculated and Experimental Values of  $C_{n\beta}$



B. Transonic

No method is presented.

C. Supersonic

The comments in Paragraph C of Section 5.1.1.1 are appropriate here.

5.2 WING-BODY COMBINATIONS IN SIDESLIP

5.2.1.1 WING-BODY SIDESLIP DERIVATIVE  $C_{Y\beta}$  IN THE  
LINEAR ANGLE-OF-ATTACK RANGE

A. All Speeds

No modifications are necessary as the methodologies are independent of sweep angle.

No substantiation was performed.

5.2.1.2 WING-BODY SIDE-FORCE COEFFICIENT  $C_Y$  AT ANGLE  
OF ATTACK

A. All Speeds

No modifications are necessary.

5.2.2.1 WING-BODY SIDESLIP DERIVATIVE  $C_{l\beta}$  IN THE  
LINEAR ANGLE-OF-ATTACK RANGE

A. Subsonic

No modifications are required other than those described in Paragraph A of Section 5.1.2.1, "Wing Sideslip Derivative  $C_{l\beta}$ ".

Good agreement (average difference = .000211) was noted between test and predicted values. Table 25 contains a summary of the planforms analyzed, their parameters, and the test and predicted results.

B. Transonic

No modifications are necessary other than those described in Paragraph B of Section 5.1.2.1, "Wing Sideslip Derivative  $C_{l\beta}$  ...".

Good agreement (average difference = .00088) was noted between test and predicted results. Table 23 contains a summary of the planforms analyzed, their parameters, and test and predicted results.

C. Supersonic

No modifications are necessary other than those described in Paragraph C of Section 5.1.2.1, "Wing Sideslip Derivative  $C_{l\beta}$  ...".

Good agreement (average difference = .00012) was noted between test and predicted values. Table 24 contains a summary of the planforms analyzed, their parameters, and test and predicted values.

5.2.3.1 WING-BODY SIDESLIP DERIVATIVE  $C_{n\beta}$  IN THE  
LINEAR ANGLE-OF-ATTACK RANGE

A. All Speeds

The comments in Paragraph A of Section 5.2.1.1, "Wing-Body Sideslip Derivative  $C_{Y\beta}$  ...", are appropriate here.

5.2.3.2 WING-BODY YAWING-MOMENT COEFFICIENT  $C_n$  AT  
ANGLE OF ATTACK

A. Subsonic

The comments in Paragraph A of Section 5.2.1.1, "Wing-Body Sideslip Derivative  $C_{Y\beta}$  ..." are appropriate here.

B. Transonic

No method is presented.

C. Supersonic

The comments in Paragraph A of this section are appropriate here.

## 5.3 TAIL-BODY COMBINATIONS IN SIDESLIP

5.3.1.1 TAIL-BODY SIDESLIP DERIVATIVE  $C_Y$  IN THE  
LINEAR ANGLE-OF-ATTACK RANGE  $\beta$ 

## A. Subsonic

No modifications are required. At this time, no sweptforward vertical tail data have been found to substantiate the methodologies.

## B. Transonic

No method is presented.

## C. Supersonic

No modifications are required other than those described in Paragraph C of Section 4.1.3.2, "Wing Lift-Curve Slope".

No sweptforward vertical tail data were found to substantiate the methodologies.

## D. Hypersonic

The comments in Paragraph C of this section are appropriate here.

5.3.1.2 TAIL-BODY SIDE-FORCE COEFFICIENT  $C_Y$  AT ANGLE  
OF ATTACK

A. Subsonic

The comments in Paragraph A of Section 5.3.1.1, "Tail-Body Sideslip Derivative  $C_{Y\beta}$  ..." are appropriate here.

B. Transonic

No method is presented.

C. Supersonic

The comments in Paragraph C of Section 5.3.1.1, "Tail-Body Sideslip Derivative  $C_{Y\beta}$  ..." are appropriate here.

5.3.2.1 TAIL-BODY SIDESLIP DERIVATIVE  $C_{Y\beta}$  IN THE  
LINEAR ANGLE-OF-ATTACK RANGE

A. Subsonic

No modifications are required.

No sweptforward vertical tail data were found to substantiate the methodology.

B. Transonic

No method is presented.

C. Supersonic

The comments in Paragraph C of Section 5.3.1.1, "Tail-Body Sideslip Derivative  $C_{Y\beta}$  ..." are appropriate here.

D. Hypersonic

The comments in Paragraph C of this section are appropriate here.

5.3.3.1 TAIL-BODY SIDESLIP DERIVATIVE  $C_{n\beta}$  IN THE  
LINEAR ANGLE-OF-ATTACK RANGE

A. Subsonic

No modifications are required other than those described in Paragraph A of Section 4.1.4.2, "Wing Pitching-Moment-Curve Slope".

No sweptforward vertical tail data were found to substantiate the methodologies.

B. Transonic

No method is presented.

C. Supersonic

No modifications are necessary other than those described in Paragraph C of Sections 4.1.4.2, "Wing Pitching-Moment-Curve Slope" and 5.3.1.1, "Tail-Body Sideslip Derivative  $C_{y\beta}$  ....

No sweptforward vertical tail data were found to substantiate the methodologies.



5.3.3.2 TAIL-BODY YAWING-MOMENT COEFFICIENT  $C_n$  AT  
ANGLE OF ATTACK

A. Subsonic

The comments in Paragraph A of Section 5.3.3.1, "Tail-Body Sideslip Derivative  $C_{n\beta}$  ..." are appropriate here.

B. Transonic

No method is presented.

C. Supersonic

No modifications are necessary other than those described in Paragraph C of Section 5.3.1.2. "Tail-Body Side-Force Coefficient  $C_Y$  at Angle of Attack".

5.4 FLOW FIELDS IN SIDESLIP

5.4.1 WING-BODY WAKE AND SIDEWASH IN SIDESLIP

A. Subsonic

No modifications are required.

No data were found to substantiate the methodology.

B. Transonic

No method is presented.

C. Supersonic

No method is presented.

5.5 LOW-ASPECT-RATIO WINGS AND WING-BODY COMBINATIONS IN  
SIDESLIP

The comments in Section 4.8 "Low-Aspect-Ratio Wings and Wing-Body Combinations..." are appropriate here.

AFWAL-TR-84-3084

5.6 WING-BODY-TAIL COMBINATIONS IN SIDESLIP

5.6.1.1 WING-BODY-TAIL SIDESLIP DERIVATIVE  $C_{Y\beta}$  IN THE  
LINEAR ANGLE-OF-ATTACK RANGE

A. Subsonic

No modifications are required.

No substantiation was performed.

B. Transonic

No method is presented.

C. Supersonic

The comments in Paragraph C of Section 5.3.1.1, "Tail-Body Sideslip Derivative  $C_{Y\beta}$ " are appropriate here.

5.6.1.2 WING-BODY-TAIL SIDE-FORCE COEFFICIENT  $C_Y$  AT  
ANGLE OF ATTACK

A. Subsonic

The comments in Paragraph A of Section 5.6.1.1, "Wing-Body-Tail Sideslip Derivative  $C_{Y\beta}$  ..." are appropriate here.

B. Transonic

No method is presented.

C. Supersonic

No modifications are required other than those described in Paragraph C of Section 5.3.1.2, "Tail-Body Side-Force Coefficient  $C_Y$  at Angle of Attack".

No substantiation was performed.

5.6.2.1 WING-BODY-TAIL SIDESLIP DERIVATIVE  $C_{l\beta}$  IN THE  
LINEAR ANGLE-OF-ATTACK RANGE

A. Subsonic

No modifications are required.

Good agreement (average difference = .000750) was noted between test and predicted values. Table 26 contains a summary of the planforms analyzed, their parameters, and test and predicted results.

B. Transonic

No method is presented.

C. Supersonic

No modifications are required other than described in Paragraph C of Section 5.3.1.1, "Tail-Body Sideslip Derivative  $C_{Y\beta}$  ...".

No substantiation was performed.

5.6.3.1 WING-BODY-TAIL SIDESLIP DERIVATIVE  $C_{n\beta}$  IN THE  
LINEAR ANGLE-OF-ATTACK RANGE

A. Subsonic

No modifications are necessary.

No substantiation was performed.

B. Transonic

No method is presented.

C. Supersonic

The comments in Paragraph A of this section are appropriate here.

5.6.3.2 WING-BODY-TAIL YAWING-MOMENT COEFFICIENT  $C_n$  AT  
ANGLE OF ATTACK

A. Subsonic

The comments in Paragraph A of Section 5.6.3.1, "Wing-Body-Tail Sideslip Derivative  $C_{n\beta}$  ..." are appropriate here.

B. Transonic

No method is presented.

C. Supersonic

No modifications are necessary other than those described in Paragraph C of Section 5.6.1.2, "Wing-Body-Tail Side-Force Coefficient  $C_Y$  at Angle of Attack".

No substantiation was performed.

6.1 SYMMETRICALLY DEFLECTED FLAPS AND CONTROL DEVICES  
ON WING-BODY AND TAIL-BODY COMBINATIONS

6.1.4.1 CONTROL DERIVATIVE  $C_{L\delta}$  OF HIGH-LIFT AND  
CONTROL DEVICES

A. Subsonic

No modifications to any of the method are required.

To obtain increased accuracy from split flap analyses, multiply the lift increment by the cosine of the sweep angle:

$$(\Delta C_{L\delta})_{\text{Split Flap}} = (\Delta C_{L\delta})_{\text{Datcom}} \cos \Lambda_c/4 \quad (8)$$

The average difference between test and predicted results was reduced from .1229 (using Datcom Equation 6.1.4.1-a) to .0506 (using Equation 8). The average difference between test and predicted single and double-slotted flap results was .0170 and .0740, respectively. Data for only one plain flap configuration was found; its average difference was .0273. Leading-edge device prediction results consistently overestimated in magnitude the test values. The average difference between nose flap test and predicted value was .0159. Slat and Krueger flap average difference was .0344 and .0150, respectively. No data were found for either internally- or internally-blown-flap configurations. Table 27 contains a summary of the planforms analyzed, their parameters, and test and predicted results.

B. Transonic

No modifications are required.

No substantiation was performed.

C. Supersonic

No modifications are required.

No substantiation was performed.



6.1.4.2 WING LIFT-CURVE SLOPE WITH HIGH-LIFT AND CONTROL  
DEVICES

A. All Speeds

No modifications are required.

Good agreement (4.33% average error) was noted between subsonic test and predicted values for both leading- and trailing-edge devices. No jet flap data were found. Transonic and supersonic substantiation was not performed. Table 28 contains a summary of the planforms analyzed, their parameters, and test and predicted results.

6.1.4.3 WING MAXIMUM LIFT WITH HIGH-LIFT AND CONTROL DEVICES

Datcom Figure 6.1.4.3-10, "Planform Correction Factor - Trailing-Edge Flaps" should be replaced with Figure 17 of this report as the Datcom figure was found to cause increasing error with increasing sweep angle. Figure 17 is based on the Datcom figure but includes the modifications suggested by J. W. Martin, Jr. of NASC as described in Reference 6. No other modifications are necessary.

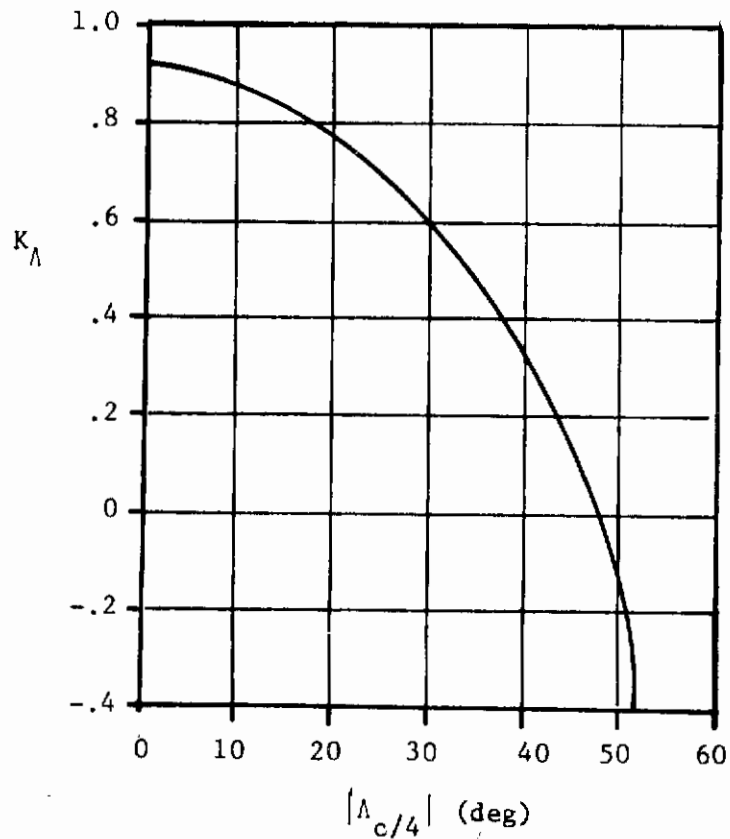


Figure 17. Planform Correction Factor - Trailing-Edge Flaps (Replaces Datcom Figure 6.1.4.3-10)

AFWAL-TR-84-3084

Correlation of test data with results from Method 1 (trailing-edge flaps) shows the improvement in accuracy gained in using Figure 17 in place of Datcom Figure 6.1.4.3-10. For split flaps, the average difference was reduced from .1998 to .0569. Also, average difference decreased from .2685 to .1040 for single-slotted flaps and from .2864 to .06577 for double-slotted flaps. Method 2, for leading-edge slats, gave fair agreement with an average difference between test and predicted results of .07833. No data were found for jet flap correlation (Method 3).

Table 29 contains a summary of the planforms analyzed, their parameters, and test results compared with both the existing and proposed method results.

### 6.1.5.1 PITCHING-MOMENT INCREMENT $\Delta C_m$ DUE TO HIGH-LIFT AND CONTROL DEVICES

#### A. Subsonic

No modifications are necessary for the jet-flap and leading-edge device methods, and for Method 1 of the trailing-edge mechanical flap section. For Method 2 of that section, Figure 18 (from Reference 33) should be used to obtain sweptforward wing loading coefficients.

Fair agreement (average difference = .08905) was noted between test and predicted trailing-edge mechanical flap values using Method 1. Method 2 substantiation was not performed. Good agreement (mean difference = .02088) was noted between test and predicted leading edge device increments. No jet flap data were found. Table 30 contains a summary of the planforms analyzed, their parameters, and test and predicted results.

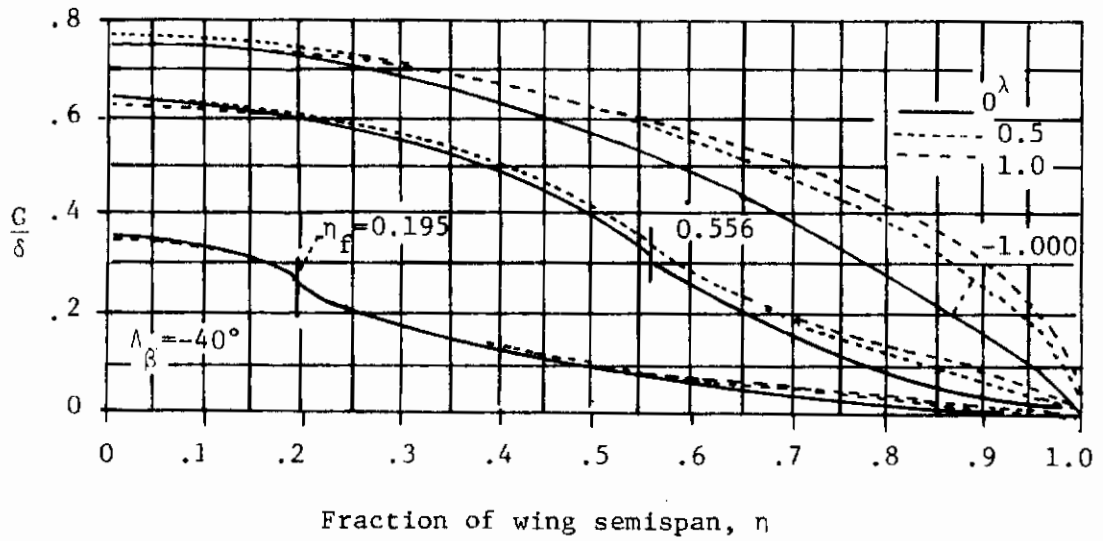
#### B. Transonic

The methodology of this section should not be used to estimate sweptforward wing characteristics. Insufficient data currently exist to validate Datcom Figure 6.1.5.1-69, "Transonic Control-Surface Pitch-Effectiveness Parameters".

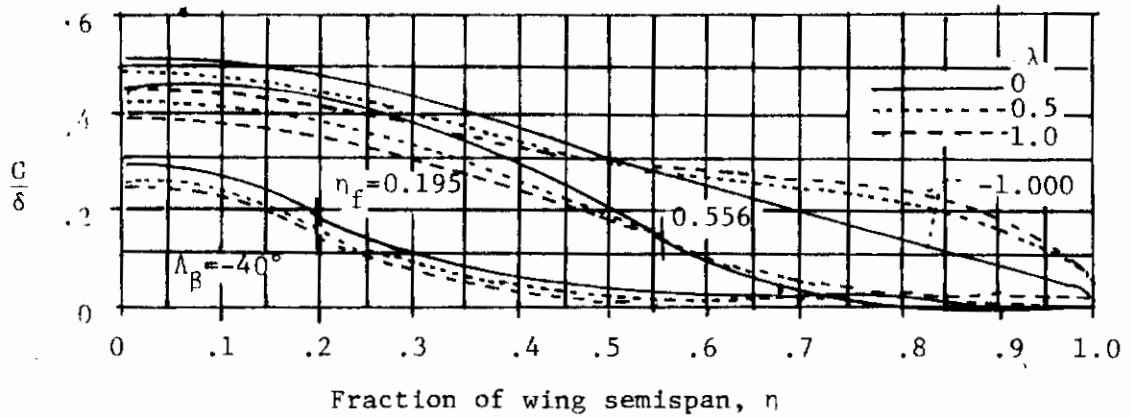
#### C. Supersonic

Figure 19 (from Reference 34) should be used for sweptforward wings having untapered controls with the outboard edge coincident with the wingtip.

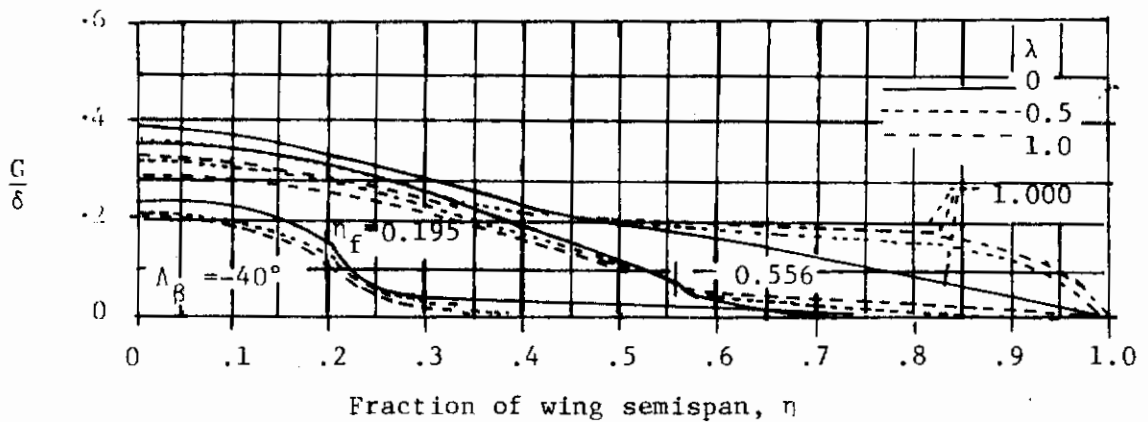
AFWAL-TR-84-3084



a)  $\frac{BA}{\kappa_{av}} = 2.0$



b)  $\frac{BA}{\kappa_{av}} = 6.0$



c)  $\frac{BA}{\kappa_{av}} = 10.0$

Figure 18. Spanwise Load Distribution Due to Symmetric Flap Deflection

AFWAL-TR-84-3084

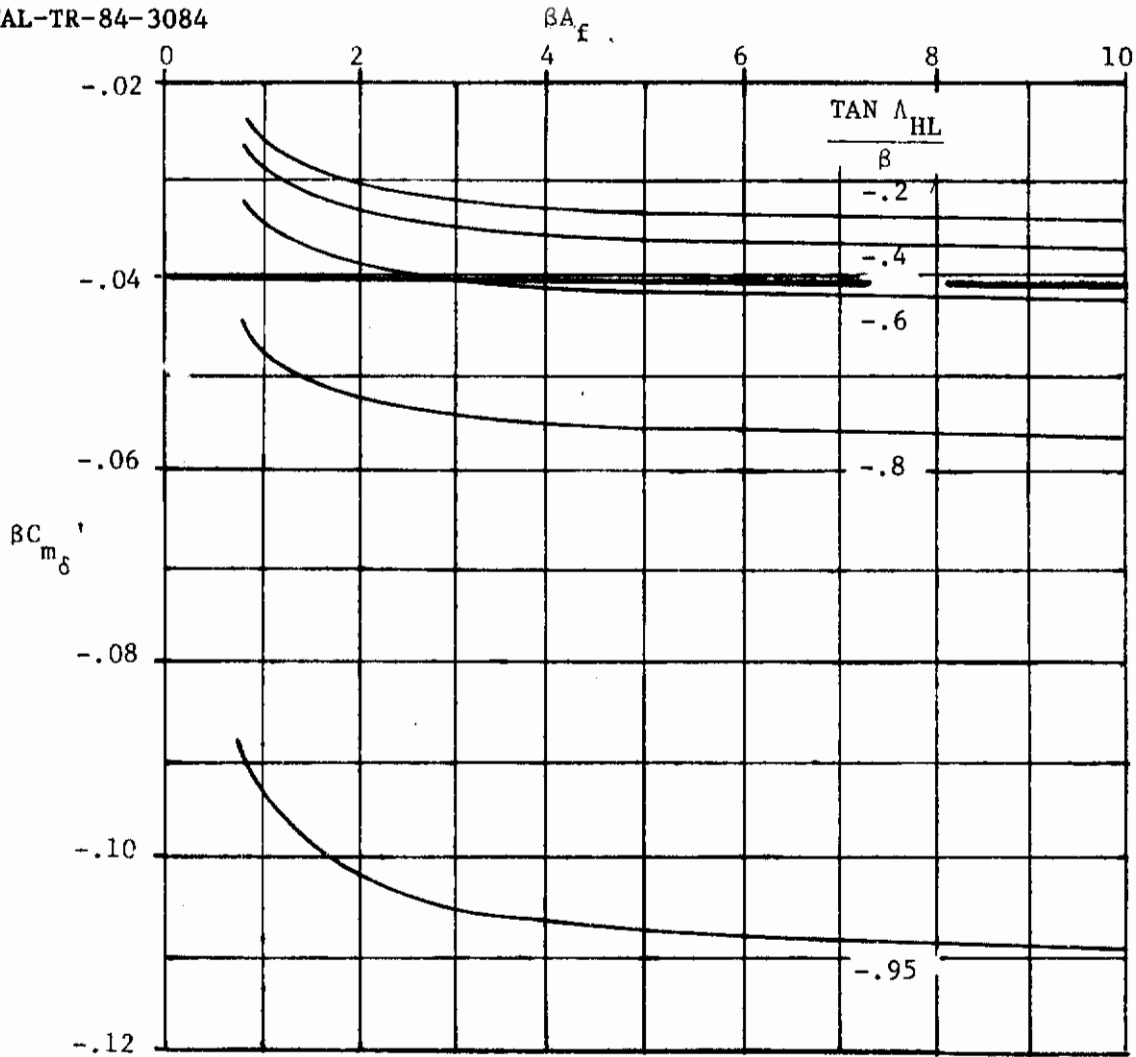


Figure 19. Pitching-Moment Derivative for Untapered Trailing-Edge Control Surfaces Located at the Wing Tip

Figure 20 (from Reference 34) should be used for tapered sweptforward controls, again, with the outboard edge coincident with the wingtip. For tapered and untapered controls having the outboard edge not coincident with the wing tip, Datcom Figure 6.1.5.1-73a, "Pitching Moment Derivative...", can be used with no modifications. No other modifications are necessary other than those described in Paragraph C of Section 6.2.1.1, "Rolling Moment Due to Control Deflection".

No substantiation was performed.

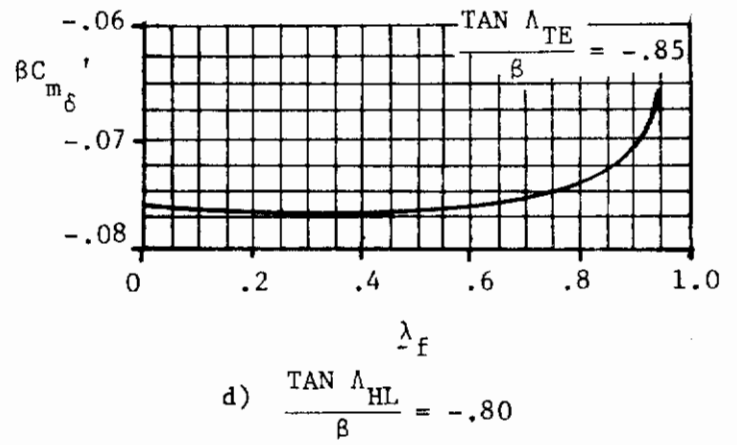
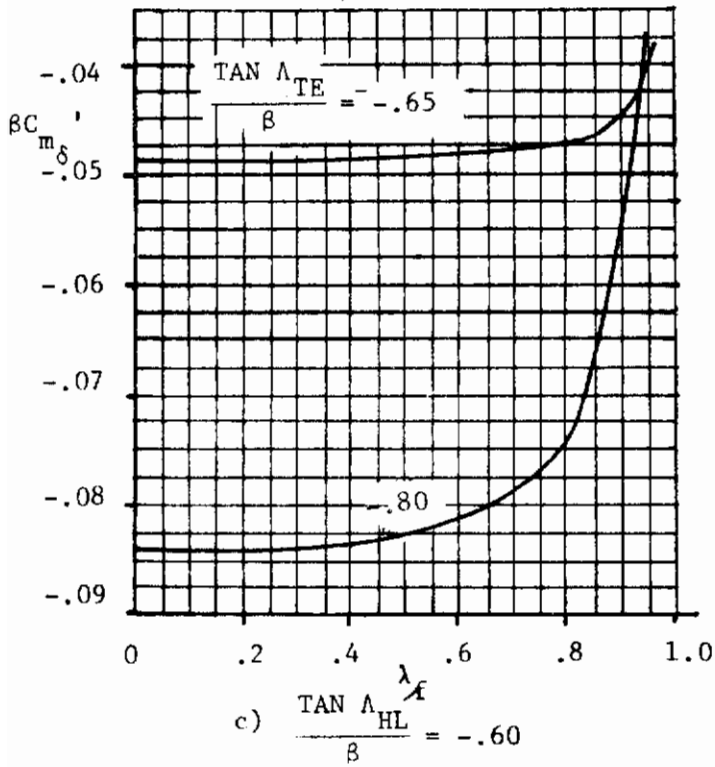
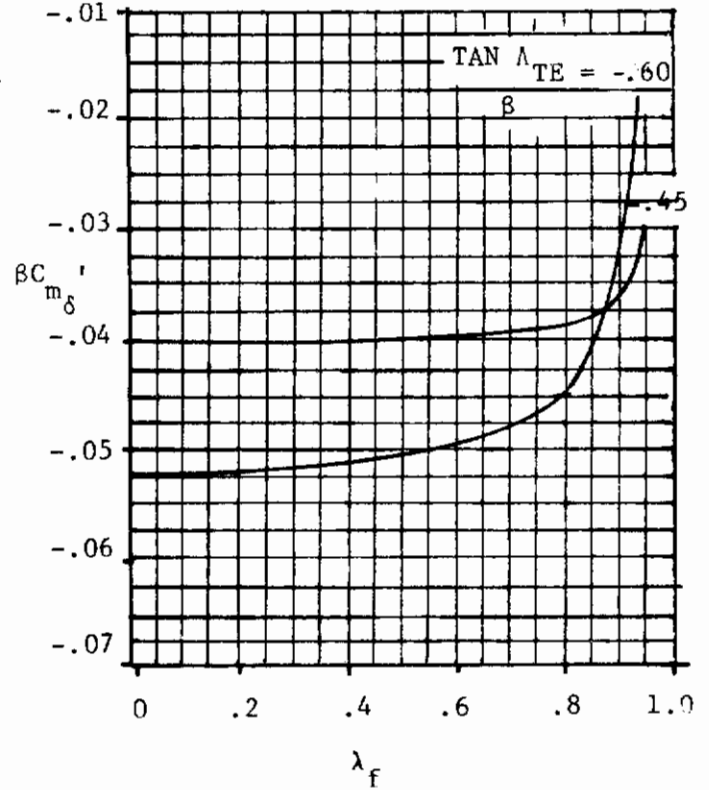
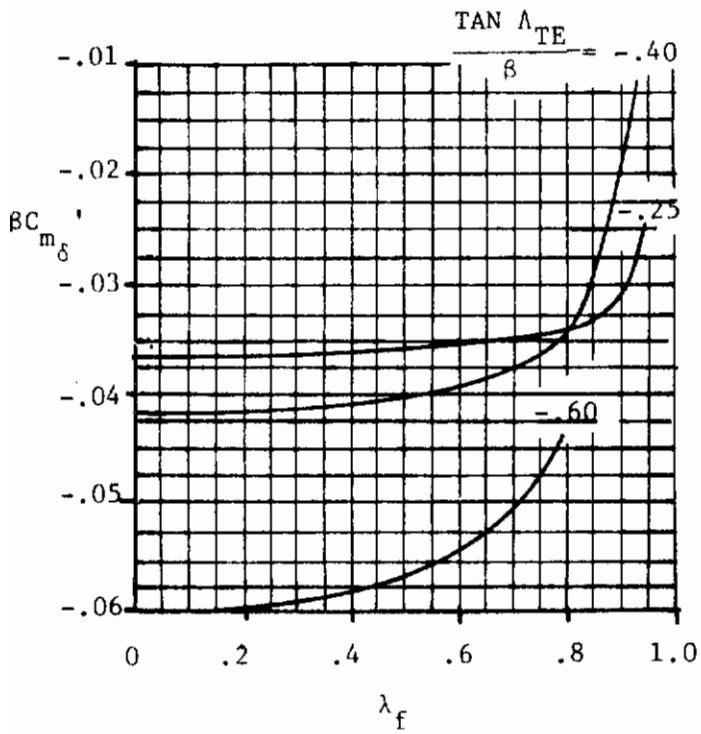


Figure 20. Pitching-Moment Derivative for Tapered Trailing-Edge Control Surfaces Having Outboard Edge Coincident with Wing Tip

6.1.5.2 WING DERIVATIVE  $C_{n\dot{\alpha}}$  WITH HIGH-LIFT AND CONTROL  
DEVICES

A. All Speeds

No modifications are necessary.

No substantiation was performed.



## 6.1.6.1 HINGE-MOMENT DERIVATIVE $C_h$ OF HIGH-LIFT AND CONTROL DEVICES $^\alpha$

### A. Subsonic

No modifications are necessary.

Good agreement (average difference = .11453) was noted between test and predicted values. Table 31 contains a summary of the planforms analyzed, their parameters, and test and predicted results.

### B. Transonic

No method is presented.

### C. Supersonic

No guidance was found in open literature to evaluate this term for sweptforward wing planforms. It is recommended that treating the control surface be analyzed as if it were on a sweptback wing having a taper ratio equal to the reciprocal of the sweptforward wing taper ratio. The modifications necessary include using the absolute value of the various sweep angles and altering the control surface description as follows (primed values denote the pseudo-aftswept wing):

$$\Lambda'_{LE} = |\Lambda_{LE}|$$

$$\Lambda'_{HL} = |\Lambda_{HL}|$$

$$\Lambda'_{TE} = |\Lambda_{TE}|$$

# Contrails

AFWAL-TR-84-3084

$$C'_r = C_t$$

$$C'_t = C_r$$

$$C'_{f_r} = C_{f_t}$$

$$C'_{f_t} = C_{f_r}$$

$$Y'_i = b/2 = Y_o$$

$$Y'_o = b/2 - Y_i$$

(9)

No substantiation was performed.

6.1.6.2 HINGE-MOMENT DERIVATIVE  $C_{h\delta}$  OF HIGH-LIFT AND  
CONTROL DEVICES

A. Subsonic

No modifications are necessary.

Insufficient data were found to allow substantiation; however, good correlation ( $\Delta C_{h\delta} = .00124$ ) was noted between the test and predicted values for the configuration found.

B. Transonic

No method is presented.

C. Supersonic

Figure 21 (from Reference 34) should be used in place of Datcom Figure 6.1.6.2-17, "Supersonic Theoretical Hinge-Moment Derivative  $C_{h\delta}$ ", for planforms having sweptforward hinge line sweep angles. No other modifications are necessary.

No substantiation was performed.

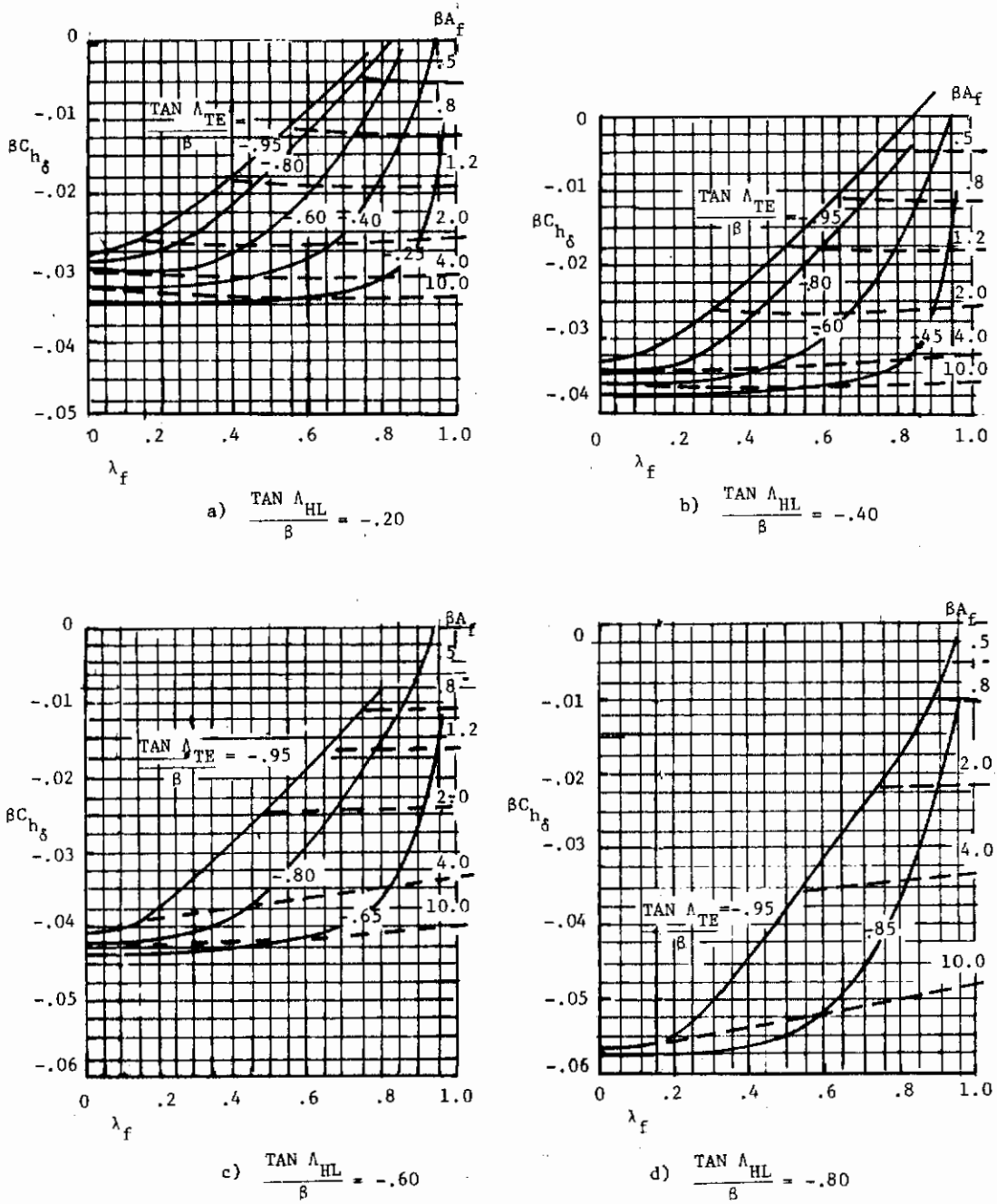


Figure 21. Supersonic Theoretical Hinge-Moment Derivative  $C_{h\delta}$

6.1.7 DRAG OF HIGH-LIFT AND CONTROL DEVICES

A. Subsonic

No modifications are required.

No substantiation was performed.

B. Transonic

No method is presented.

C. Supersonic

No modifications are required.

No substantiation was performed.

6.2 ASYMMETRICALLY DEFLECTED CONTROLS  
ON WING-BODY AND TAIL-BODY COMBINATIONS

6.2.1.1 ROLLING MOMENT DUE TO CONTROL DEFLECTION

A. Subsonic

No modifications are required.

Fair agreement was noted between test and predicted values for plain-trailing-edge flaps (average difference = .06475) and spoilers (average difference = .00257). Table 32 contains a summary of the planforms analyzed, their parameters, and test and predicted results.

B. Transonic

No modifications are necessary other than those described in Paragraph B of Section 4.1.3.2, "Wing Lift-Curve Slope".

No substantiation was performed.

C. Supersonic

Figures 22 through 25 (from Reference 34) should be used as described for the following control surface configurations:

- a. Tapered control surfaces with outboard edge coincident with wing tip: use Figure 22.
- b. Tapered control surface with outboard edge not coincident with wing tip: use Figure 23.
- c. Untapered control surface with outboard edge coincident with wing tip: use Figure 24.

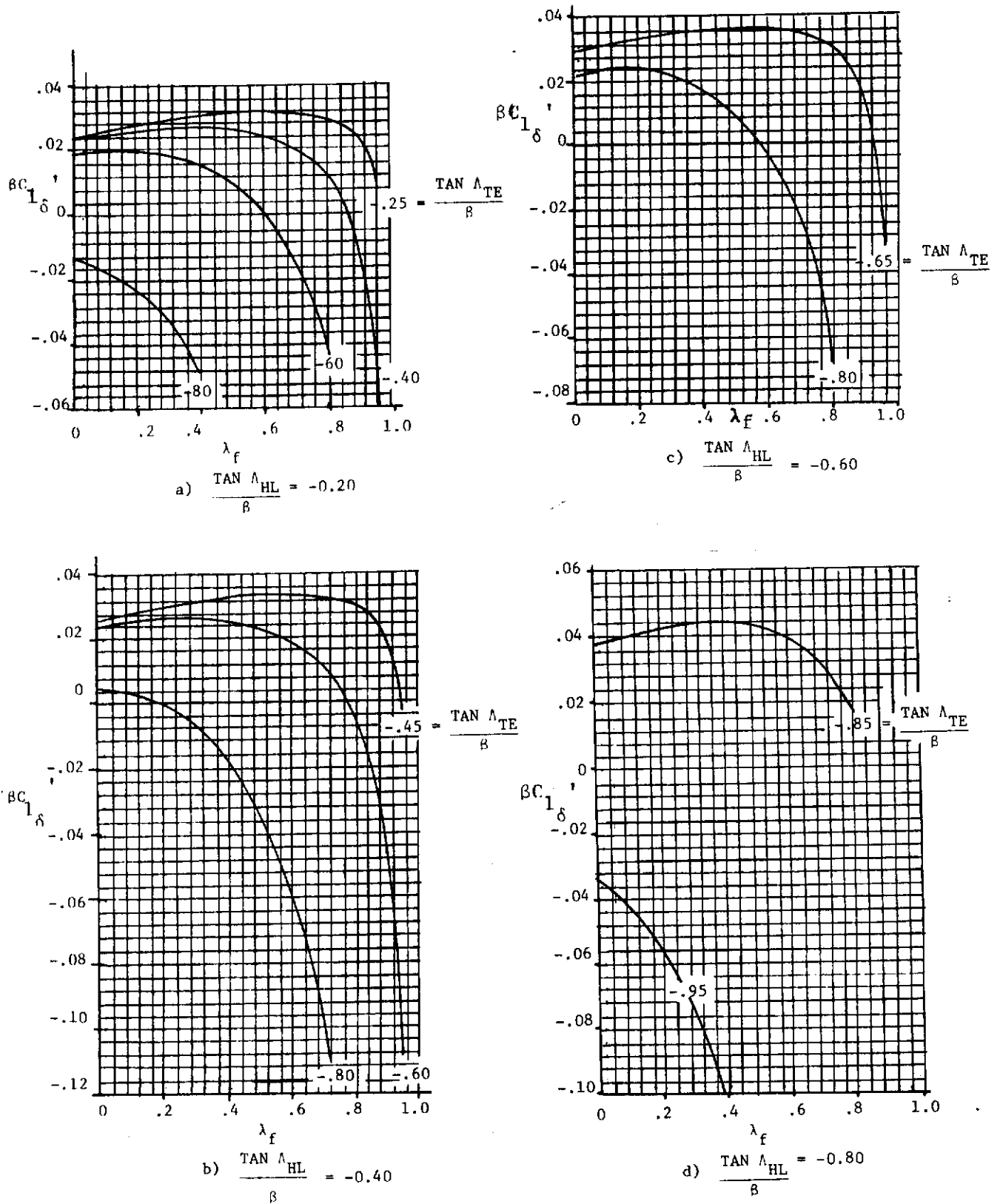
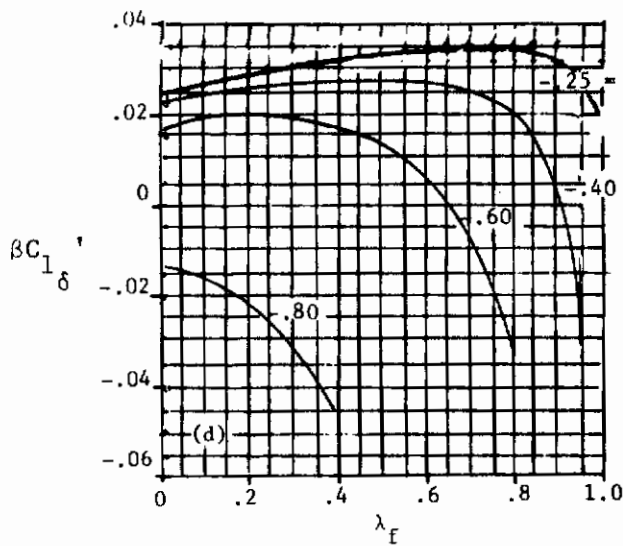
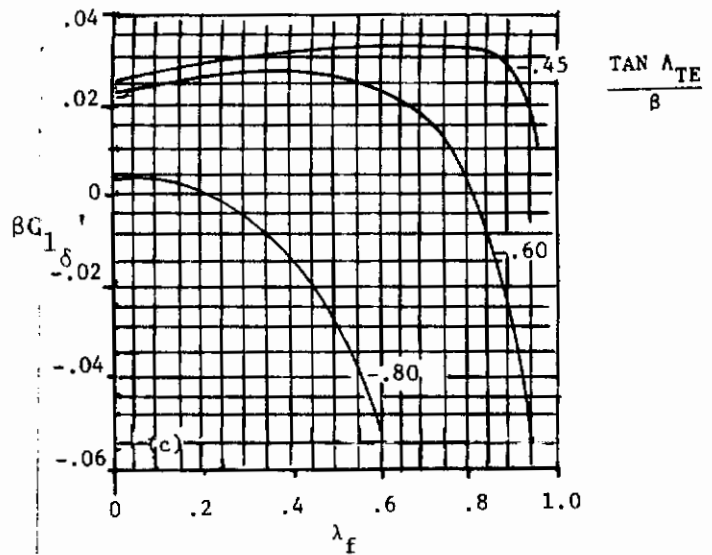


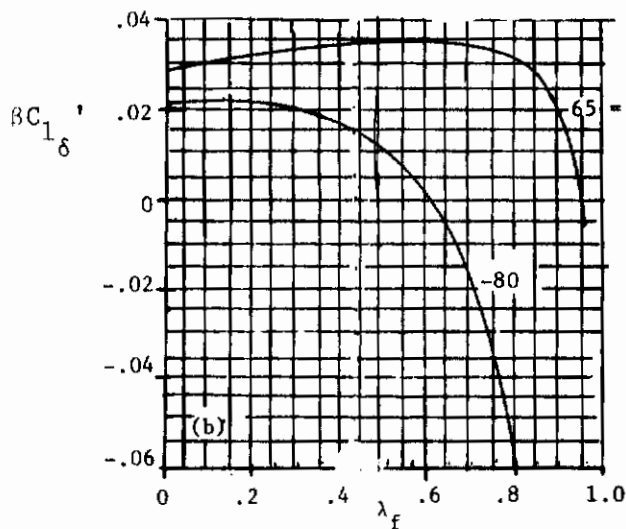
Figure 22. Rolling-Moment Derivative for Tapered Control Surfaces Having Outboard Edge Coincident with Wing Tip



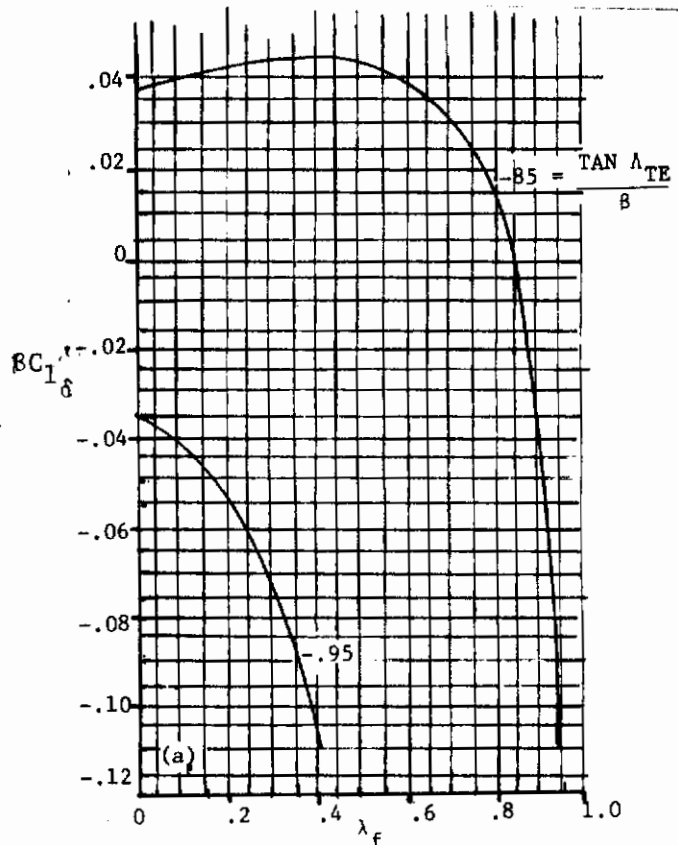
a)  $\frac{TAN \Lambda_{HL}}{\beta} = -0.20$



b)  $\frac{TAN \Lambda_{HL}}{\beta} = -0.40$



c)  $\frac{TAN \Lambda_{HL}}{\beta} = -0.60$



d)  $\frac{TAN \Lambda_{HL}}{\beta} = -0.80$

Figure 23. Rolling-Moment Derivative for Tapered Control Surfaces Having Outboard Edge Not Coincident with Wing-Tip



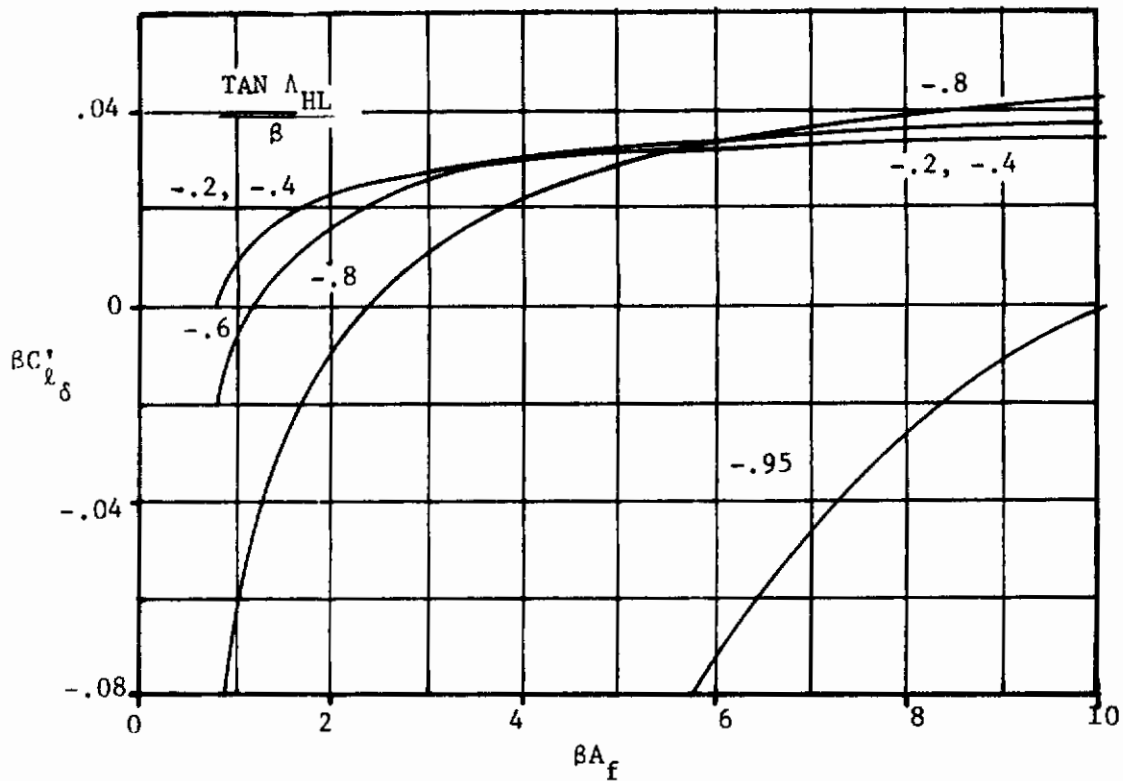


Figure 24. Rolling-Moment Derivative for Untapered Control Surfaces Having Outboard Edge Coincident with Wing Tip

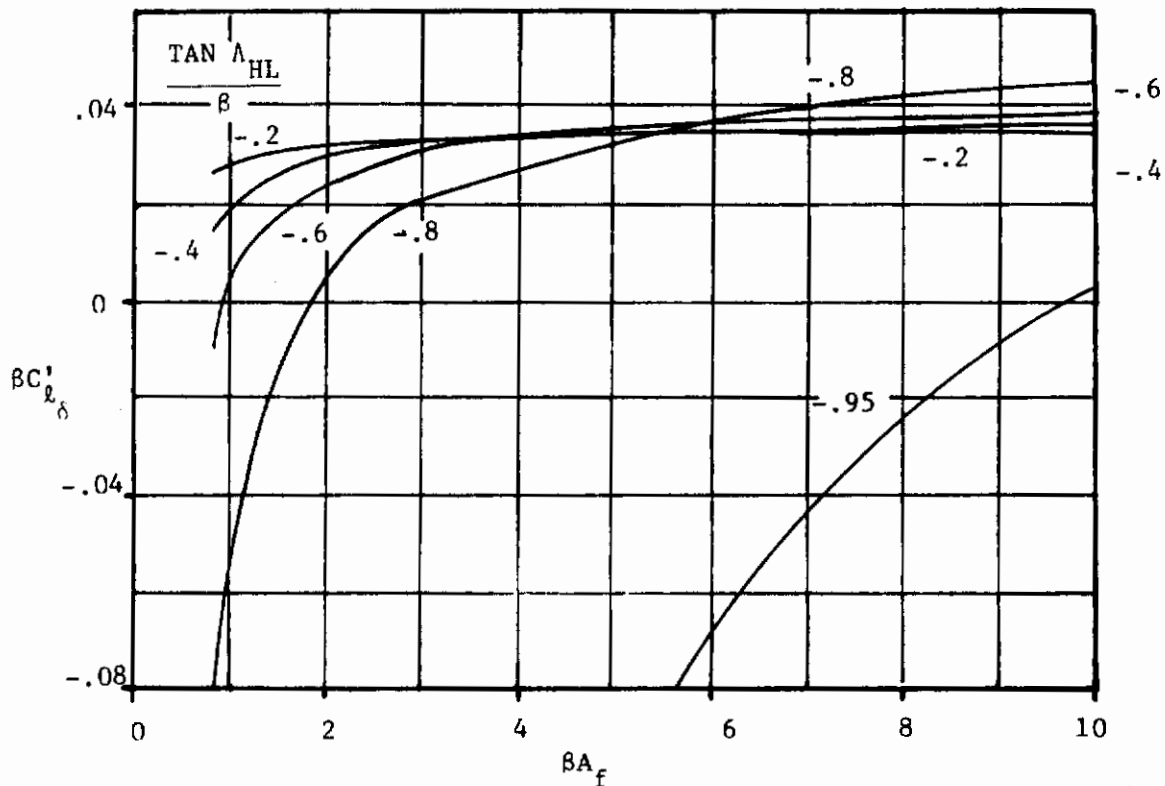


Figure 25. Rolling Moment Derivative for Untapered Control Surfaces Having Outboard Edge Not Coincident with Wing Tip

AFWAL-TR-84-3084

d. Untapered control surface with outboard edge not coincident with wing tip: use Figure 25.

Also, the absolute value of the quarter-chord sweep angle should be used in Datcom Figure 6.2.1.1-30, "Spoiler Rolling Moments...".

No substantiation was performed.

6.2.1.2 ROLLING-MOMENT DUE TO A DIFFERENTIALLY DEFLECTED  
HORIZONTAL STABILIZER

A. Subsonic

No modifications are required other than those described in Paragraph A of Sections 4.3.1.3, "Wing-Body Lift in the Nonlinear Angle-of-Attack Range" and 4.4.1 "Wing-Wing Combinations at Angle of Attack".

No substantiation was performed.

B. Transonic

No modifications are required other than those described in Paragraph B of Sections 4.1.3.2, "Wing Lift-Curve Slope"; 4.3.1.3, "Wing-Body Lift in the Nonlinear Angle-of-Attack Range"; and 4.4.1 "Wing-Wing Combinations at Angle of Attack". The comments in Paragraphs A and C of this section are also applicable here.

No substantiation was performed.

C. Supersonic

No modifications are required other than those described in Paragraph C of Sections 4.1.3.2, "Wing Lift-Curve Slope"; 4.3.1.2, "Wing-Body Lift-Curve Slope"; and 4.3.1.3, "Wing-Body Lift in the Nonlinear Angle-of-Attack Range".

No substantiation was performed.

## 6.2.2.1 YAWING MOMENT DUE TO CONTROL DEFLECTION

## A. Subsonic

No modifications are necessary other than the use of the absolute value of the leading-edge sweep angle in Datcom Figure 6.2.2.2-11, "Yawing Moment Due to Spoiler...".

Fair agreement was noted between test and predicted values for plain flap (average difference = .00111) and spoiler configurations (average difference = .00365). Table 33 contains a summary of the planforms analyzed, their parameters, and test and predicted results.

## B. Transonic

No modifications are necessary other than those described in Paragraph A of this section and Paragraph B of Section 4.1.3.2, "Wing Lift-Curve Slope".

No substantiation was performed.

## C. Supersonic

The absolute value of the midchord sweep angle should be used in Datcom Figure 6.2.2.1-13, "Yawing Moment Due to Aileron Deflection...". Also, the modifications described in Paragraph C of Sections 4.1.3.2, "Wing Lift-Curve Slope" and 6.2.1.1, "Rolling Moment Due to Control Deflection" are appropriate here. No other modifications are necessary.

No substantiation was performed.

6.3 SPECIAL CONTROL METHODS

No modifications are required.

No substantiation was performed.

7.1 WING DYNAMIC DERIVATIVES

7.1.1.1 WING PITCHING DERIVATIVE  $C_{Lq}$

A. Subsonic

No modifications are required other than those described in Paragraph A of Section 4.1.4.2, "Wing Pitching-Moment-Curve Slope".

Good agreement (5.13% error) was noted between test and predicted results for the single sweptforward planform found. Table 34 contains a summary of the planforms analyzed, their parameters, and test and predicted results.

B. Transonic

No method is presented.

C. Supersonic

Based on the reversibility theorem, the relation

$$(C_{Lq})_{FSW} = 2(C_{m\alpha})_{ASW} \tag{10}$$

should be used to obtain sweptforward wing characteristics, using an aft swept wing identical in planform to the forward swept wing in reverse flow. Care must be taken with respect to the moment reference center location, as the root quarterchord location for the sweptback planform is the three-quarter chord location for the sweptforward planform. Also, the modifications described in Paragraph C of Section 4.1.3.2, "Wing Lift-Curve Slope" are relevant here as well.

Analyses were performed using twice the sweptforward pitching-moment-curve slope value (using methods described in this report) to obtain the sweptback value of  $C_{Lq}$ . The values derived from using reversibility theorem assumptions were then compared to results obtained from this section with fair correlation (an average of 14%) was noted.

7.1.1.2 WING PITCHING DERIVATIVE  $C_{nq}$

A. Subsonic

No modifications are required other than those described in Paragraph A of Section 4.1.4.2, "Wing Pitching-Moment-Curve Slope".

An error of 16.12% was noted between test and predicted results for the single sweptforward planform found. Table 35 contains a summary of the planforms analyzed, their parameters, and test and predicted results.

B. Transonic

No modifications are required other than those described in Paragraphs A and C of this section and Paragraphs B and C of Section 4.1.3.2, "Wing Lift-Curve Slope".

No substantiation was performed.

C. Supersonic

The reversibility theorem states that

$$(C_{mq})_{FSW} = (C_{mq})_{ASW} \quad (11)$$

Hence, to obtain values of this derivative use the absolute value of the trailing-edge sweep angle. Also, the modifications described in Paragraph C of Sections 7.1.1.1, "Wing Pitching Derivative  $C_{Lq}$ " and 4.1.4.2, "Wing Pitching-Moment-Curve Slope" are applicable here.

No substantiation was performed.

7.1.1.3 WING PITCHING DERIVATIVE  $C_{Dq}$ 

## A. Subsonic

Other than using the absolute value of the leading-edge sweep angle, no modifications are necessary.

## B. Transonic

No method is presented.

## C. Supersonic

No method is presented.



7.1.2.1 WING ROLLING DERIVATIVE  $C_{Y_P}$ 

## A. Subsonic

No modifications are required.

Good agreement (average  $\Delta C_{Y_P} = .0145$ ) was noted between test and predicted values. Table 36 contains a summary of the planforms analyzed, their parameters, and test and predicted results.

## B. Transonic

No method is presented.

## C. Supersonic

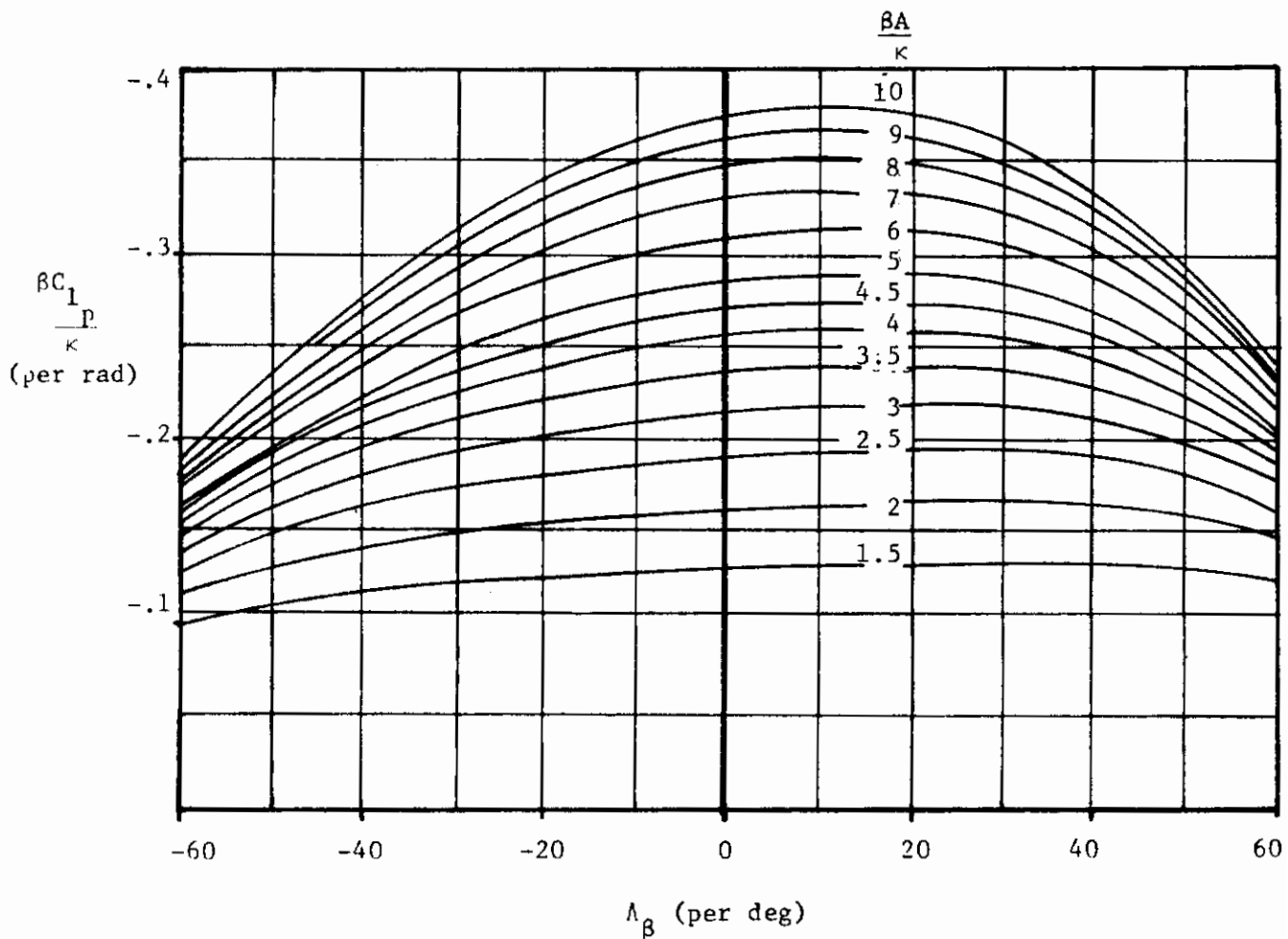
The methodology of this section is unsuited for sweptforward planforms. No method is presented to determine forward swept wing characteristics.

7.1.2.2 WING ROLLING DERIVATIVE  $C_{\ell p}$ 

## A. Subsonic

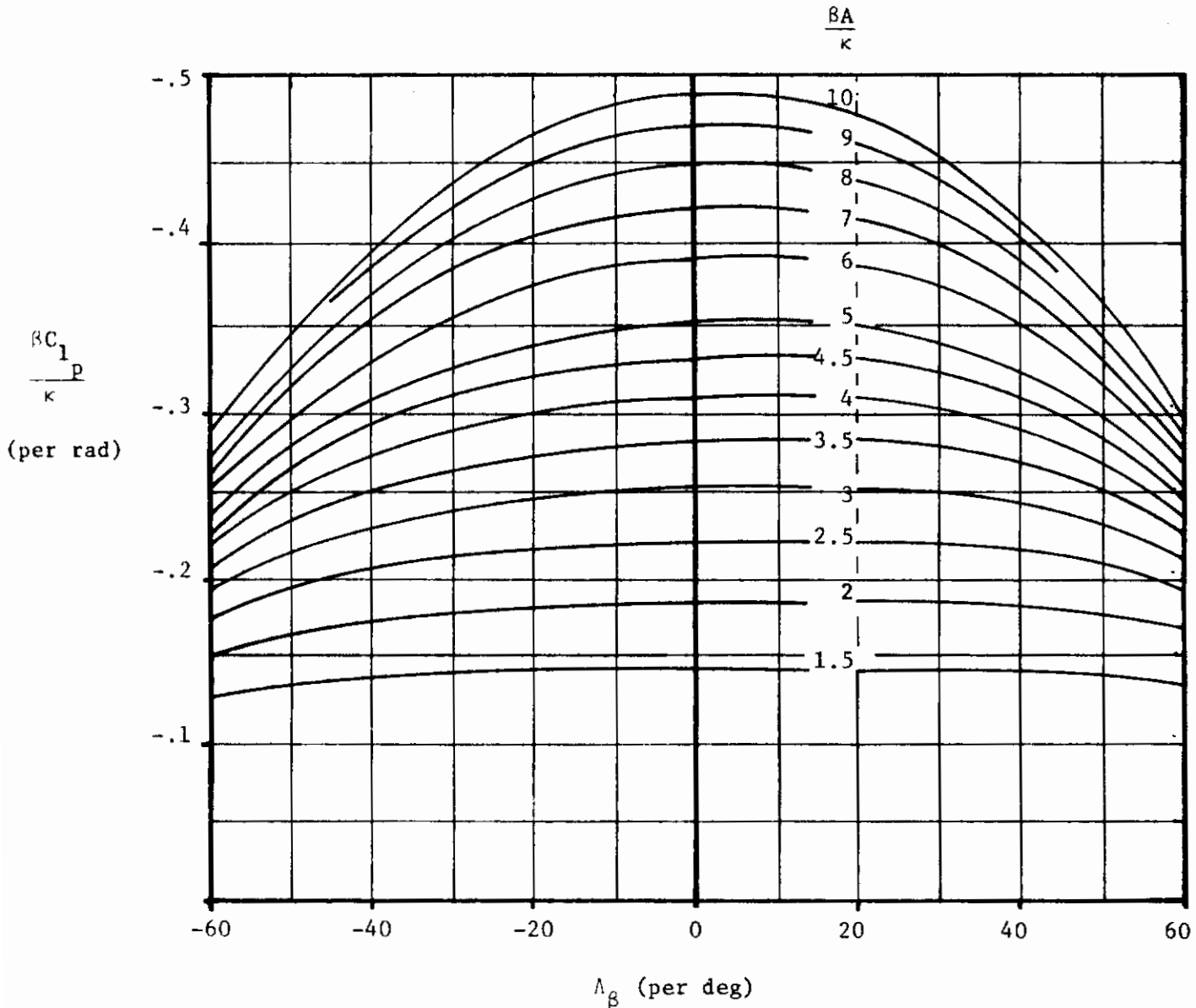
Figure 26 (from Reference 35) should be used in place of Datcom Figure 7.1.2.2-20, "Rolling-Damping Parameter at Zero Lift". The absolute value of the quarter-chord sweep angle should be used in Datcom Figure 7.1.2.2.-24, "Drag-Due-To-Lift Roll-Damping Parameter". Also, the modifications discussed in Paragraph A of Sections 4.1.5.1, "Wing Zero-Lift Drag", 4.1.3.3; "Wing Lift in the Nonlinear Angle-of-Attack Range"; and 4.1.3.2, "Wing Lift-Curve Slope" are appropriate here.

Good agreement (9.08% average error) was noted between test and predicted results. Table 37 contains a summary of the planforms analyzed, their parameters, and test and predicted values.



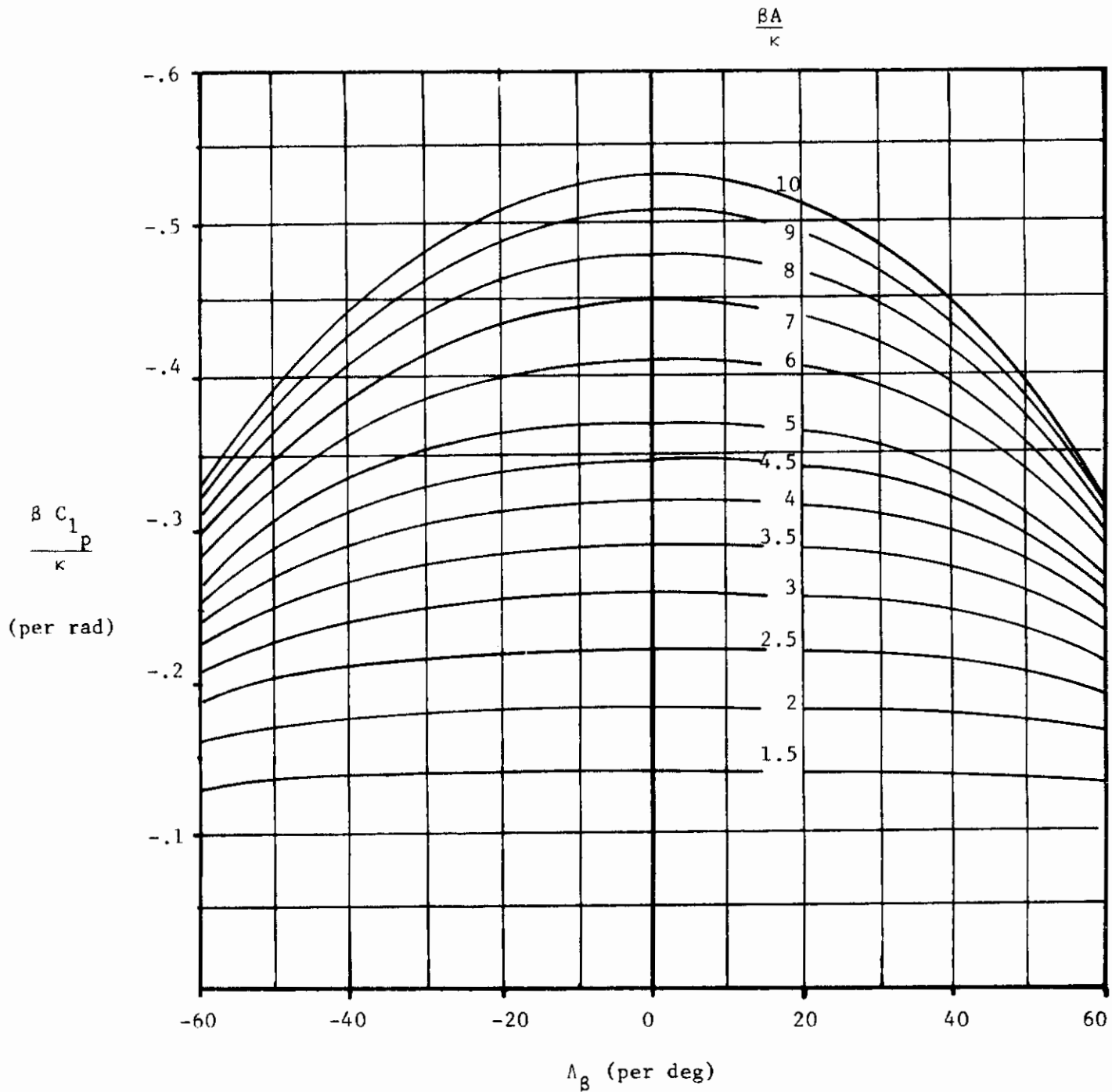
a. Taper Ratio = 0.0

Figure 26. Roll-Damping Parameter at Zero Lift



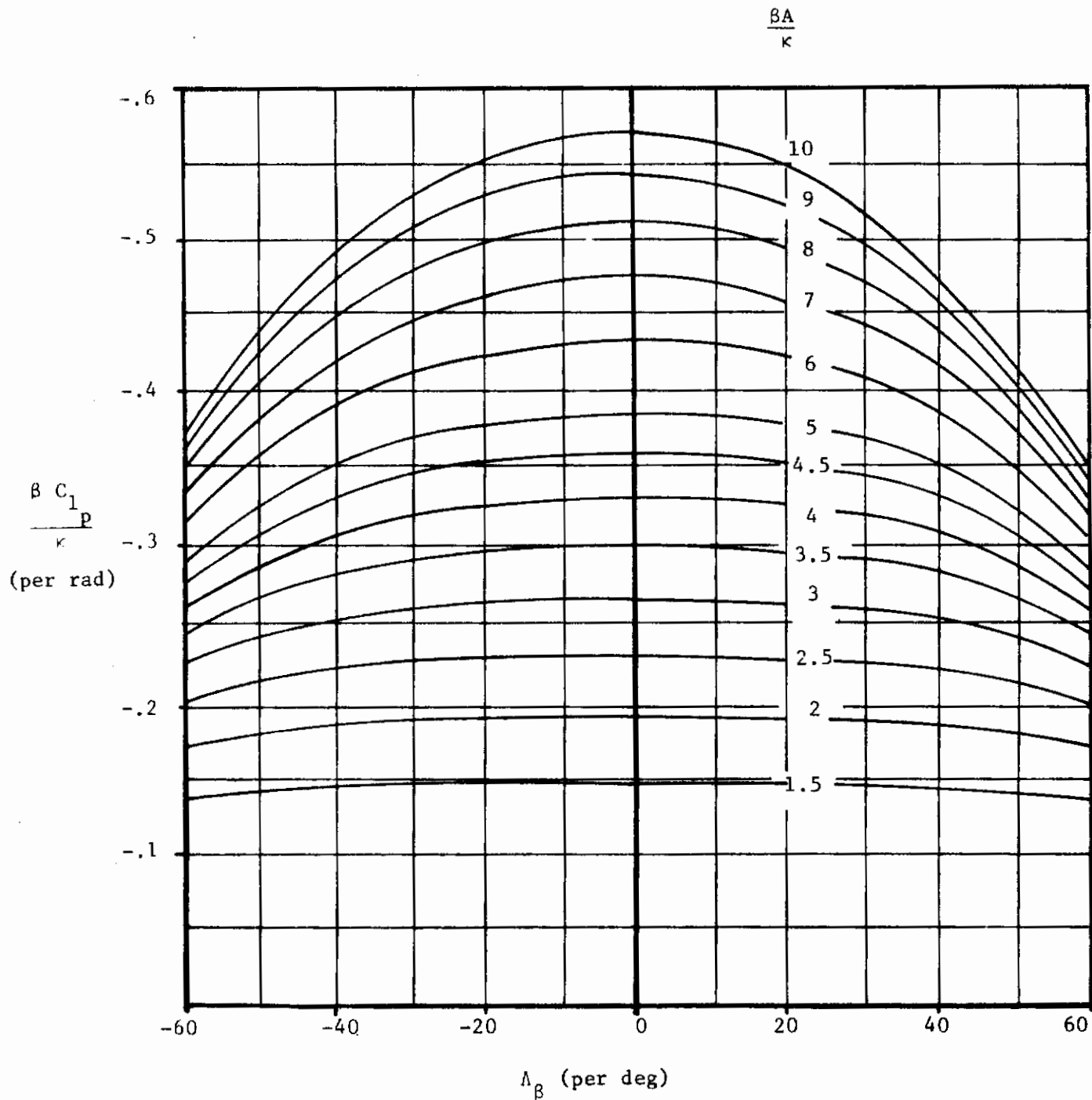
b) Taper Ratio = 0.25

Figure 26. Roll-Damping Parameter at Zero Lift



c) Taper Ratio = 0.5

Figure 26. Roll-Damping Parameter at Zero Lift



d) Taper Ratio = 1.0

Figure 26. Roll-Damping Parameter at Zero Lift

AFWAL-TR-84-3084

B. Transonic

No method is presented.

C. Supersonic

The absolute value of the designated sweep angle should be used in Datcom Figures 7.1.2.2-25, "Roll-Damping Parameter" and 7.1.2.2-27, "Damping-In-Roll Correction Factor for Sonic-Leading-Edge Region". No other modifications are necessary.

No substantiation was performed.

7.1.2.3 WING ROLLING DERIVATIVE  $C_{n_p}$

A. Subsonic

No modifications are necessary other than those discussed in Paragraph A of Sections 7.1.2.2, "Wing Rolling Derivative  $C_{l_p}$ "; 4.1.5.1, "Wing Zero-Lift Drag"; and 4.1.5.2, "Wing Drag at Angle of Attack".

B. Transonic

No method is presented.

C. Supersonic

The comments in Paragraph C of Section 7.1.2.1, "Wing Rolling Derivative  $C_{y_p}$ " are appropriate here.



7.1.3.1 WING YAWING DERIVATIVE  $C_{Y_r}$

A. All Speeds

No method is presented.

7.1.3.2 WING YAWING DERIVATIVE  $C_{\ell_r}$

A. Subsonic

Insufficient data currently exist to validate this section. Existing data indicate using the unswept quarter-chord line in Datcom Figure 7.1.3.2-10, "Wing Yawing Derivative  $C_{\ell_r}$ " to obtain approximations for sweptforward wing planforms.

B. Transonic

No method is presented.

C. Supersonic

No method is presented.

7.1.3.3 WING YAWING DERIVATIVE  $C_{n_r}$

A. Subsonic

Figure 27 should be used in lieu of Datcom Figure 7.1.3.3-6, "Low-Speed Drag-Due-To-Lift Yaw-Damping Parameter". Figure 28 should be used in lieu of Datcom Figure 7.1.2.2-7, "Low-Speed Profile-Drag-Yaw-Damping Parameter". These new figures are based on work done by Toll and Queijo (Reference 7).

No substantiation was performed.

B. Transonic

No method is presented.

C. Supersonic

No method is presented.

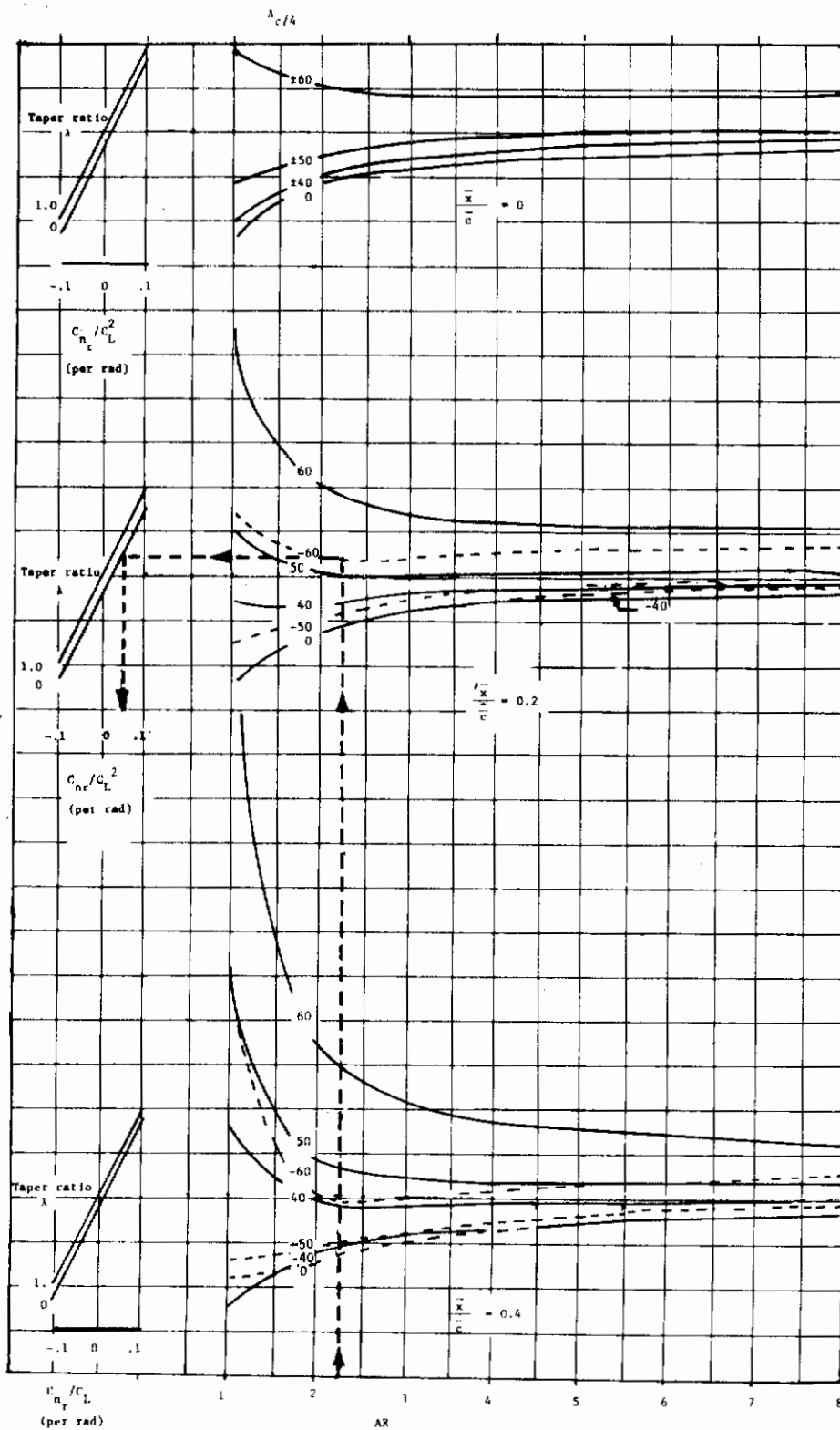


Figure 27. Low-Speed Drag-Due-To-Lift Yaw-Damping Parameter

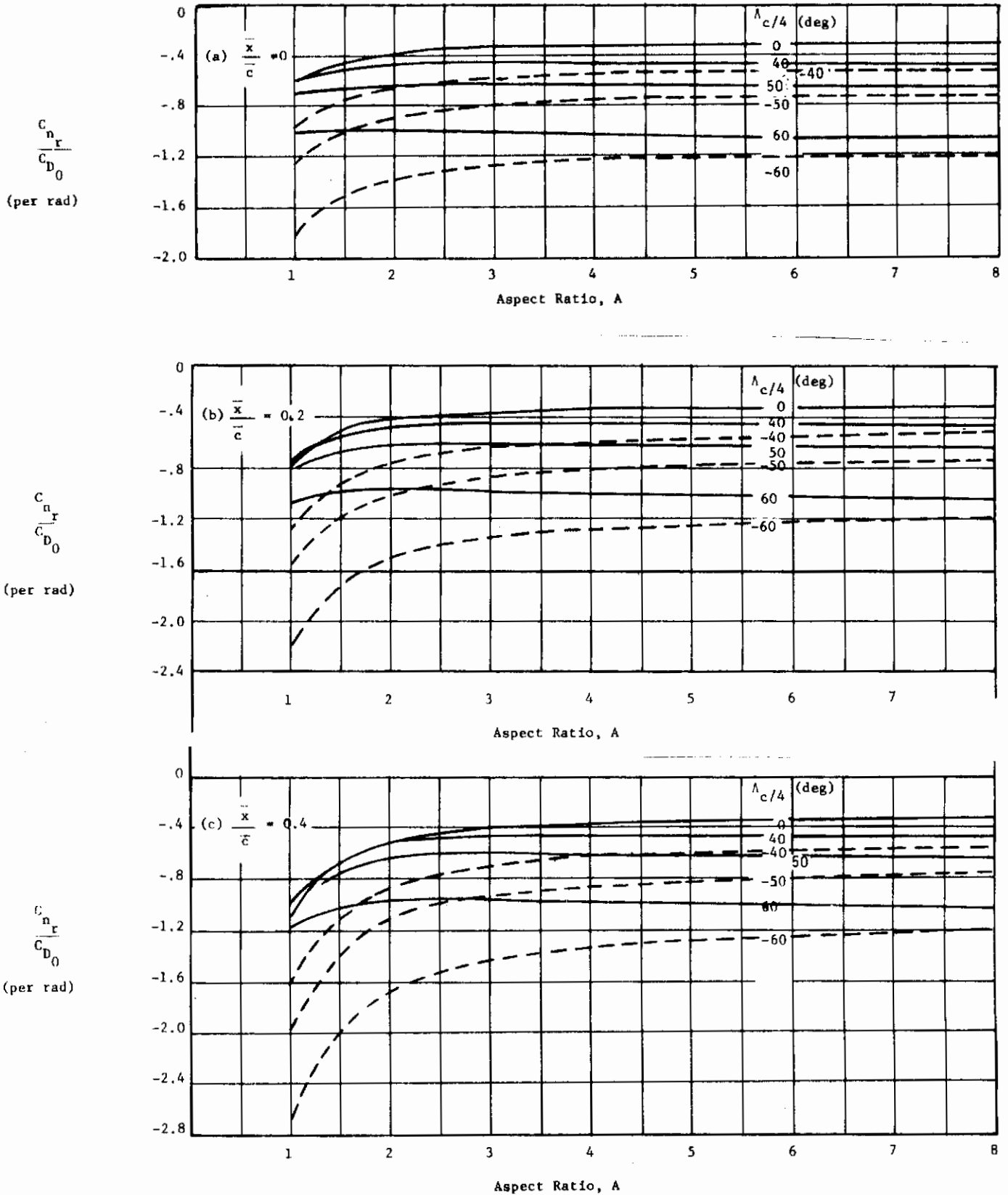


Figure 28. Low-Speed Profile-Drag Yaw-Damping Parameter

7.1.4.1 WING ACCELERATION DERIVATIVE  $C_{L_{\alpha}}$

A. Subsonic

No modifications are necessary other than those described in Paragraph A of Section 4.1.4.2, "Wing Pitching-Moment-Curve Slope".

No substantiation was performed.

B. Transonic

The comments of Paragraph A of this section are applicable here.

No substantiation was performed.

C. Supersonic

The reversibility theorem states that this derivative is identical whether in forward or reverse flight. Use the absolute value of the trailing-edge sweep angle to obtain forward swept wing characteristics.

No substantiation was performed.

7.1.4.2 WING ACCELERATION DERIVATIVE  $C_{m\dot{\alpha}}$

A. Subsonic

The comments of Paragraph A of Section 7.1.4.1, "Wing Acceleration Derivative  $C_{L\dot{\alpha}}$ " are appropriate here.

No substantiation was performed.

B. Transonic

The comments of Paragraph B of Section 7.1.4.1, "Wing Acceleration Derivative  $C_{L\dot{\alpha}}$ " are appropriate here.

No substantiation was performed.

C. Supersonic

No guidance was found in literature. The author suggests using the absolute value of the trailing-edge sweep angle to obtain forward-swept-wing characteristics.

No substantiation was performed.

AFWAL-TR-84-3084

7.1.4.3 WING DERIVATIVE  $C_{D,\alpha}$

A. Subsonic

No modifications are necessary.

No substantiation was performed.

B. Transonic

No method is presented.

C. Supersonic

No method is presented.

## 7.3 WING-BODY DYNAMIC DERIVATIVES

7.3.1.1 WING-BODY PITCHING DERIVATIVE  $C_{Lq}$ 

## A. All Speeds

No modifications to either method are necessary other than those described in Sections 7.1.1.1, "Wing Pitching Derivative C" and 4.3.1.2, "Wing-Body Lift-Curve Slope" in the appropriate speed range.

No substantiation was performed.



7.3.1.2 WING-BODY PITCHING DERIVATIVE  $C_{m_q}$

A. All Speeds

No modifications to either method are necessary other than those described in Sections 7.1.1.2, "Wing Pitching Derivative  $C_{m_q}$ ", and 4.3.1.2, "Wing-Body Lift-Curve Slope".

No substantiation was performed.

7.3.2.1 WING-BODY ROLLING DERIVATIVE  $C_{Yp}$

A. Subsonic

No modifications are necessary.

No substantiation was performed.

B. Transonic

No method is presented.

C. Supersonic

No method is presented.

7.3.2.2 WING-BODY ROLLING DERIVATIVE  $C_{\ell p}$ 

## A. Subsonic

No modifications are necessary other than those described in Paragraph A of Section 7.1.2.2, "Wing Rolling Derivative  $C_{\ell p}$ ".

No substantiation was performed.

## B. Transonic

No method is presented.

## C. Supersonic

The absolute value of the leading-edge sweep angle should be used in Datcom Figure 7.3.2.2-13, "Effect of the Fuselage on Roll Damping". Also, the modifications described in Paragraph C of Section 7.1.2.2, "Wing Rolling Derivative  $C_{\ell p}$ " should be incorporated.

7.3.2.3 WING-BODY ROLLING DERIVATIVE  $C_{n_p}$

A. Subsonic

No modifications are necessary other than those described in Paragraph A of Section 7.1.2.3, "Wing Rolling Derivative  $C_{n_p}$ ".

No substantiation was performed.

B. Transonic

No method is presented.

C. Supersonic

No method is presented.

7.3.3.1 WING-BODY ROLLING DERIVATIVE  $C_{Y_r}$

A. All Speeds

No methods are presented.

7.3.3.2 WING-BODY ROLLING DERIVATIVE  $C_{\ell_r}$

A. Subsonic

No modifications are necessary other than those described in Paragraph A of Section 7.1.3.2, "Wing Rolling Derivative  $C_{\ell_r}$ ".

No substantiation was performed.

B. Transonic

No method is presented.

C. Supersonic

No method is presented.

7.3.3.3 WING-BODY ROLLING DERIVATIVE  $C_{n_r}$ 

## A. Subsonic

The comments of Paragraph A of Section 7.1.3.3, "Wing Rolling Derivative  $C_{n_r}$ " are appropriate here.

No substantiation was performed.

## B. Transonic

No method is presented.

## C. Supersonic

No method is presented.

7.3.4.1 WING-BODY ACCELERATION DERIVATIVE  $C_{L\dot{\alpha}}$ 

## A. All Speeds

No modifications to either method are necessary other than those at the appropriate speed of Sections 7.1.4.1, "Wing Acceleration Derivative  $C_{L\dot{\alpha}}$ " and 4.3.1.2, "Wing-Body Lift-Curve Slope".

No substantiation was performed.

7.3.4.2 WING-BODY ACCELERATION DERIVATIVE  $C_{m\dot{\alpha}}$ 

## A. All Speeds

No modifications to either method are necessary other than those at the appropriate speed of Sections 4.3.1.2, "Wing-Body Lift-Curve Slope" and 7.1.4.2, "Wing Acceleration Derivative  $C_{n\dot{\alpha}}$ ".

No substantiation was performed.

## 7.4 WING-BODY-TAIL DYNAMIC DERIVATIVES

7.4.1.1 WING-BODY-TAIL PITCHING DERIVATIVE  $C_{Lq}$ 

## A. All Speeds

No modifications are necessary for either method other than those described at the appropriate speed in Sections 7.3.1.1, "Wing-Body Pitching Derivative  $C_{Lq}$ "; 4.4.1, "Wing-Wing Combinations at Angle of Attack"; 4.3.1.2, "Wing-Body Lift-Curve Slope"; and 4.1.3.2, "Wing Lift-Curve Slope".

No substantiation was performed.

7.4.1.2 WING-BODY-TAIL PITCHING DERIVATIVE  $C_{mq}$ 

## A. All Speeds

No modifications are necessary for either method other than those described at the appropriate speed in Sections 7.3.1.2, "Wing-Body Pitching Derivative  $C_{mq}$ ", 4.4.1, "Wing-Wing Combinations at Angle of Attack"; 4.3.1.2, "Wing-Body Lift-Curve Slope"; and 4.1.3.2, "Wing Lift-Curve Slope".

No substantiation was performed.



7.4.1.3 WING-BODY-TAIL PITCHING DERIVATIVE,  $C_{Dq}$ 

## A. Subsonic

Other than use of the absolute value of the leading-edge sweep angle in Datcom Figure 7.4.1.3 -4, "Variation in Downwash with Pitch Rate", no modifications are necessary.

No substantiation was performed.

## B. Transonic

No method is presented.

## C. Supersonic

No method is presented.

7.4.2.1 WING-BODY-TAIL ROLLING DERIVATIVE  $C_{Yp}$ 

## A. Subsonic

No modifications are necessary for either method.

No substantiation was performed.

## B. Transonic

No method is presented.

## C. Supersonic

No method is presented.

7.4.2.2 WING-BODY-TAIL ROLLING DERIVATIVE  $C_{lp}$ 

## A. Subsonic

No modifications are necessary for either method other than those described in Paragraph A of Section 7.1.2.2, "Wing Rolling Derivative  $C_{lp}$  ...".

No substantiation was performed.

## B. Transonic

No method is presented.

## C. Supersonic

No method is presented.

7.4.2.3 WING-BODY-TAIL ROLLING DERIVATIVE  $C_{n_p}$ 

## A. Subsonic

No modifications are necessary for either method other than those described in Paragraph A of Section 7.3.2.3, "Wing-Body Rolling Derivative  $C_{n_p}$ ".

No substantiation was performed.

## B. Transonic

No method is presented.

## C. Supersonic

No method is presented.

7.4.3.1 WING-BODY-TAIL YAWING DERIVATIVE  $C_{Y_r}$ 

## A. Subsonic

No modifications are required.

No substantiation was performed.

## B. Transonic

No method is presented.

## C. Supersonic

No method is presented.

7.4.3.2 WING-BODY-TAIL YAWING DERIVATIVE  $C_{\ell_r}$ 

## A. Subsonic

No modifications are required other than those described in Paragraph A of Section 7.3.3.2, "Wing-Body Yawing Derivative  $C_{\ell_r}$ ".

No substantiation was performed.

## B. Transonic

No method is presented.

## C. Supersonic

No method is presented.

7.4.3.3 WING-BODY-TAIL YAWING DERIVATIVE  $C_{n_r}$ 

## A. Subsonic

No modifications are required other than those described in Paragraph A of Section 7.3.3.3, "Wing-Body Yawing Derivative  $C_{n_r}$ ".

No substantiation was performed.

## B. Transonic

No method is presented.

## C. Supersonic

No method is presented.

7.4.4.1 WING-BODY-TAIL ACCELERATION DERIVATIVE  $C_{L\dot{\alpha}}$ 

## A. All Speeds

No modifications to either method are necessary other than those described at the appropriate speed of Sections 7.3.4.1, "Wing-Body Acceleration Derivative  $C_{L\dot{\alpha}}$ "; 4.4.1, "Wing-Wing Combinations at Angle of Attack"; 4.3.1.2, "Wing-Body Lift-Curve Slope"; and 4.1.3.2, "Wing Lift-Curve Slope".

No substantiation was performed.

7.4.4.2 WING-BODY-TAIL ACCELERATION DERIVATIVE  $C_{m\dot{\alpha}}$ 

## A. All Speeds

No modifications to either method are necessary other than those described at the appropriate speeds of Sections 7.3.4.2, "Wing-Body Acceleration Derivative C"; 4.4.1, "Wing-Wing Combinations at Angle of Attack"; 4.3.1.2, "Wing-Body Lift-Curve Slope"; and 4.1.3.2, "Wing Lift-Curve Slope".

No substantiation was performed.

7.4.4.3 WING-BODY-TAIL DERIVATIVE  $C_{D\dot{\alpha}}$

A. Subsonic

No modifications are necessary other than those described in Paragraph A of Section 4.4.1, "Wing-Wing Combinations at Angle of Attack".

No substantiation was performed.

B. Transonic

No method is presented.

C. Supersonic

No method is presented.

7.4.4.4 WING-BODY-TAIL DERIVATIVE  $C_{Y\dot{\beta}}$ 

## A. Subsonic

The absolute value of the vertical tail leading-edge sweep angle should be used in Datcom Figures 7.4.4.4-6, "Sidewash Contribution Due to Angle of Attack"; 7.4.4.4 - 22, "Sidewash Contribution Due to Dihedral"; 7.4.4.4-26, "Sidewash Contribution Due to Wing Twist"; and 7.4.4.4-42, "Sidewash Contribution Due to Body Effect".

No substantiation was performed.

## B. Transonic

No method is presented.

## C. Supersonic

No method is presented.



7.4.4.5 WING-BODY-TAIL DERIVATIVE  $C_{l\dot{\beta}}$ 

## A. Subsonic

No modifications are necessary other than those described in Paragraph A of Section 7.4.4.4, "Wing-Body-Tail Derivative  $C_{Y\dot{\beta}}$ ".

No substantiation was performed.

## B. Transonic

No method is presented.

## C. Supersonic

No method is presented.

7.4.4.6 WING-BODY-TAIL DERIVATIVE  $C_{n\dot{\beta}}$ 

## All Speeds

The comments of Section 7.4.4.5 at the appropriate speed are relevant here.

No substantiation was performed.

# *Contrails*

## APPENDIX - SUMMARY OF METHODOLOGY MODIFICATIONS

<u>SECTION</u>	<u>DERIVATIVE</u>	<u>MODIFICATIONS</u>
4.1	WINGS AT ANGLE OF ATTACK	
4.1.3.1	$\alpha_o$	<p>Subsonic: Use Equation 2 in place of Datcom Equation 4.1.3.1-b. Use Figure 2 to obtain FSW Twist Effect Factors.</p> <p>Transonic: NDM</p> <p>Supersonic: NDM</p>
4.1.3.2	$C_{L_\alpha}$	<p>Subsonic: No modifications are required for Method 1. Method 2 should not be used.</p> <p>Transonic: Use <math> \Lambda_{c/2} </math> in Datcom Figure 4.1.3.2-53b.</p> <p>Supersonic: In Datcom Figure 4.1.3.2-56a through -56f use <math> \Lambda_{TE} </math> in place of <math>\Lambda_{LE}</math>. Use <math> \Lambda_{LE} </math> in Datcom Figure 4.1.3.2-60.</p> <p>Hypersonic: Supersonic comments are applicable here.</p>
4.1.3.3	$C_{L @ \alpha}$	<p>Subsonic: Use <math> \Lambda_{LE} </math> in Datcom Equation 4.1.3.3-e. See report text if planform parameter <math>J &gt; 1</math>.</p> <p>Transonic: Use <math> \Lambda_{LE} </math> in all equations and charts.</p> <p>Supersonic: Use <math> \Lambda_{LE} </math> in all equations and charts. See modifications, Section 4.1.3.2, Supersonic.</p> <p>Hypersonic: See modifications, this section and 4.1.3.2, Supersonic.</p>
4.1.3.4	$C_{L_{max}}$ & $\alpha_{C_{L_{max}}}$	<p>Subsonic: Method 1: No modifications are necessary.</p> <p>Method 2: Use <math> \Lambda_{LE} </math> in Datcom Figures 4.1.3.4-21a, -21b and -22. See modifications, Section 4.1.3.1, Subsonic.</p> <p>Method 3: Use <math> \Lambda_{LE} </math> in Datcom Figures 4.1.3.4-24a and -25b.</p>

<u>SECTION</u>	<u>DERIVATIVE</u>	<u>MODIFICATIONS</u>
4.1.3.4 con't		<p>Transonic: Use <math> \Lambda_{LE} </math> in Datcom Figures 4.1.3.4-24a, -25b and -26b.</p> <p>Supersonic: See Modifications, Sections 4.1.3.2 and 4.1.3.3, Supersonic</p> <p>Hypersonic: See Modifications, Sections 4.1.3.2 and 4.1.3.3, Supersonic</p>
4.1.4.1	$C_{m_o}$	<p>Subsonic: Method 1: Use Figure 5 to obtain FSW twist effect factor Method 2: Do not use</p> <p>Transonic: NDM</p> <p>Supersonic: NDM</p>
4.1.4.2	$\frac{dC_m}{dC_L}$	<p>Subsonic: Use Figure 6 to obtain FSW aerodynamic-center locations.</p> <p>Transonic: No sweptforward wing method presented. Do not use existing Datcom method.</p> <p>Supersonic: Use Figure 6 to obtain FSW aerodynamic-center locations.</p> <p>Hypersonic: Use Figure 6 to obtain FSW aerodynamic-center locations.</p>
4.1.4.3	$C_m @ \alpha$	<p>All speeds: No sweptforward wing method presented. Do not use existing Datcom methods. However, Datcom Figure 4.1.4.3-25 can be used to determine pitch-up/down trend by use of <math> \Lambda_{c/4} </math>.</p>
4.1.5.1	$C_{D_o}$	<p>All speeds: No modifications necessary. Do not use results for performance estimation.</p>
4.1.5.2	$C_{D_L}$	<p>Subsonic: Use <math> \Lambda_{LE} </math> in Datcom Figures 4.1.5.2-53a and -53b. Use <math> \Lambda_{c/4} </math> in Datcom Figure 4.1.5.2-48. Use Figure 8 in place of Datcom Figure 4.1.5.2-42 for sweptforward wing planforms. Do not use results for performance estimation.</p>

<u>SECTION</u>	<u>DERIVATIVE</u>	<u>MODIFICATIONS</u>
4.1.5.2 con't		<p>Transonic: Use <math> \Lambda_{LE} </math> in Datcom Figure 4.1.5.2-55. Do not use results for performance estimation.</p> <p>Supersonic: No modifications necessary. Do not use results for performance estimation.</p>
4.3	Wing-Body, Tail-Body Combinations at Angle of Attack	
4.3.1.2	$C_{L\alpha}$	<p>Subsonic: No modifications for either method.</p> <p>Transonic: Use <math> \Lambda_{TE} </math> for <math>\Lambda_{LE}</math> in Datcom Figure 4.3.1.2-11. See modifications Section 4.1.3.2, Transonic.</p> <p>Supersonic: Use <math> \Lambda_{TE} </math> for <math>\Lambda_{LE}</math> in Datcom Figure 4.3.1.2-11. See Section 4.1.3.2, Supersonic.</p>
4.3.1.3	$C_L @ \alpha$	<p>Subsonic: See Sections 4.1.3.3 and 4.4.1, Subsonic.</p> <p>Transonic: See Sections 4.1.3.2, 4.1.3.3, 4.3.1.2, and 4.4.1, Transonic.</p> <p>Supersonic: See Sections 4.1.3.2, 4.1.3.3, 4.3.1.2 and 4.4.1, Supersonic.</p>
4.3.1.4	$C_{L_{max}} @ \alpha C_{L_{max}}$	<p>Subsonic: Method 1: No modifications necessary. Method 2: Use Figure 9a in place of Datcom Figure 4.3.1.4-12b and Figure 9b in place of Datcom Figure 4.3.1.4-12c.</p> <p>Transonic: NDM</p> <p>Supersonic: Method 1: See Sections 4.1.3.4 and 4.3.1.2, Supersonic. Method 2: See Section 4.3.1.3</p>
4.3.2.1	$C_{m\alpha}$	<p>Subsonic: Method 1: See Section 4.1.4.1, Method 1, Subsonic. Method 2: Do not use.</p> <p>Transonic: Method 1: Section 4.1.4.1, Method 1, Subsonic Method 2: Do not use.</p> <p>Supersonic: No sweptforward wing method presented. Do not use existing Datcom method.</p>

<u>SECTION</u>	<u>DERIVATIVE</u>	<u>MODIFICATIONS</u>
4.3.2.2	$\frac{dC_m}{dC_L}$	<p>Subsonic: See Section 4.1.4.2, Subsonic.</p> <p>Transonic: No sweptforward wing method presented. Do not use existing Datcom method.</p> <p>Supersonic: Use <math> \Lambda_{LE} </math> in Datcom Figures 4.3.2.2-36b and 4.3.2.2-37. See Sections 4.1.3.2, 4.1.4.2, and 4.3.1.2, Supersonic.</p>
4.3.3.1	$C_{D_o}$	<p>Subsonic: No modifications necessary. Do not use results for performance estimation.</p> <p>Transonic: No modifications necessary. Do not use results for performance estimation.</p> <p>Supersonic: Use <math> \Lambda_{LE} </math> in all equations and figures in this speed range. Do not use results for performance estimation.</p>
4.3.3.2	$C_D @ \alpha$	<p>All speeds: Method 1: Do not use. Method 2: See section 4.1.5.2 in the appropriate speed range. Do not use results for performance estimation.</p>
4.4	Wing-Wing Combinations at Angle of Attack	
4.4.1	Downwash	<p>Subsonic: Method 1: Use Figure 10 in place of Datcom Figure 4.4.1-66, use <math> \Lambda_{c/l} </math> in Datcom Figure 4.4.1-67. See Sections 4.1.3.1 and 4.1.3.4, Subsonic. See text to increase accuracy of this method. Method 2: No modifications. Method 3: Use Figure 11 in place of Datcom Figure 4.4.1-71. See Section 4.3.1.3, Subsonic.</p>
	Downwash due to flap deflection	No modifications necessary.
	Upwash	Method unsuited for swept wings. No method presented.
	Dynamic pressure ratio	No modifications necessary.

<u>SECTION</u>	<u>DERIVATIVE</u>	<u>MODIFICATIONS</u>
	Downwash	Transonic: See Sections 4.1.3.2 and 4.1.3.3, Transonic.
	Dynamic pressure ratio	No modifications necessary.
	Downwash	Supersonic: Method 1: No modifications necessary. Method 2: Applicable to rectangular and sweptback planforms only. Method 3: Use Figure 12 in place of Datcom Figure 4.4.1-80.
	Dynamic pressure ratio	No modifications necessary.
<hr/>		
4.5	Wing-Body Tail Combinations at Angle of Attack	
4.5.1.1	$C_{L_{\alpha}}$	All speeds: For both methods, see Sections 4.1.3.2, 4.3.1.2, and 4.4.1 in the appropriate speed range.
4.5.1.2	$C_L @ \alpha$	All speeds: For both methods, see Sections 4.1.3.2, 4.1.3.3, 4.1.3.4, 4.3.1.2, 4.3.1.3, and 4.4.1 in the appropriate speed range.
4.5.1.3	$C_{L_{max}} @ \alpha_{C_{L_{max}}}$	All speeds: See Sections 4.1.4.2, 4.1.4.3, 4.3.1.4, 4.3.2.2, 4.3.3.1, 4.3.3.2, and 4.4.1 in the appropriate speed range.
4.5.2.1	$C_{m_{\alpha}}$	All speeds: See Sections 4.3.1.2, 4.3.2.2, 4.3.3.2, and 4.4.1 in the appropriate speed range.
4.5.3.1	$C_{D_o}$	Subsonic: No modifications necessary. Do not use results for performance estimation.  Transonic: Use $ A_{c/4} $ in Datcom Figure 4.5.3.1-19. Do not use results for performance estimation.  Supersonic: See Section 4.3.3.1, Supersonic. Do not use results for performance estimation.

<u>SECTION</u>	<u>DERIVATIVE</u>	<u>MODIFICATIONS</u>
4.5.3.2	$C_{D_{\alpha}}$	All speeds: See Sections 4.1.3.1, 4.1.5.1, 4.3.1.2, 4.3.2.1, 4.3.2.2, 4.3.3.1, 4.3.3.2, and 4.4.1 in the appropriate speed range. Do not use results for performance estimation.
4.6	Power effects at Angle of Attack	No modifications are expected other than those described for power-off coefficients.
4.7	Ground effects at angle of attack	No modifications are expected other than those described for out-of-ground-effect coefficients.
4.8	Low-Aspect-Ratio Wings and Wing-Body Combination at Angle of Attack	This section is unsuited for sweptforward wing applications and should not be used.
5.1	Wings in Sideslip	
5.1.1.1	$C_{Y_{\beta}}$	Subsonic: No modifications are necessary. Transonic: NDM Supersonic: Method applicable to rectangular planforms only.
5.1.2.1	$C_{l_{\beta}}$	Subsonic: See text for modified use of Datcom Figure 5.1.2.1-27. Transonic: See Section 4.1.3.2, Transonic. Supersonic: See Sections 4.1.3.2 and 7.1.2.2, Supersonic.
5.1.3.1	$C_{n_{\beta}}$	Subsonic: No modifications necessary Transonic: NDM Supersonic: See Sections 5.1.1.1, Supersonic.
5.2	Wing-Body Combinations in Sideslip	



<u>SECTION</u>	<u>DERIVATIVE</u>	<u>MODIFICATIONS</u>
5.2.1.1	$C_{y\beta}$	All speeds: No modifications necessary
5.2.2.1	$C_{\ell\beta}$	All speeds: See Section 5.1.2.1 in the appropriate speed range.
5.2.3.1	$C_{n\beta}$	All speeds: No modifications necessary.
5.3	Tail-Body Combinations in Sideslip	
5.3.1.1	$C_{y\beta}$	Subsonic: No modifications necessary. Transonic: NDM Supersonic: See Section 4.1.3.2, Supersonic. Hypersonic: See Section 4.1.3.2, Hypersonic.
5.3.2.1	$C_{\ell\beta}$	Subsonic: No modifications required. Transonic: NDM Supersonic: See Section 5.3.1.1, Supersonic.
5.3.3.1	$C_{n\beta}$	Subsonic: See Section 4.1.4.2, Subsonic. Transonic: NDM Supersonic: See Sections 4.1.4.2 and 5.3.1.1, Supersonic.
5.4	Flow Fields in Sideslip	
5.4.1	Wake and Sidewash	Subsonic: No modifications necessary. Transonic: NDM Supersonic: NDM
5.5	Low-Aspect-Ratio Wings and Wing-Body Combinations in Sideslip	This section is unsuited for swept-forward wing applications and should not be used.

# Contrails

AFWAL-TR-84-3084

<u>SECTION</u>	<u>DERIVATIVE</u>	<u>MODIFICATIONS</u>
5.6	Wing-Body-Tail Combinations in Sideslip	
5.6.1.1	$C_{y\beta}$	Subsonic: No modifications necessary. Transonic: NDM Supersonic: See Section 5.3.1.1, Supersonic.
5.6.2.1	$C_{\ell\beta}$	Subsonic: No modifications necessary. Transonic: NDM Supersonic: See Section 5.3.1.1, Supersonic.
5.6.3.1	$C_{n\beta}$	Subsonic: No modifications necessary. Transonic: NDM Supersonic: No modifications necessary
6.1	Symmetrically Deflected Flaps and Control Devices on Wing-Body and Tail-Body Combinations	
6.1.4.1	$C_{L\delta}$	All speeds: No modifications necessary. See text to obtain increased accuracy at subsonic speeds.
6.1.4.2	$(C_{L\alpha})_{\delta}$	All speeds: No modifications necessary.
6.1.4.3	Maximum Lift with High-Lift and Control Devices	Use Figure 17 in place of Datcom Figure 6.1.4.3-10.
6.1.5.1	$C_{m\delta}$	Subsonic: No modifications are necessary, to the jet-flap methods and leading-edge device and to Method 1, for trailing-edge mechanical flaps. Figure 18 should be used to obtain sweptforward wing estimates in Method 2 for trailing-edge mechanical flaps. Transonic: Existing methodologies should not be used for FSW estimation. No method is presented.

<u>SECTION</u>	<u>DERIVATIVES</u>	<u>MODIFICATIONS</u>
6.1.5.1 con't		Supersonic: Use Figure 19 in place of Datcom Figure 6.1.5.1-70 for sweptforward wings. Use Figure 20 in place of Datcom Figure 6.1.5.1-73b for sweptforward wings. See Section 6.2.1.1, Supersonic.
6.1.5.2	$(C_{m_{\alpha}})_{\delta}$	All speeds: No modifications necessary.
6.1.6.1	$C_{h_{\alpha}}$	Subsonic: No modifications necessary. Transonic: NDM  Supersonic: Treat sweptforward control as if on sweptback wing with inverse taper. See text for notation modifications.
6.1.6.2	$C_{h_{\delta}}$	Subsonic: No modifications necessary.  Transonic: NDM  Supersonic: Use Figure 21 in place of Datcom Figure 6.1.6.2-17.
6.1.7	$(C_{D})_{\delta}$	Subsonic: No modifications necessary.  Transonic: NDM  Supersonic: No modifications necessary.
6.2	Asymmetrically Deflected Controls on Wing-Body and Tail-Body Combinations	
6.2.1.1	$C_{L_{\delta}}$	Subsonic: No modifications necessary.  Transonic: See Section 4.1.3.2, Transonic.  Supersonic: Use $ A'_{c/4} $ in Datcom Figure 6.2.1.1-30. Use Figure 22 in place of Datcom Figure 6.2.1.1-27 for sweptforward wings. Use Figure 23 in place of Datcom Figure 6.2.1.1-28 for sweptforward wings.

<u>SECTION</u>	<u>DERIVATIVE</u>	<u>MODIFICATIONS</u>
6.2.1.1 (Cont'd)		Use Figure 24 in place of Datcom Figure 6.2.1.1-29a for sweptforward wings. Use Figure 25 in place of Datcom Figure 6.2.1.1-29b for sweptforward wings.
6.2.1.2	$(C_\ell)_{H.S.}$	<p>Subsonic: See Sections 4.3.1.3 and 4.4.1, Subsonic.</p> <p>Transonic: See Sections 4.1.3.2, 4.3.1.3, and 4.4.1, Transonic.</p> <p>Supersonic: See Sections 4.1.3.2, 4.3.1.2, and 4.3.1.3, Supersonic.</p>
6.2.2.1	$C_{n_\delta}$	<p>Subsonic: Use <math> \Lambda_{LE} </math> in Datcom Figure 6.2.2.1-11.</p> <p>Transonic: See Section 4.1.3.2, transonic</p> <p>Supersonic: Use <math> \Lambda_{c/2} </math> in Datcom Figure 6.2.2.1-13. See Sections 4.1.3.2 and 6.2.1.1, Supersonic.</p>
6.3	Special Control Methods	No modifications necessary.
7.1	Wing Dynamic Derivatives	
7.1.1.1	$C_{L_q}$	<p>Subsonic: See Section 4.1.4.2, Subsonic.</p> <p>Transonic: NDM</p> <p>Supersonic: Use the equation,</p> $(C_{L_q})_{FSW} = 2(C_{m_\alpha})_{ASW}$ <p>See text for details. See also Section 4.1.3.2, Supersonic.</p>
7.1.1.2	$C_{m_q}$	<p>Subsonic: See Section 4.1.4.2, Subsonic.</p> <p>Transonic: See Section 4.1.3.2, Transonic.</p> <p>Supersonic: Use <math> \Lambda_{TE} </math> for <math>\Lambda_{LE}</math> in all equations and charts. See Sections 4.1.4.2 and 7.1.1.1, Supersonic.</p>

<u>SECTION</u>	<u>DERIVATIVES</u>	<u>MODIFICATIONS</u>
7.1.1.3	$C_{Dq}$	<p>Subsonic: Use <math> \Lambda_{LE} </math> in all equations and charts.</p> <p>Transonic: NDM</p> <p>Supersonic: NDM</p>
7.1.2.1	$C_{Yp}$	<p>Subsonic: No modifications necessary.</p> <p>Transonic: NDM</p> <p>Supersonic: The methodology of this section is unsuited for sweptforward wings and should not be used. No method is presented.</p>
7.1.2.2	$C_{lp}$	<p>Subsonic: Use Figure 26 in place of Datcom Figure 7.1.2.2-20, use <math> \Lambda_{c/4} </math> in Datcom Figure 7.1.2.2-24. See Sections 4.1.3.3 and 4.1.5.1, Subsonic.</p> <p>Transonic: NDM</p> <p>Supersonic: Use <math> \Lambda_{c/2} </math> in Datcom Figure 7.1.2.2-25 and <math> \Lambda_{LE} </math> in Datcom Figure 7.1.2.2-27.</p>
7.1.2.3	$C_{np}$	<p>Subsonic: See Sections 4.1.5.1, 4.1.5.2, and 7.1.2.2, Subsonic.</p> <p>Transonic: NDM</p> <p>Supersonic: The methodology of this section is unsuited for sweptforward wings and should not be used. No method is presented.</p>
7.1.3.1	$C_{Yr}$	All speeds: NDM
7.1.3.2	$C_{lr}$	<p>Subsonic: Section not validated due to lack of data. For all sweptforward planforms, use unswept quarter-chord line in Datcom Figure 7.1.3.2-10.</p> <p>Transonic: NDM</p> <p>Supersonic: NDM</p>

<u>SECTION</u>	<u>DERIVATIVES</u>	<u>MODIFICATIONS</u>
7.1.3.3	$C_{n_r}$	Subsonic: Use Figure 27 in place of Datcom Figure 7.1.3.3-6 and Figure 28 in place of Datcom Figure 7.1.3.3-7.  Transonic: NDM  Supersonic: NDM
7.1.4.1	$C_{L_{\dot{\alpha}}}$	Subsonic: See Section 4.1.4.2, Subsonic.  Transonic: See Sections 4.1.3.2, Transonic and 4.1.4.2, Subsonic.  Supersonic: Use $ \Lambda_{TE} $ whenever $\Lambda_{LE}$ is called for.
7.1.4.2	$C_{m_{\dot{\alpha}}}$	Subsonic: See Section 4.1.4.2, Subsonic.  Transonic: See Sections 4.1.3.2, Transonic and 4.1.4.2, Subsonic.  Supersonic: Use $ \Lambda_{TE} $ whenever $\Lambda_{LE}$ is called for.
7.1.4.3	$C_{D_{\dot{\alpha}}}$	Subsonic: No modifications necessary.  Transonic: NDM  Supersonic: NDM
7.3	Wing-Body Dynamic Derivatives	
7.3.1.1	$C_{L_q}$	All speeds: See Sections 7.1.1.1 and 4.3.1.2 in the appropriate speed range.
7.3.1.2	$C_{m_q}$	All speeds: See Sections 7.1.1.2 and 4.3.1.2 in the appropriate speed range.
7.3.2.1	$C_{Y_P}$	Subsonic: No modifications necessary.  Transonic: NDM  Supersonic: NDM
7.3.2.2	$C_{L_P}$	Subsonic: See Section 7.1.2.2, subsonic.  Transonic: NDM  Supersonic: Use $ \Lambda_{LE} $ in Datcom figure 7.3.2.2-13. See Section 7.1.2.2, Supersonic.

<u>SECTION</u>	<u>DERIVATIVES</u>	<u>MODIFICATIONS</u>
7.3.2.3	$C_{n_p}$	Subsonic: See Section 7.1.2.3, Subsonic. Transonic: NDM Supersonic: NDM
7.3.3.1	$C_{Y_r}$	All speeds: NDM
7.3.3.2	$C_{\ell_r}$	Subsonic: See Section 7.1.3.2, Subsonic. Transonic: NDM Supersonic: NDM
7.3.3.3	$C_{n_r}$	Subsonic: See Section 7.1.3.3, Subsonic. Transonic: NDM Supersonic: NDM
7.3.4.1	$C_{L_\alpha}$	All speeds: See Sections 4.3.1.2 and 7.3.1.1 in the appropriate speed range.
7.3.4.2	$C_{m_\alpha}$	All speeds: See Sections 4.3.1.2 and 7.3.1.1 in the appropriate speed range.
7.4	Wing-Body-Tail Dynamic Derivatives	
7.4.1.1	$C_{L_q}$	All speeds: See Sections 4.1.3.2, 4.3.1.2, 4.4.1, and 7.3.1.1 in the appropriate speed range.
7.4.1.2	$C_{m_q}$	All speeds: See Sections 4.1.3.2, 4.3.1.2, 4.4.1, and 7.3.1.2 in the appropriate speed range.
7.4.1.3	$C_{D_q}$	Subsonic: Use $ \Lambda_{LE} $ in Datcom Figure 7.4.1.3-4. Transonic: NDM Supersonic: NDM

<u>SECTION</u>	<u>DERIVATIVES</u>	<u>MODIFICATIONS</u>
7.4.2.1	$C_{Y_p}$	Subsonic: No modifications necessary. Transonic: NDM Supersonic: NDM
7.4.2.2	$C_{\ell_p}$	Subsonic: See Section 7.1.2.2, Subsonic. Transonic: NDM Supersonic: NDM
7.4.2.3	$C_{n_p}$	Subsonic: See Section 7.3.2.3, Subsonic. Transonic: NDM Supersonic: NDM
7.4.3.1	$C_{Y_r}$	Subsonic: No modifications necessary. Transonic: NDM Supersonic: NDM
7.4.3.2	$C_{\ell_r}$	Subsonic: See Section 7.3.3.2, Subsonic Transonic: NDM Supersonic: NDM
7.4.3.3	$C_{n_r}$	Subsonic: See Section 7.3.3.3, Subsonic. Transonic: NDM Supersonic: NDM
7.4.4.1	$C_{L_{\dot{\alpha}}}$	All speeds: See Sections 4.1.3.2, 4.3.1.2, 4.4.1, and 7.3.4.1 in the appropriate speed range.
7.4.4.2	$C_{m_{\dot{\alpha}}}$	All speeds: See Sections 4.1.3.2, 4.3.1.2, 4.4.1, and 7.3.4.2 in the appropriate speed range.



<u>SECTION</u>	<u>DERIVATIVE</u>	<u>MODIFICATIONS</u>
7.4.4.3	$C_{D\dot{\alpha}}$	Subsonic: See Section 4.4.1. Transonic: NDM Supersonic: NDM
7.4.4.4	$C_{Y\dot{\beta}}$	Subsonic: Use $ \Lambda_{LE} $ in Datcom Figures 7.4.4.4-6, 7.4.4.4-22, 7.4.4.4-26, and 7.4.4.4-42. Transonic: NDM Supersonic: NDM
7.4.4.5	$C_{L\dot{\beta}}$	Subsonic: See Section 7.4.4.4, Subsonic. Transonic: NDM Supersonic: NDM
7.4.4.6	$C_{n\dot{\beta}}$	Subsonic: See Section 7.4.4.4, Subsonic. Transonic: NDM Supersonic: NDM

## REFERENCES

1. "USAF Stability and Control Datcom", Project Engineer: D. E. Hoak; Flight Control Division, Flight Dynamics Laboratory, Wright-Patterson Air Force Base, Ohio, October 1960 (Revised April 1978).
2. DeYoung, John and Harper, Charles W., "Theoretical Symmetric Span Loading at Subsonic Speeds for Wings Having Arbitrary Plan Form", NACA Report 921, 1948.
3. Williams, J. E. and Vukelich, S. R., "Analysis of Datcom Methods as Applied to Modern Configurations", McDonnell Douglas Corporation, MDC E2265, 1980.
4. Lundry, Jerry L., "Charts for Obtaining Subsonic Inviscid Induced Drag of Twisted Swept Wings", Douglas Aircraft Company, Report LB-31689, 1964.
5. Polhamus, Edward C. and Sleeman, William C., Jr., "The Rolling Moment Due to Sideslip of Swept Wings at Subsonic and Transonic Speeds", NASA TN D-209, 1960.
6. Bauer, C. R., Anderson, A.K., Jr., and Lee, R.F., "Investigation of USAF Stability and Control Datcom Prediction Methods and Related Data", McDonnell Douglas Corporation, Report MDC J8328, 1978.
7. Toll, Thomas A., and Queijo, M. J., "Approximate Relations and Charts for Low-Speed Stability Derivatives of Swept Wings", NACA TN 1581, 1948.
8. Sharpes, D. G., "Validation of USAF Stability and Control Datcom Methodologies for Sweptforward Wing Planforms - Subsonic Wing Lift", AFWAL-TM-219-FIGC, 1982.
9. Martina, Albert P. and Deters, Owen J., "Maximum Lift and Longitudinal Stability Characteristics at Reynolds Number Up to  $7.8 \times 10^6$  of a  $35^\circ$  Sweptforward Wing Equipped with High-Lift and Stall-Control Devices, Fuselage, and Horizontal Tail", NACA RM L9H18a, 1950.
10. McCormack, Gerald M. and Cook, Woodrow L., "Effects of Several Leading-Edge Modifications on the Stalling Characteristics of a  $45^\circ$  Swept-Forward Wing", NACA RM A9D29, 1949.
11. Purser, Paul E. and Spearman, M. Leroy, "Wing-Tunnel Tests at Low Speed of Swept and Yawed Wings Having Various Plan Forms", NACA RM L7D23, 1947.
12. Feigenbaum, David and Goodman, Alex, "Preliminary Investigation at Low Speeds of Swept Wings in Rolling Flow", NACA RM L7E09, 1947.
13. Paniszczyn, T. F. and Paulovich, K. F., "Summary Report, Tests of 1/10-Scale XB-53 Complete Model, Galcit 10-ft Tunnel", Consolidated Vultee Aircraft Corp., Report No. FZT-112-007, 1946.

14. Vincenti, Walter G., Van Dyke, Milton D., and Matteson, Frederick H., "Investigation of Wing Characteristics at a Mach Number of 1.53. II - Swept Wings of Taper Ratio 0.5", NACA RM A8E05, 1948.
15. Hopkins, Edward J., "Lift, Pitching Moment, and Span Load Characteristics of Wings at Low Speed as Affected by Variations of Sweep and Aspect Ratio", NACA TN 2284, 1950.
16. McCormack, Gerald M. and Stevens, Victor I., Jr., "An Investigation of the Low-Speed Stability and Control Characteristics of Swept-Forward and Swept-Back Wings in the Ames 40- by 80-Foot Wind Tunnel", NACA RM A6K15, 1947.
17. Cahill, Jones F. and Gottlieb, Stanley M., "Low-Speed Aerodynamic Characteristics of a Series of Swept Wings Having NACA 65A006 Airfoil Sections", NACA RM L50F16, 1951.
18. Savage, Paul W., "Experimental Analysis of the Effects of Sweep and Aspect Ratio on Incompressible Flow About Forward Swept Wings", Master's Thesis, AFIT/GAE/AA/81D-26, 1981.
19. Hieser, Gerald and Whitcomb, Charles F., "Investigation of the Effects of a Nacelle on the Aerodynamic Characteristics of a Swept Wing and the Effects of Sweep on a Wing Alone", NACA TN 1709, 1948.
20. Mendelsohn, Robert A. and Brewer, Jack D., "Comparison Between the Measured and Theoretical Span Loadings on a Moderately Swept-Forward and a Moderately Swept-Back Semispan Wing", NACA TN 1351, 1946.
21. Conner, D. William and Cancro, Patrick A., "Low-Speed Characteristics in Pitch of a  $34^{\circ}$  Sweptforward Wing with Circular-Arc Airfoil Sections", NACA RM L7F04a, 1948.
22. Alexander, Sidney R., "Drag Measurements of a  $34^{\circ}$  Swept- Forward and Swept-Back NACA 65-009 Airfoil of Aspect Ratio 2.7 as Determined by Flight Tests at Supersonic Speeds", NACA RM L6I11, 1946.
23. Paulovich, K. F., "Summary Report, Galcit Power-Off Wind Tunnel Tests on a Revised 1/10-Scale XA-44 Complete Model", Consolidated Vultee Aircraft Corp., Report No. FZT-001A, 1946.
24. McCormack, Gerald M. and Cook, Woodrow L., "Effects of Boundary-Layer Control on the Longitudinal Characteristics of a  $45^{\circ}$  Swept-Forward Wing-Fuselage Combination", NACA RM A9K02a, 1950.
25. Graham, Robert R., "Lateral-Control Investigation at a Reynolds Number of 5,300,000 of Wing Aspect Ratio 5.8 Sweptforward  $32^{\circ}$  at the Leading Edge", NACA RM L9H18, 1950.

26. Spearman, M. Leroy and Comisarow, Paul, "An Investigation of the Low-Speed Static Stability Characteristics of Complete Models Having Sweptback and Sweptforward Wings", NACA RM L8H31, 1948.
27. Tolhurst, William H., Jr., "An Investigation of the Downwash and Wake Behind Large-Scale Swept and Unswept Wings", NACA RM A7L05, 1948.
28. Hoggard, H. Page, Jr. and Hagerman, John R., "Downwash and Wake Behind Untapered Wings of Various Aspect Ratios and Angles of Sweep", NACA TN 1703, 1948.
29. Paulovich, K. F., "Tests of Revised 1/10-Scale XA-44 Complete Model (Modified Wing No. 10) in Galcitt 10-ft. Tunnel - Summary Report", Consolidated Vultee Aircraft Corp. Report No. FZT-112-005, 1946.
30. Luoma, Arvo A., Bielat, Ralph P., and Whitcomb, Richard T., "High-Speed Wind-Tunnel Investigation of the Lateral Control Characteristics of Plain Ailerons on a Wing with Various Amounts of Sweep", NACA RM L7I15, 1947.
31. MacLachlan, Robert and Fisher, Lewis R., "Wind-Tunnel Investigation at Low Speeds of the Pitching Derivatives of Untapered Swept Wings", NACA RM L8G19, 1948.
32. Maggin, Bernard and Bennett, Charles, "Low-Speed Stability and Damping-in-Roll Characteristics of Some High Swept Wings", NACA TN 1286, 1946.
33. DeYoung, J., "Theoretical Symmetric Span Loading Due to Flap Deflection for Wings of Arbitrary Plan Form at Subsonic Speeds", NACA Rept. 1071, 1952.
34. Goin, K. L., "Equations and Charts for the Rapid Estimation of Hinge-Moment and Effectiveness Parameters for Trailing Edges Swept Ahead of the Mach Lines", NACA Rept. 1041, 1951.
35. DeYoung, J., "Theoretical Antisymmetric Span Loading for Wings of Arbitrary Plan Form at Subsonic Speeds", NACA Rept. 1056, 1951.

TABLE 1. SUBSONIC WING-ALONE LIFT-CURVE SLOPE  
DATA SUMMARY AND SUBSTANTIATION

<u>REF</u>	<u>A</u>	<u><math>\Lambda_{c/2}</math></u>	<u><math>C_{L\alpha}</math></u>		<u>E percent error</u>
			<u>CALC</u>	<u>TEST</u>	
9	5.8	-38	.0628	.0630	-0.3
10	3.6	-47	.0468	.0488	-4.1
11	2.6	60	.0346	.0380	-8.9
	4.5	30	.0588	.0550	6.9
	6.0	0	.0726	.0730	-0.5
	4.5	-30	.0588	.0530	10.9
	2.1	-52	.0358	.0400	-10.5
12	2.6	45	.0431	.0400	7.8
	2.6	-45	.0431	.0480	-10.2
28	3.0	60	.0353	.0380	-7.1
	3.0	-60	.0353	.0350	0.9
13	4.1	-33	.0588	.0600	-2.0

$$\text{average error} = \frac{\sum |E|}{n} = 5.85$$

TABLE 2. SUPERSONIC WING-BODY NORMAL-FORCE-CURVE SLOPE  
DATA SUMMARY AND SUBSTANTIATION

<u>REF</u>	<u><math>\Lambda_{c/2}</math></u>	<u>A</u>	<u>d/b</u>	<u>M</u>	<u><math>C_{N\alpha}</math></u>		<u>E percent error</u>
					<u>CALC</u>	<u>TEST</u>	
14	-30	3.5	.067	1.53	.0592	.0585	1.2
	-43	2.9	.073	1.53	.0580	.0550	5.5
	-60	2.0	.088	1.53	.0390	.0365	6.8
Unpub.	-38	4.0	.164	1.40	.0813	.0760	7.0
				1.50	.0745	.0720	3.5

$$\text{average error} = \frac{\sum |E|}{n} = 4.79$$

TABLE 3. SUBSONIC WING-ALONE LIFT VARIATION  
WITH ANGLE OF ATTACK  
DATA SUMMARY AND SUBSTANTIATION

REF	$\Lambda_{LE}$	A	J	$C_{L_{max}}$	$\alpha C_{L_{max}}$	$\alpha$	CALC	$C_L$ TEST	E percent error
9	-32	5.8	7.6	0.945	19.04	6	0.3905	0.418	-6.58
						8	0.5242	0.545	-3.82
						12	0.7855	0.770	2.01
						16	0.9318	0.915	1.84
						18	0.9525	0.960	-0.78
10	-42	3.5	2.4	1.015	25.58	6	0.3095	0.310	-0.16
						8	0.4231	0.420	0.74
						12	0.6594	0.620	6.35
						16	0.8826	0.780	13.15
						20	1.0114	0.920	9.93
						24	1.0545	1.000	5.45
15	46	3.4	3.0	1.000	25.05	6	0.3412	0.375	-9.01
						8	0.4622	0.470	-1.66
						12	0.7087	0.720	-1.57
						16	0.9515	0.870	9.37
						20	1.0560	0.960	10.00
	46	2.8	2.6	0.970	25.50	6	0.3070	0.360	-14.72
						8	0.4191	0.460	-8.89
						12	0.6516	0.670	-2.74
						16	0.8860	0.820	8.05
						20	0.9801	0.960	2.09
-37	4.2	4.9	1.083	23.19	6	0.3569	0.385	-7.30	
					8	0.4862	0.495	-1.78	
					12	0.7530	0.697	8.03	
					16	0.9899	0.855	15.78	
					20	1.0981	0.980	12.05	
					22	1.0979	1.010	8.70	
-37	3.4	3.8	0.975	23.61	6	0.3314	0.370	-10.43	
					8	0.4509	0.480	-6.06	
					12	0.6967	0.720	-3.24	
					16	0.9369	0.845	10.88	
					20	1.0388	0.970	7.09	
					22	1.0378	0.990	4.83	
-37	2.8	3.0	0.860	22.50	6	0.3099	0.360	-13.92	
					8	0.4230	0.460	-8.04	
					12	0.6578	0.670	-1.82	
					16	0.8529	0.820	4.01	
					20	0.9217	0.955	-3.49	

TABLE 3. CONTINUED

REF	$\Lambda_{LE}$	A	J	$C_{Lmax}$	$\alpha C_{Lmax}$	$\alpha$	CALC $C_L$	TEST	E percent error
16	-41	3.1	2.3	1.085	27.60	6	0.3000	0.290	3.45
						8	0.3837	0.380	0.97
						12	0.6524	0.580	12.48
						16	0.8798	0.789	11.51
						20	1.0192	0.920	10.78
	24	1.1036	1.040	6.12					
	-26	3.6	5.2	1.261	23.21	6	0.3890	0.405	-3.95
						8	0.5310	0.530	0.19
						12	0.8260	0.780	5.90
						16	1.0900	0.990	10.10
						20	1.2230	1.145	6.81
	5	4.6	0.9	1.352	21.09	6	0.4255	0.445	-4.38
						8	0.5761	0.580	-0.67
						12	0.8642	0.845	2.27
						16	1.1350	1.110	2.25
20						1.3178	1.340	-1.66	
48	3.6	2.9	1.053	25.89	6	0.3301	0.360	-8.31	
					8	0.4494	0.460	-2.30	
					12	0.6954	0.680	2.26	
					16	0.9291	0.895	3.81	
					20	1.0585	1.090	-2.89	
					22	1.0852	1.145	-5.22	
					24	1.0862	1.180	-7.95	
33	4.8	7.1	1.075	23.70	6	0.3916	0.440	-11.00	
					8	0.5261	0.565	-6.88	
					12	0.7938	0.820	-3.20	
					16	1.0678	1.070	-0.21	
					20	1.1200	1.280	-12.50	
					22	1.1087	1.220	-9.12	
17	-47	4.0	2.6	1.075	28.03	6	0.3292	0.315	4.51
						8	0.4482	0.430	4.23
						12	0.6935	0.685	1.24
						16	0.9410	0.840	12.02
						20	1.0966	0.930	17.91
						24	1.1527	0.980	17.62
						26	1.1592	0.980	18.29
						4	4.0	7.2	0.862
8	0.5473	0.500	9.46						
10	0.6786	0.620	9.45						
12	0.7765	0.705	10.14						
14	0.8403	0.730	15.11						

TABLE 3. CONCLUDED

<u>REF</u>	<u><math>\Lambda_{LE}</math></u>	<u>A</u>	<u>J</u>	<u><math>C_{L_{max}}</math></u>	<u><math>^{\alpha}C_{L_{max}}</math></u>	<u><math>\alpha</math></u>	<u>CALC</u>	<u>TEST</u>	<u>E percent error</u>
17	43	4.0	2.5	1.051	27.30	6	0.3384	0.360	-6.00
						8	0.4585	0.495	-7.37
						12	0.7029	0.705	-0.30
						16	0.9457	0.875	8.08
						20	1.0789	0.970	11.23
						24	1.1110	1.040	6.83
						26	1.0969	1.010	8.60

$$\text{average error} = \frac{\sum |E|}{n} = 6.67$$





TABLE 6) SUBSONIC WING-ALONE  
AERODYNAMIC-CENTER LOCATION  
DATA SUMMARY AND SUBSTANTIATION

REF	$\Lambda_{c/4}$	A	M	$\frac{X_{ac}}{c_r}$		$\Delta X_{ac}$
				CALC	TEST	
9	-36	5.8	.19	-.3332	-.3157	-.0175
10	-45	3.6	.14	-.3073	-.2968	-.0105
11	-30	5.2	.10	-.4110	-.4476	.0366
	-30	4.5		-.3260	-.3713	.0453
	-30	3.6		-.2130	-.4446	.2316
	-32	3.6		-.0839	-.1111	.0272
	-30	3.5		-.0334	-.0567	.0233
	-45	2.1		-.2120	-.2587	.0467
	-47	2.1		-.0998	.0558	-.1556
	-45	2.2		-.0597	-.1267	.0670
	-60	3.0		-.8240	-.8696	.0456
	-60	1.5		-.2900	-.3225	.0325
12	-45	2.6	.17	-.3120	-.3466	.0346
15	-40	5.3	.16	-.3935	-.2519	-.1416
		4.2		-.3225	-.2081	-.1144
		3.4		-.2522	-.1735	-.0787
		2.8		-.1886	-.1424	-.0462
	-30	6.8		-.3378	-.2052	-.1326
		5.3		-.2496	-.1276	-.1220
		4.2		-.1760	-.1037	-.0723
		3.4		-.1275	-.0614	-.0661
16	-45	3.1	.12	-.2046	-.2303	.0257
	-30	4.7		-.1542	-.1545	.0003
18	-15	4.8	.14	-.0480	-.0649	.0169
		4.3		-.0220	-.0501	.0281
		3.8		.0060	-.0136	.0196
	-30	3.9		-.2450	-.3077	.0627
		3.5		-.1970	-.2625	.0655
		3.2		-.1660	-.2140	.0480
	-45	2.6		-.3020	-.3985	.0965
		2.3		-.2520	-.3434	.0914
		2.1		-.2020	-.3081	.1061
19	-45	2.7	.20	-.1800	-.1290	-.0510
			.30	-.1825	-.1319	-.0506
			.40	-.1820	-.1264	-.0556
			.51	-.1830	-.1269	-.0561
			.56	-.1850	-.1279	-.0571
			.61	-.1850	-.1306	-.0544
			.66	-.1860	-.1230	-.0630
			.70	-.1840	-.1247	-.0593
20	-12	6.1	.26	.0620	.0563	.0057

$$\text{average difference} = \frac{\sum |\Delta X_{ac}|}{n} = .0625$$

TABLE 7. SUPERSONIC WING-BODY  
AERODYNAMIC-CENTER LOCATION  
DATA SUMMARY AND SUBSTANTIATION

REF	$\Lambda_{c/2}$	A	d/b	CALC.	$\frac{x_{ac}}{c_r}$		$\Delta x_{ac}$	
					TEST			
14	-60	2.0	.088	-.1997	.0148		-.2145	
	-43	2.9	.073	.0193	-.0104		.0297	
	-30	3.5	.067	.1394	.1013		.0381	
Unpub.	-34	4.0	.164	-.0914	-.2208		.1293	
					average error = $\frac{\Sigma  \Delta x_{ac} }{n}$			.1029

*Contrails*

TABLE 8. ZERO-LIFT DRAG  
DATA SUMMARY AND SUBSTANTIATION

REF	$\Lambda_{c/4}$	A	PLANFORM*	M	$C_{D_0}$		$\Delta C_{D_0}$
					CALC	TEST	
9	-35	5.8	W	0.19	.00919	.00893	.00026
10	-45	3.6	W	0.14	.00770	.01222	-.00452
11	30	5.2	W	0.12	.01169	.01884	-.00715
	-30	5.2	W	0.12	.01169	.01986	-.00817
	58	2.1	W	0.12	.00829	.01224	-.00395
	-47	2.1	W	0.12	.00902	.01486	-.00584
16	45	3.6	W	0.16	.00786	.02296	-.01510
	30	4.8	W	0.16	.00846	.02583	-.01737
	-30	4.7	W	0.16	.00848	.02581	-.01733
	-45	3.1	W	0.16	.00741	.01990	-.01249
17	-45	4.0	W	0.20	.00699	.00507	.00192
Unpub.	-12	5.6	WB	0.80	.01744	.0561	-.03866
				0.90	.01974	.0676	-.04786
				0.95	.02684	.0762	-.04936
				1.05	.04524	.0969	-.05166
	-33	4.0	WB	0.80	.01845	.0364	-.01795
				0.90	.01845	.0375	-.01905
				0.95	.01845	.0402	-.02175
				1.05	.03635	.0551	-.01875
	-54	1.9	WB	0.80	.02252	.0194	.00312
				0.90	.02252	.0193	.00322
				0.95	.02252	.0213	.00122
				1.05	.03112	.0343	-.00318
22	34	2.7	W	1.20	.07476	.02643	.04833
				1.25	.06877	.02492	.04385
				1.30	.06326	.02580	.03746
	-34	2.7	W	1.20	.07476	.03550	.03926
				1.25	.06877	.03342	.03535
				1.30	.06326	.03121	.03205

\*W - Wing-Alone  
WB - Wing-Body

$$\text{average difference} = \frac{|\Delta C_{D_0}|}{n}$$

Subsonic = .00855  
Transonic = .02298  
Supersonic = .03938

TABLE 9. SUBSONIC WING-ALONE DRAG DUE TO LIFT  
DATA SUMMARY AND SUBSTANTIATION

REF	$\Lambda_{c/4}$	A	$C_L$	CALC	$C_{DL}$ TEST	$\Delta C_{DL}$ ( $\times 10^4$ )
9	-35	5.8	.1	.00084	-.00012	9.6
			.2	.00324	.00197	12.7
			.3	.00718	.00749	-3.1
			.4	.01266	.01374	-10.8
			.5	.01970	.02179	-20.9
			.6	.02828	.04316	-148.8
10	-45	3.6	.1	.00095	.00081	1.4
			.2	.00382	.00398	-1.6
			.3	.00859	.00891	-3.2
			.4	.01527	.01877	-35.0
			.5	.02386	.02954	-56.8
			.6	.03436	.05028	-159.2
11	-47	2.1	.1	.00187	-.00019	20.6
			.2	.00746	.00285	46.1
			.3	.01679	.01162	51.7
			.4	.02985	.02362	62.3
			.5	.04665	.04266	39.9
			.6	.06717	.07371	-65.4
	-30	5.2	.1	.00078	.00143	-6.5
			.2	.00314	.00598	-28.4
			.3	.00706	.01159	-45.3
			.4	.01255	.01869	-61.4
			.5	.01961	.02717	-75.6
			.6	.02824	.04178	-135.4
16	-45	3.1	.1	.00107	.00065	4.2
			.2	.00423	.00323	10.0
			.3	.00950	.00933	1.7
			.4	.01687	.01881	-19.4
			.5	.02635	.03333	-69.8
			.6	.03793	.05397	-160.4
	-30	4.7	.1	.00074	0	7.4
			.2	.00294	.00022	27.2
			.3	.00660	.00135	52.5
			.4	.01172	.00484	68.8
			.5	.01831	.01352	47.9
			.6	.02635	.02064	57.1
17	-45	4.0	.1	.00132	.00019	11.3
			.2	.00527	.00332	19.5
			.3	.01185	.01117	6.8
			.4	.02106	.02523	-41.7
			.5	.03291	.05399	-210.8
			.6	.04739	.09157	-441.8

*Contrails*

TABLE 9. CONCLUDED

<u>REF</u>	<u><math>\Lambda_{c/4}</math></u>	<u>A</u>	<u><math>C_L</math></u>	<u>CALC</u>	$C_{DL}$ <u>TEST</u>	$\Delta C_{DL}$ <u>(x 10<sup>4</sup>)</u>
21	-36	3.9	.1	.00271	.00078	19.3
			.2	.01082	.00867	21.5
			.3	.02435	.02500	-6.5
			.4	.04330	.04571	-24.1
			.5	.06765	.07965	-120.0
			.6	.09741	.12698	-295.7

$$\text{average difference} = \frac{\sum |\Delta C_{DL}|}{n} = 58.2$$

# Contrails

AFWAL-TR-84-3084

TABLE 10. TRANSONIC WING-BODY DRAG DUE TO LIFT  
DATA SUMMARY AND SUBSTANTIATION

REF	$\Lambda_{c/4}$	A	d/b	M	$C_L$	CALC $C_{DL}$	TEST	$\Delta C_{DL}$ ( $\times 10^4$ )	
Unpub.	-12	5.6	.133	0.80	.009	.00001	.00072	-7.1	
					.084	.00069	-.00910	97.9	
					.164	.00262	-.01692	195.4	
					.332	.01077	-.01535	261.2	
					.674	.04447	.00817	363.0	
					.735	.05295	.02415	288.0	
					.772	.05839	.03375	246.4	
					0.90	.207	.00486	-.01390	187.6
					.372	.01569	-.00662	223.1	
					.518	.03045	.01445	160.0	
					.579	.03796	.02928	86.8	
					.613	.04252	.03850	40.2	
					.704	.05610	.05854	-24.4	
					0.95	.325	.01332	-.00733	206.5
					.484	.02947	.00751	219.6	
	.550	.03808	.02672	113.6					
	.577	.04192	.03652	54.0					
	.612	.04714	.04733	-1.9					
	.670	.05652	.06694	-104.2					
	1.05	.101	.00149	-.00673	82.2				
	.271	.01067	-.00701	176.8					
	.459	.03063	.01365	169.8					
	.530	.04087	.02148	193.9					
	.564	.04631	.02845	178.6					
	.595	.05153	.03909	124.4					
	.677	.06280	.06038	24.2					
	-33	4.0	.153	0.80	.059	.00056	-.00539	59.6	
					.138	.00310	-.00961	127.1	
					.214	.00743	-.01083	182.6	
					.383	.02371	-.00467	283.8	
					.536	.04647	.00850	379.7	
					.698	.07881	.03106	477.5	
					.771	.09623	.04545	507.8	
0.90					.021	.00007	-.00169	17.6	
.109					.00198	-.00765	96.3		
.193					.00617	-.00980	159.7		
.374					.02321	-.00371	269.2		
.537					.04791	.01217	357.4		
.690					.07922	.03744	417.8		
.825					.11332	.07430	390.2		
0.95					.101	.00173	-.00701	87.4	
.185					.00586	-.00916	150.2		
.360					.02226	-.00472	269.8		
.523					.04682	.01192	349.0		
.692					.08201	.04116	408.5		
.762					.09954	.05737	421.7		
.840					.12093	.07819	427.4		



TABLE 10. CONCLUDED

REF	$\Lambda_{c/4}$	A	d/b	M	$C_L$	$C_{DL}$		$\Delta C_{DL}$ (x 10 <sup>4</sup> )				
						CALC	TEST					
Unpub.	-33	4.0	.153	1.05	.093	.00154	-.00320	47.4				
					.277	.01380	-.00182	156.2				
					.474	.04046	.01317	272.9				
					.662	.07882	.04022	386.0				
					.743	.09922	.05611	431.1				
					.824	.12199	.07623	457.6				
					.905	.14727	.09898	482.9				
					-54	1.9	.206	0.80	.026	.00021	-.00092	11.3
									.081	.00197	-.00065	26.2
									.179	.00970	.00334	63.6
	.290	.02552	.01355	119.7								
	.403	.04913	.03114	179.9								
	.465	.06542	.04431	211.1								
	.525	.08356	.06063	229.3								
	0.90	.075	.00165	.00044					12.1			
		.174	.00877	.00409					46.8			
		.282	.02320	.01474					84.6			
		.401	.04685	.03420	126.5							
		.458	.06105	.04743	136.2							
	0.95	.522	.07927	.06465	146.2							
.578		.09709	.08348	136.1								
.082		.00196	-.00004	20.0								
.189		.01051	.00414	63.7								
.304		.02711	.01577	113.4								
.422		.05221	.03599	162.2								
.485		.06883	.05041	184.2								
.547		.08768	.06662	210.6								
.601		.10586	.08603	198.3								
1.05		.068	.00131	-.00064	19.5							
	.184	.00950	.00349	60.1								
	.312	.02715	.01600	111.5								
	.437	.05327	.03622	170.5								
	.509	.07242	.05064	217.8								
	.571	.09102	.06665	243.7								
	.634	.11250	.08546	270.4								

$$\text{average difference} = \frac{\sum |\Delta C_{DL}|}{n} = 188.8$$



*Contrails*

TABLE 11. SUPERSONIC WING-BODY DRAG DUE TO LIFT  
DATA SUMMARY AND SUBSTANTIATION

REF	$\Lambda_{c/4}$	A	d/b	M	$C_L$	CALC $C_{DL}$	TEST	$\Delta C_{DL}$ (x $10^4$ )					
Unpub.	-12	5.6	.133	1.2	-.070	.00095	.0067	-57.5					
					.081	.00201	.0009	11.1					
					.205	.01012	.0025	76.2					
					.348	.02734	.0157	116.4					
					.424	.03996	.0275	124.6					
					.502	.05545	.0461	93.5					
					.577	.07296	.0691	38.6					
	1.3	-078	.00139	.0063	-49.1	.070	.00189	.0009	9.9				
						.185	.01000	.0013	87.0				
						.307	.02606	.0133	127.6				
						.372	.03773	.0251	126.3				
						.438	.05186	.0336	182.6				
						.502	.06791	.0532	147.1				
						-33	4.0	.153	1.2	.044	.00046	.0024	-19.4
										.211	.00951	.0028	67.1
										.380	.03077	.0150	157.7
										.554	.06557	.0393	262.7
.633	.08602	.0554	306.2										
.720	.11158	.0749	366.8										
.796	.13713	.0955	416.3										
1.3	.036	.00038	.0012	-8.2	.187					.00885	.0019	69.5	
					.340					.02913	.0136	155.3	
					.503					.06376	.0371	266.6	
					.579	.08478	.0520	327.8					
-54	1.9	.206	1.2	.058	.00135	.0006	7.5						
				.174	.01224	.0040	82.4						
				.285	.03321	.0156	176.1						
				.407	.06814	.0349	332.4						
				.473	.09218	.0480	441.8						
				.539	.11996	.0636	563.6						
				.602	.15012	.0816	685.2						
				1.3	.060	.00145	.0003	11.5	.169	.01171	.0036	81.1	
									.284	.03335	.0151	182.5	
									.403	.06763	.0351	325.3	
.467	.09101	.0481	429.1										
.530	.11755	.0636	539.5										
.597	.14942	.0811	683.2										

$$\text{average difference} = \frac{\sum |\Delta C_{DL}|}{n} = 215.6$$

TABLE 12. SUBSONIC WING-BODY LIFT-CURVE SLOPE  
DATA SUMMARY AND SUBSTANTIATION

<u>REF</u>	<u><math>\Lambda_{c/2}</math></u>	<u>A</u>	<u>d/b</u>	<u>CALC</u>	$C_{L\alpha}$ <u>TEST</u>	<u>E</u> <u>percent</u> <u>error</u>
13	-33	4.1	.127	.06744	.06408	
23	-17	6.0	.108	.07631	.07772	-1.81
Unpub.	-36	4.0	.164	.07542	.07000	7.74
24	-48	3.6	.142	.05400	.04950	9.09
25	-38	5.8	.120	.06893	.06830	0.92
26	-18	6.6	.143	.08233	.07754	6.18
	-33	5.1	.160	.06893	.06427	7.25
	-48	3.2	.197	.05007	.05414	-7.52

$$\text{average error} = \frac{\sum |\%E|}{n} = 5.72$$

TABLE 13. SUBSONIC WING-BODY LIFT VARIATION  
WITH ANGLE OF ATTACK  
DATA SUMMARY AND SUBSTANTIATION

REF	$\Lambda_{c/4}$	d/b	J	$C_{L_{max}}$	$\alpha_{C_{L_{max}}}$	$\alpha$	METHOD $C_L$		TEST	E percent error	
							1	2		1	2
9	-35	.120	3.4	1.070	20.53	7	0.442	0.465	0.382	15.7	21.7
							0.634	0.598	0.540	17.4	10.7
							0.784	0.731	0.592	32.4	23.5
							0.932	0.864	0.692	34.7	24.9
							1.045	0.997	0.791	32.1	26.0
							1.136	1.130	0.874	30.0	29.3
							1.198	1.263	0.929	29.0	36.0
23	-12	.108	7.7	1.008	14.17	7	0.592	0.545	0.52	13.8	4.8
							0.763	0.700	0.67	13.9	4.5
							0.940	0.856	0.79	19.0	8.4
							1.116	1.012	0.81	37.8	24.9
24	-45	.142	2.0	1.057	28.24	7	0.379	0.334	0.382	-0.8	-12.6
							0.429	0.429	0.485	-11.5	-11.5
							0.487	0.524	0.592	-17.7	-11.5
							0.556	0.619	0.692	-19.7	-10.5
							0.636	0.715	0.791	-19.6	-9.6
							0.727	0.810	0.874	-16.8	-7.3
							0.832	0.905	0.929	-10.4	-2.6
							0.950	1.001	0.977	-2.8	2.5
							1.083	1.096	1.031	5.0	6.3
							1.232	1.191	1.064	15.8	11.9
1.398	1.286	1.085	28.8	18.5							
average error = $\frac{\Sigma  \%E }{n} =$										19.3	14.5

TABLE 14: SUBSONIC WING-BODY MAXIMUM LIFT  
DATA SUMMARY AND SUBSTANTIATION

REF	$\Lambda_{c/4}$	A	d/b	$C_{L_{max}}$		$\alpha C_{L_{max}}$		E percent error	
				CALC	TEST	CALC	TEST	$C_L$	$\alpha$
9	-35	5.8	.120	1.070	1.21	20.53	26.0	-11.6	-21.0
13	-26	4.1	.127	0.976	0.90	18.75	21.6	8.4	-13.2
23	-12	6.0	.108	1.008	0.82	14.17	12.4	22.9	14.3
24	-45	3.6	.142	1.025	1.10	24.45	30.3	-6.8	-19.3
average error = $\frac{\Sigma  \%E }{n}$								12.4	17.0

TABLE 15. SUBSONIC WING-BODY  
AERODYNAMIC CENTER LOCATION

REF	$\Lambda_{c/4}$	A	d/b	$\frac{x_{ac}}{c_r}$		$\Delta x_{ac}$
				CALC	TEST	
26	-15	6.6	.143	-.41399	-.39027	-.0237
	-30	5.1	.160	-.28243	-.30655	.0241
	-45	3.2	.197	-.09601	-.16497	.0690
Unpub.	-34	4.0	.164	-.41386	-.44400	.0301
average difference = $\frac{\Sigma  \Delta x_{ac} }{n}$						.0367

TABLE 16. SUBSONIC WING-BODY ZERO-LIFT DRAG  
DATA SUMMARY AND SUBSTANTIATION

REF	$\Lambda_{c/4}$	A	d/b	$C_{D_0}$		$\Delta C_{D_0}$
				CALC	TEST	
9	-35	5.8	.120	.01096	.01673	-.00577
13	-30	4.1	.127	.01339	.01002	.00337
21	-36	3.9	.123	.00943	.00979	-.00036
23	-12	6.0	.108	.01423	.01128	.00295
24	-45	3.6	.142	.01000	.01895	-.00895
Unpub.	-34	4.0	.197	.01936	.03310	-.01374
average difference = $\frac{\Sigma  \Delta C_{D_0} }{n}$						.00586

TABLE 17. SUPERSONIC WING-BODY ZERO-LIFT DRAG  
DATA SUMMARY AND SUBSTANTIATION

REF	$\Lambda_{c/2}$	A	d/b	M	$C_{D_0}$		$\Delta C_{D_0}$
					CALC	TEST	
14	60	2.0	.088	1.53	.01881	.02031	-.00150
	43	2.9	.073		.01977	.02510	-.00533
	30	3.5	.067		.01991	.02474	-.00483
	-30	3.5	.067		.01991	.02540	-.00549
	-43	2.9	.073		.01977	.02722	-.00745
	-60	2.0	.088		.01881	.02110	-.00229

$$\text{average difference} = \frac{\sum |\Delta C_{D_0}|}{n} = .00448$$

TABLE 18. SUBSONIC WING-BODY DRAG DUE TO LIFT  
DATA SUMMARY AND SUBSTANTIATION

REF	$\Lambda_{LE}$	A	d/b	$C_L$	$C_{D_L}$		$\Delta C_{D_L}$ (x 10 <sup>4</sup> )
					CALC	TEST	
Unpub.	-7.9	5.6	.133	.239	.00578	0	57.8
				.391	.01352	.00378	97.4
				.540	.02542	.01939	60.3
				.681	.04095	.03536	55.9
				.745	.04960	.03925	103.5
				.820	.06055	.04623	143.2
				.898	.07314	.05795	151.9
-28.3	4.0	.153	.237	.00853	.00017	83.6	
			.378	.02089	.00691	139.8	
			.519	.03952	.01847	210.5	
			.652	.06337	.03556	278.1	
			.720	.07790	.04718	307.2	
			.784	.09319	.06162	315.7	
			.858	.11233	.08047	318.6	
-48.7	1.9	.206	.080	.00243	.00041	20.2	
			.179	.01015	.00423	59.2	
			.283	.02493	.01306	118.7	
			.398	.04932	.02891	204.1	
			.451	.06363	.04034	232.9	
			.516	.08327	.05578	274.9	
			.578	.10470	.07323	314.7	

$$\text{average difference} = \frac{\sum |\Delta C_{D_L}|}{n} = 169.0$$

TABLE 19: SUBSONIC DOWNWASH - METHOD 1  
DATA SUMMARY AND SUBSTANTIATION

REF	$\Lambda_{c/4}$	A	$\frac{2h_H}{b}$	$\alpha$	DOWNWASH ANGLE		$\Delta\epsilon$	
					CALC	TEST		
27	45	3.6	0	0.1	0.05	1.50	-1.45	
			.20		0.05	0.40	-0.35	
			0	12.7	6.50	5.30	1.20	
			.20		6.60	6.40	0.20	
			0	21.1	10.30	6.00	4.30	
			.20		11.01	8.25	2.76	
	30	4.8	4.8	-.10	-1.0	-0.52	0.49	-1.01
				0		-0.53	1.50	-2.03
				.30		-0.45	0.53	-0.98
				-.10	8.5	4.19	3.45	0.74
				0		4.38	3.82	0.56
				.30		3.96	3.80	0.16
				-.10	15.9	7.50	4.40	3.10
				0		7.93	4.84	3.09
	-30	4.7	4.7	-.10	-1.0	-0.43	-0.20	-0.23
				0		-0.44	0.40	-0.84
				.20		-0.40	0.70	-1.10
				-.10	9.9	3.63	3.60	0.03
				0		4.00	4.20	-0.20
				.20		4.24	4.40	-0.16
				-.10	16.4	5.18	4.80	0.38
				0		6.17	4.95	1.22
	-45	3.1	3.1	-.10	3.3	1.96	2.35	-0.39
				0		2.14	3.00	-0.86
.20					2.22	3.10	-0.88	
-.10				9.9	4.79	4.70	0.09	
0					5.22	5.00	0.22	
.20					5.84	8.40	-2.56	
9	-35	5.8	-.11	0.0	0.21	-2.1	2.31	
			.25		0.07	1.8	-1.73	
			-.11	4.0	1.86	0	1.86	
			.25		1.70	4.2	-2.50	
			-.11	8.0	3.34	1.8	1.54	
			.25		3.43	6.0	-2.57	

$$\text{average difference} = \frac{\sum |\Delta\epsilon|}{n} = 1.37$$

TABLE 20. SUBSONIC DOWNWASH GRADIENT  
METHOD 2  
DATA SUMMARY AND SUBSTANTIATION

REF	$\Lambda_{c/4}$	A	CALC	$\frac{\partial \epsilon}{\partial \alpha}$	TEST	$\Delta \left( \frac{\partial \epsilon}{\partial \alpha} \right)$
9	-35	5.8	.2989		.3654	.0665
26	45	3.7	.4993		.4079	.0914
	30	5.6	.4058		.4000	.0058
	15	7.2	.3488		.3775	-.0287
	-15	7.2	.3407		.4124	-.0717
	-30	5.4	.3922		.4315	-.0393
	-45	3.3	.4607		.4219	.0388
27	30	4.8	.4200		.3911	.0289
	-30	4.7	.4304		.4706	-.0402
	-45	3.1	.4597		.4489	.0108

$$\text{average difference} = \frac{\sum \left| \Delta \left( \frac{\partial \epsilon}{\partial \alpha} \right) \right|}{n} = .0422$$

TABLE 21. DOWNWASH DUE TO FLAP DEFLECTION  
DATA SUMMARY AND SUBSTANTIATION

REF	$\Lambda_{c/4}$	A	$\frac{2b_f}{b}$	CALC	$\Delta \epsilon$	TEST	$\Delta(\Delta \epsilon)$
26	45	3.7	.82	1.0535		2.7789	-1.7254
	30	5.6	.87	1.1414		3.6632	-2.5218
	15	7.2	.88	1.1338		3.0316	-1.8978
	-15	7.2	.90	1.0720		3.7474	-2.6754
	-30	5.4	.86	0.9978		3.1421	-2.1443
	-45	3.3	.82	1.0955		2.0632	-0.9677

$$\text{average difference} = \frac{\sum |\Delta(\Delta \epsilon)|}{n} = 1.9887$$

TABLE 22. SUBSONIC DYNAMIC PRESSURE RATIO  
DATA SUMMARY AND SUBSTANTIATION

REF	$\Lambda_{c/4}$	A	$C_L$	CALC	$\frac{q}{q_\infty}$	TEST	$\frac{\Delta q}{q_\infty}$
28	60	3.0	.004	.836		.970	-.134
			.154	.956		.925	.031
	30	5.2	.028	.895		.952	-.057
			.259	.991		.950	.041
	-30	5.2	0	.893		.890	.003
			.231	.994		.949	.045
	-60	3.0	.022	.837		.780	.057
			.162	.957		.900	.057

$$\text{average difference} = \frac{\sum \left| \frac{\Delta q}{q_\infty} \right|}{n} = .053$$

TABLE 23. TRANSONIC WING-BODY ROLLING MOMENT  
DUE TO SIDESLIP  
DATA SUMMARY AND SUBSTANTIATION

<u>REF</u>	<u><math>\Lambda_{LE}</math></u>	<u>A</u>	<u>d/b</u>	<u>M</u>	<u><math>C_L</math></u>	<u>CALC</u>	<u><math>C_{\ell_B}</math></u>	<u>TEST</u>	<u><math>\Delta C_{\ell_B}</math></u> <u>(x 10<sup>3</sup>)</u>
Unpub.	-7.9	5.6	.133	0.6	.161	-.000259	.001130	-1.389	
					.540	-.000309	.001490	-1.799	
				0.9	-.031	-.000237	-.001750	1.513	
					.400	-.000245	.000833	-1.078	
				1.2	-.150	-.000332	-.001025	0.693	
					.218	-.000239	-.000468	0.229	
	-28.3	4.0	.153	0.6	.160	.000154	.00134	-1.186	
					.519	.000864	.00188	-1.016	
				0.9	.122	.000107	.001145	-1.038	
					.559	.001075	.001821	-0.746	
				1.2	-.026	-.000395	-.000305	-0.090	
					.396	.000351	.000597	-0.246	
-48.7	1.9	.206	0.6	.032	-.000235	.000740	-0.975		
				.284	.000221	.001060	-0.839		
			0.9	.022	-.000253	.000690	-0.943		
				.012	-.000412	.000540	-0.952		
			1.2	.299	-.000032	.001125	-1.157		
-29.3	4.0	.164	0.6	-.042	.000695	.001060	-0.365		
			0.9	-.067	.000632	.001072	-0.440		

$$\text{average difference} = \frac{\sum |\Delta C_{\ell_B}|}{n} = 0.879$$



TABLE 24. SUPERSONIC WING-BODY ROLLING MOMENT  
DUE TO SIDESLIP  
DATA SUMMARY AND SUBSTANTIATION

REF	$\Lambda_{LE}$	A	d/b	M	$C_N$	$C_{l_B}$		$\Delta C_{l_B}$ (x 10 <sup>3</sup> )
						CALC...	TEST	
Unpub.	-29	4.0	.164	1.5	-.113	.000484	.000472	.012
				1.6	-.104	.000505	.000478	.027
					.258	.000844	.000527	.317
				1.8	-.108	.000364	.000436	-.072
					.225	.000801	.000650	.151
						average difference = $\frac{\sum  \Delta C_{l_B} }{n} = .116$		

TABLE 25. SUBSONIC WING-BODY ROLLING MOMENT  
DUE TO SIDESLIP  
DATA SUMMARY AND SUBSTANTIATION

REF	$\Lambda_{c/4}$	A	d/b	$\Gamma$	$C_L$	$C_{l_B}$		$\Delta C_{l_B}$ (x 10 <sup>3</sup> )
						CALC...	TEST	
13	-30	4.0	.112	7	-.019	-.001463	-.001350	-.113
23	-12	6.0	.108	3	.139	-.000989	-.000870	-.119
				5		-.001393	-.001370	-.023
29	-30	4.9	.112	8	-.014	-.001817	-.001175	-.642
Unpub.	-34	4.0	.164	0	-.012	.000755	.000946	-.191
					.316	.001349	.001169	.180
						average difference = $\frac{\sum  \Delta C_{l_B} }{n} = .211$		

*Contrails*

TABLE 26. SUBSONIC WING-BODY-TAIL  
ROLLING MOMENT DUE TO SIDESLIP  
DATA SUMMARY AND SUBSTANTIATION

REF	$\Lambda_{c/4}$	A	d/b	$\Gamma$	$C_L$	$C_{l_B}$		$\Delta C_{l_B}$ ( $\times 10^3$ )				
						CALC	TEST					
23	-12	6.0	.108	3	.139	-.001784	-.00141	-0.374				
						-.002188	-.00191	-0.278				
26	-15	7.2	.143	0	-.120	-.0013	-.0023	1.0				
					.097	-.0010	-.0018	0.8				
					.237	-.0007	-.0013	0.6				
					.472	-.0003	-.0011	0.8				
					.669	0	-.0004	0.4				
					-30	5.4	.160	0	-.076	-.0014	-.0022	0.8
									.088	-.0010	-.0018	0.8
									.241	-.0005	-.0013	0.8
									.392	-.0001	-.0008	0.7
									.561	.0004	-.0007	1.1
									.698	.0008	-.0003	1.1
					-45	3.3	.197	0	-.063	-.0016	-.0024	0.8
									.059	-.0011	-.0021	1.0
									.182	-.0007	-.0017	1.0
.290	-.0003	-.0011	0.8									
.412	.0002	-.0006	0.8									
.533	.0006	-.0003	0.9									
29	-30	4.9	.112	8	-.014	-.002486	-.002688	0.202				
						-.002458	-.002613	0.155				

$$\text{average difference} = \frac{\sum |\Delta C_{l_B}|}{n} = 0.750$$

# Contrails

TABLE 27. EFFECT OF CONTROL SURFACE DEFLECTION ON LIFT  
DATA SUMMARY AND SUBSTANTIATION

Ref	$\Lambda c/4$	A	Flap Type	$\eta_i$	$\eta_o$	CALC * $C_{L\delta}$	TEST	$\Delta C_{L\delta}$			
9	-35	5.8	Split	.10	.60	.4162	.3667	.0495			
					.97	.5918	.5733	.0185			
					.37	.2967	.3133	-.0166			
					.97	.3514	.4075	-.0561			
					.80	.2831	.3110	-.0279			
16	-45	3.1		0	.62	.3490	.295	.0540			
					.97	.4579	.400	.0579			
					-30	4.7		0	.62	.5489	.467
.97	.7202	.665	.0552								
21	-36	3.9		0	.50	.3648	.2989	.0659			
26	-15	7.2			.14	.5097	.5883	-.0786			
					.16	.3783	.3290	.0493			
					.18	.2594	.2126	.0468			
30	-45	4.4	Plain	.53	.90	.0470	.0743	-.0273			
9	-35	5.8	Single-	.10	.60	.6253	.6001	.0252			
					slotted	.97	.8893	.8784	.0109		
						.37	.4457	.4615	-.0158		
						.97	.5780	.5940	-.0160		
					Double-	slotted	.10	.60	.8486	.6976	.1510
								.97	1.2068	1.1362	.0706
								.37	.6049	.5686	.0363
								.97	.7165	.7545	-.0380
					Leading-	edge	0	.41	-.0334	-.0224	-.0110
								.58	-.0444	-.0350	-.0094
.41	-.0446	-.0360	-.0086								
10	-45	3.6		0	1.00	-.0383	-.0143	-.0240			
						-.0638	-.0371	-.0267			
9	-35	5.8	Slat	0	.41	-.0394	-.0054	-.0340			
					.58	-.0524	-.0197	-.0327			
					.75	-.0658	-.0293	-.0365			
			Kreuger	0	.41	-.0421	-.0185	-.0236			
					.58	-.0617	-.0517	-.0100			
					.75	-.0848	-.0733	-.0115			

$$\text{Average Difference} = \frac{\sum |\Delta C_{L\delta}|}{n}$$

- Split Flap = .0506
- Single Slotted Flap = .0170
- Double Slotted Flap = .0740
- Plain Flap = .0273
- Leading Edge Flap = .0159
- Slat = .0344
- Kreuger = .0150

\*Equation 8 used to obtain split flap results.

TABLE 28. EFFECT OF CONTROL SURFACE DEFLECTION ON LIFT-CURVE SLOPE  
DATA SUMMARY AND SUBSTANTIATION

Ref	$\Lambda c/4$	A	Flap Type	$\eta_i$	$\eta_o$	$(C_{L\alpha})_\delta$		E percent error				
						CALC	TEST					
21	-36	3.94	Kreuger	0	.98	.06232	.06615	-5.79				
9	-35	5.79	Leading-edge	0	.75	.06557	.06901	-4.98				
					.58	.06520	.06284	3.76				
					.41	.06482	.06202	4.51				
				Slat	0	.75	.07083	.06415	10.41			
						.58	.06939	.06372	8.90			
						.41	.06791	.06174	9.99			
			Single-slotted	.10	.60	.97	.06630	.06532	1.50			
						.97	.06743	.06754	-.16			
						.37	.06570	.06602	-.48			
				.37	.80	.97	.06639	.06750	-1.64			
						Double-slotted	.10	.60	.97	.06886	.06517	5.66
									.97	.07111	.06980	1.88
.37	.06766	.06849	-1.21									
			.97	.06904	.07193	-4.02						

$$\text{Average Difference} = \frac{\sum |\%E|}{n} = 4.33$$

TABLE 29. EFFECT OF CONTROL SURFACE DEFLECTION ON MAXIMUM LIFT COEFFICIENT DATA SUMMARY AND SUBSTANTIATION

Ref	$\Lambda_c/4$	A	Re (x 10 <sup>-6</sup> )	Flap Type	$\eta_i$	$\eta_o$	CALC *	$\Delta C_{L_{max}}$	$\Delta(\Delta C_{L_{max}})$
								TEST	
16	-45	3.12	8.08	Split	0	.62	.23512	.15142	.08370
						.97	.31728	.23243	.08485
	-30	4.69	4.92		0	.62	.40149	.29370	.10779
						.97	.53215	.42176	.11039
21	-36	3.94	6.90	0	.50	.26949	.28656	-.01707	
9	-35	5.79	7.00	Single slotted	.10	.60	.24139	.24	.00139
						.97	.35963	.35	.00963
					.37	.80	.16968	.14	.02968
						.97	.21763	.15	.06763
					.10	.60	.37515	.28	.09515
						.97	.55891	.42	.13891
					.37	.80	.26370	.18	.08370
						.97	.33822	.24	.09822
					.10	.60	.46969	.40	.06969
						.97	.64976	.61	.03976
					.37	.80	.33016	.24	.09016
						.97	.42345	.36	.06345
Slats	0	.41	.1123	.1064	.0059				
		.58	.2209	.1796	.0413				
		.75	.3758	.1880	.1878				

$$\text{Average Difference} = \frac{\sum |\Delta(\Delta C_{L_{max}})|}{n}$$

- Split Flap = .05690
- Single-Slotted Flap = .10400
- Double-Slotted Flap = .06577
- Slats = .07833

\*Trailing edge flap values obtained by using Figure 17 in place of Datcom Figure 6.1.4.3-10.

TABLE 30. EFFECT OF CONTROL SURFACE DEFLECTION ON PITCHING MOMENT DATA SUMMARY AND SUBSTANTIATION

Ref	$\Delta c/4$	A	Flap Type	$\eta_i$	$\eta_o$	CALC	$\Delta C_{m_{TEST}}$	$\Delta(\Delta C_m)$	
16	-45	3.12	Split	0	.62	-.31723	-.13250	-18473	
					.97	-.26135	-.12347	-.13788	
	-30	4.69		0	.62	-.30393	-.17542	-.12851	
					.97	-.27169	-.16183	-.10986	
21	-36	3.94		0	.98	-.27518	-.178	-.09718	
26	-15	7.15			.14	.56	-.16651	-.08424	-.08227
					.16	.58	-.16289	-.09012	-.07277
					.18	.59	-.15321	-.05926	-.09395
9	-35	5.79			.10	.60	-.25204	-.20329	-.04875
					.97		-.17162	-.15829	-.01333
					.37	.80	-.00487	-.03514	.03027
					.97		.03891	-.00357	.04248
30	-30	6.80	Plain		.55	.91	.01147	.01066	.00081
					.53	.90	.01549	.01655	-.00106
9	-35	5.79	Single-slotted		.10	.60	-.36121	-.20543	-.15578
					.97		-.30565	-.19257	-.11308
					.37	.80	-.08068	-.05229	-.02839
					.97		-.03244	.06000	-.09244
					.10	.60	-.47582	-.36486	-.11096
					.97		-.46036	-.26221	-.19815
			Double-slotted		.37	.80	-.15520	-.06514	-.09006
					.97		-.12138	.00500	-.12638
					.10	.60	-.47582	-.36486	-.11096
					.97		-.46036	-.26221	-.19815
10	-45	3.55	Leading-edge Flap	0	.50		-.01427	-.01847	.00420
					.75		-.03029	-.02275	-.00754
					1.00		-.04363	-.12504	.08141
9	-35	5.79		0	.41		-.01757	-.00975	-.00782
					.58		-.03258	-.01718	-.01540
					.41		-.02037	-.01857	-.00180
					.58		-.03820	-.02257	-.01563
					.75		-.06118	-.03186	-.02932
					.41		-.02600	-.01714	-.00886
			Kreuger	0	.58		-.04878	-.02657	-.02221
					.75		-.08083	-.04529	-.03554

$$\text{Average Difference} = \frac{\sum |\Delta(\Delta C_m)|}{n}$$

Trailing Edge Devices = .08905

Leading Edge Devices = .02088

TABLE 31. EFFECT OF ANGLE OF ATTACK ON CONTROL SURFACE HINGE MOMENT  
DATA SUMMARY AND SUBSTANTIATION

<u>Ref</u>	<u><math>\Lambda c/4</math></u>	<u>A</u>	<u>Flap Type</u>	<u><math>\eta_i</math></u>	<u><math>\eta_o</math></u>	<u>CALC</u>	<u><math>C_{h\alpha}</math> TEST</u>	<u><math>\Delta C_{h\alpha}</math></u>
30	-30	6.80	Plain	.55	.91	-.15601	-.13188	-.02413
25	-45	4.40		.53	.90	-.11899	-.25956	.14057
	-35	5.79		.59	.98	-.08466	-.26356	.17890

$$\text{Average Difference} = \frac{\Sigma |\Delta C_{h\alpha}|}{n} = .11453/\text{rad}$$

TABLE 32. EFFECT OF CONTROL SURFACE DEFLECTION ON ROLLING MOMENT  
DATA SUMMARY AND SUBSTANTIATION

<u>Ref</u>	<u><math>\Lambda c/4</math></u>	<u>A</u>	<u>Flap Type</u>	<u><math>\eta_i</math></u>	<u><math>\eta_o</math></u>	<u>CALC</u>	<u><math>C_{\ell\delta}</math> TEST</u>	<u><math>\Delta C_{\ell\delta}</math></u>
30	-30	6.86	Plain	.55	.91	.14576	.09090	.05489
	-45	4.40		.53	.90	.12506	.04562	.07944
25	-35	5.79		.59	.98	.12570	.06574	.05996
			Spoiler	0	.40	.00122	.00327	-.00205
					.63	.00204	.00538	-.00334
					.98	.02067	.01985	.00082
				0	.40	.00896	.01387	-.00491
					.63	.01501	.01848	-.00347
					.98	.02067	.01985	.00082

$$\text{Average Difference} = \frac{\Sigma |\Delta C_{\ell\delta}|}{n}$$

Plain = .06475

Spoiler = .00257

TABLE 33. EFFECT OF CONTROL SURFACE DEFLECTION  
ON YAWING MOMENT  
DATA SUMMARY AND SUBSTANTIATION

<u>REF</u>	<u><math>\Lambda_{c/4}</math></u>	<u>A</u>	<u>FLAP TYPE</u>	<u><math>\eta_i</math></u>	<u><math>\eta_o</math></u>	<u><math>C_L</math></u>	<u>CALC</u>	<u><math>C_n</math></u>	<u>TEST</u>	<u><math>\Delta C_n</math></u>		
25	-35	5.8	PLAIN	.59	.98	.089	-.00018	-.00092	.00074			
						.334	-.00065	-.00168	.00103			
						.641	-.00116	-.00272	.00156			
								<u><math>h_s</math></u>				
					SPOILER	0	.40	.04	.00118	.00344	-.00226	
			.63	.00222					.00478	-.00256		
			.98	.00464					.00478	-.00014		
					0	.40	.10	.00296	.00993	-.00697		
.63	.00554	.01356	-.00802									
.98	.01160	.01356	-.00196									

$$\text{average difference} = \frac{\sum |\Delta C_n|}{n}$$

PLAIN = .00111

SPOILER = .00365



TABLE 34. SUBSONIC WING-ALONE  $C_{Lq}$   
DATA SUMMARY AND SUBSTANTIATION

<u>REF</u>	<u><math>\Lambda_{c/4}</math></u>	<u>A</u>	<u><math>C_{Lq}</math></u>		<u>E percent error</u>
			<u>CALC</u>	<u>TEST</u>	
31	45	2.6	0.9079	0.9200	-1.32
	-45	2.6	1.3915	1.4667	-5.13

TABLE 35. SUBSONIC WING-ALONE  $C_{Mq}$   
DATA SUMMARY AND SUBSTANTIATION

<u>REF</u>	<u><math>\Lambda_{c/4}</math></u>	<u>A</u>	<u><math>C_{Mq}</math></u>		<u>E percent error</u>
			<u>CALC.</u>	<u>TEST</u>	
31	45	2.6	-.5869	-.5655	3.78
	-45	2.6	-.7000	-.8345	-16.12



TABLE 36. SUBSONIC WING-ALONE  $C_{Y_P}$   
DATA SUMMARY AND SUBSTANTIATION

REF	$\Lambda_{c/4}$	A	$C_L$	CALC $C_{Y_P}$	TEST $C_{Y_P}$	$\Delta C_{Y_P}$
12	45	2.6	.038	.0384	.0311	.0073
			.050	.0498	.0494	.0004
			.100	.0997	.0962	.0035
	-45	2.6	.050	-.0133	-.0424	.0291
			.100	-.0267	-.0589	.0322

$$\text{average difference} = \frac{\sum |\Delta C_{Y_P}|}{n} = .0145$$

TABLE 37. SUBSONIC WING-ALONE  $C_{L_P}$   
DATA SUMMARY AND SUBSTANTIATION

REF	$\Lambda_{c/4}$	A	$C_L$	CALC $C_{L_P}$	TEST $C_{L_P}$	E percent error	
12	45	2.6	0	-.1984	-.2249	-11.78	
	-45	2.6	0	-.1984	-.2158	-8.06	
32	42	5.9	.060	-.3164	-.3097	2.16	
			.269	-.3179	-.2951	7.73	
			.311	-.2213	-.2600	-14.88	
	-38	5.9	3.0	.669	-.2360	-.2310	2.16
				.335	-.3193	-.3504	-8.88
				.800	-.3292	-.3613	-8.88
	3.0	.310	-.2198	-.2351	-6.51		
		.689	-.2330	-.2903	-19.74		

$$\text{average error} = \frac{\sum |\%E|}{n} = 9.08$$